Erika E. Holt

Early age autogenous shrinkage of concrete

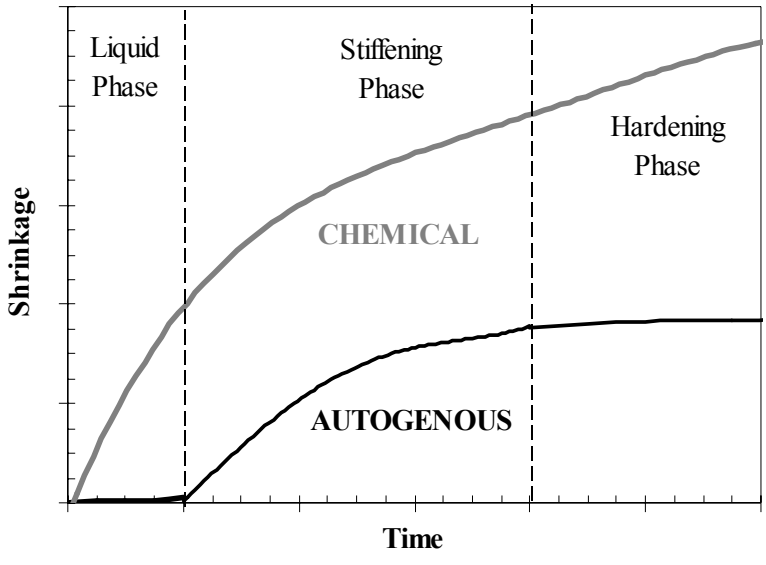

TECHNICAL RESEARCH CENTRE OF FINLAND ESPOO 2001

VTT PUBLICATIONS 446

Early age autogenous shrinkage of concrete

Erika E. Holt

VTT Building and Transport

TECHNICAL RESEARCH CENTRE OF FINLAND
ESPOO 2001

ISBN 951–38–5870–7 (soft back ed.)
ISSN 1235–0621 (soft back ed.)

ISBN 951–38–6250–X (URL: http://www.vtt.fi/inf/pdf/)
ISSN 1455–0849 (URL: http://www.vtt.fi/inf/pdf/)

JULKAISIJA – UTGIVARE – PUBLISHER

Valtion teknillinen tutkimuskeskus (VTT), Vuorimiehentie 5, PL 2000, 02044 VTT
puh. vaihde (09) 4561, faksi (09) 456 4374

Statens tekniska forskningscentral (VTT), Bergsmansvägen 5, PB 2000, 02044 VTT
tel. växel (09) 4561, fax (09) 456 4374

Technical Research Centre of Finland (VTT), Vuorimiehentie 5, P.O.Box 2000, FIN–02044 VTT, Finland
phone internat. + 358 9 4561, fax + 358 9 456 4374

VTT Rakennus- ja yhdyskuntatekniikka, Materiaalit ja tuotteet, Kemistintie 3, PL 1805, 02044 VTT,
puh. vaihde (09) 4561, faksi (09) 456 7004

VTT Bygg och Transport, Material och produkter, Kemistvägen 3, PB 1805, 02044 VTT,
tel. växel (09) 4561, fax (09) 456 7004

VTT Building and Transport, Materials and Products, Kemistintie 3, P.O. Box 1805,
FIN–02044 VTT, Finland
phone internat. + 358 9 4561, fax + 358 9 456 7004

Technical editing Maini Manninen

Tummavuoren Kirjapaino Oy, Vantaa 2001

Holt, Erika E. Early age autogenous shrinkage of concrete. Espoo 2001. Technical Research Centre of Finland, VTT Publications 446. 184 p. + app. 9 p.

Keywords concrete, shrinkage, fresh concrete, volume change, measuring methods, tests, modeling

Abstract

Volume change of concrete resulting from structural and environmental factors is an acceptable phenomenon. In the majority of cases this volume change, or shrinkage, is assumed to begin at the time of loading or drying. In reality, a volume change commences immediately after the cement and water come in contact during concrete mixing. These early age volume changes are typically ignored in design of concrete structures since their magnitude can be much less than shrinkage resulting from drying. But even when the concrete curing conditions are ideal, the first day shrinkage can significantly contribute to the ultimate shrinkage and thus the cracking risk.

The goal of this work was to establish a clearer understanding of the mechanisms causing autogenous shrinkage of concrete during the early ages. Autogenous shrinkage is a volume change resulting when there is no moisture transfer to the surrounding environment. It is most prominent in high strength, or high performance concrete where the water-to-cement ratio is under approximately 0.42. Autogenous shrinkage at later ages has been well documented and explained by self-desiccation behavior but the presence of autogenous shrinkage during the first day of concrete hardening has not been theoretically explained.

This work aimed at developing a test method to assess the shrinkage occurring immediately after mixing the concrete and continuing for the first 24 hours. Once a test method was established it was possible to investigate the chemical and physical phenomena causing the autogenous shrinkage in the first hours for neat paste, mortar and concrete. The shrinkage was well correlated to the cements' chemistry and the development of internal capillary pressure within the cement paste. Material parameters influencing the magnitude of the early age autogenous shrinkage were studied, such as the use of superplasticizer and different cement types. The three factors most significantly contributing to the autogenous shrinkage were identified as the concrete's chemical shrinkage, amount of bleeding, and time of hardening. Finally, a generalized model was proposed for reducing early age autogenous shrinkage in future practice.

Preface

This publication is based on work done from 1997 - 2001 for the degree of Doctor of Philosophy from the University of Washington in Seattle, Washington, USA. All laboratory testing was done in the Building and Transport Institute of VTT, the Technical Research Centre of Finland.

"[Cement paste] will obey the general law of gel formation and contract in volume. It is convenient to refer to this type of shrinkage as 'autogenous shrinkage' to distinguish it from others which are due to thermal causes or loss of moisture to the air."

– C.G. Lynam 1934

Contents

1. Introduction

Concrete is a vital component of our infrastructure and society, from roads to buildings. Its durability is essential in preserving resources and maintaining a sound construction system. The majority of material durability issues are focused on later ages, when the concrete has gained adequate strength. This includes standard drying shrinkage in which the concrete loses water to the environment and undergoes a volumetric change. Such drying shrinkage contributes to the material's performance due to induced stresses that may facilitate deterioration, such as curling of pavement slabs or cracking in facade elements. At early ages, the tensile capacity of the concrete is lowest therefore posing the greatest risk of material faults such as cracking. Early age drying shrinkage can be eliminated by proper handling and curing techniques to prevent moisture loss and provide time for the material to strengthen. In practice, actual measurements of this early age shrinkage are rarely obtained due to difficulty in measuring and lack of standardization.

Even without exact measurements there are still visual observations of concrete shrinkage on a construction site. This includes the occurrence of concrete cracking soon after casting even though adequate measures were taken to prevent shrinkage. For instance, the Denver airport runways had noticeable concrete cracks 7 days after placing though curing techniques were as specified, with a continuous water spraying system. These occurrences can be attributed to an additional type of concrete behavior: autogenous shrinkage.

Autogenous shrinkage is defined as a concrete volume change occurring without moisture transfer to the environment. It is merely a result of the internal chemical and structural reactions of the concrete components. The contribution of autogenous shrinkage has previously been viewed as "insignificant" in typical concrete mixtures due to the dominant role of drying shrinkage. In recent years the increasing use of high performance concretes has lead to the re-introduction of autogenous concerns as the mixtures are using more "special" cements and multiple admixtures while reducing water. The combination of a variety of material properties provides a basis for evaluating and quantifying the contribution of early age autogenous shrinkage to the total performance of concrete.

This work aims at establishing the factors that contribute to early age autogenous shrinkage. Background information is provided to relate autogenous volume changes to other shrinkage types and to define the different shrinkage stages. Laboratory testing of autogenous shrinkage is correlated to chemical shrinkage measuring and modeling based on cement composition. These tests and models provide a basis for a new method to predict the likelihood of early age autogenous shrinkage.

2. Background

Concrete shrinkage is of increasing concern when focusing on maintaining durable structures. Over time, the shrinkage induces cracking which can severely decrease concrete life expectancy. These volume changes are often attributed to drying of the concrete over a long time period, though recent observations have also focused on early age or plastic drying problems. At early ages the concrete is still moist and there are difficulties in measuring the fluid material. These difficulties have hindered comprehensive physical testing and understanding of the factors influencing plastic shrinkage. The most common solution to reduce early age volume changes is to avoid drying by proper handling of the concrete for the first few hours after placement. It is imperative that the concrete curing begins immediately and follows correct methods. [Holt 2000]

A supplementary problem to drying shrinkage at early ages is the change that occurs when no moisture transfer is permitted with the environment. This volume reduction is called *autogenous shrinkage* and is attributed to chemistry and internal structural changes. Autogenous shrinkage is usually a concern in high strength or high performance concrete (> 40 MPa or 6000 psi) where there is a low water-to-cement (w/c) ratio. Overall, early age concrete shrinkage is of increasing concern, as it can be responsible for cracking when the concrete has not gained significant strength to withstand internal stresses.

Shrinkage of concrete takes place in two distinct *stages*: early and later ages. The early stage is commonly defined as the first day, while the concrete is setting and starting to harden. Later ages, or long term, refers to the concrete at an age of 24 hours and beyond. During this later stage the concrete is demolded and standardized shrinkage measurements are conducted. The long-term shrinkage is typically the only part that is identified and addressed in literature, as well as being the portion that is accommodated in structural design.

Within each of these two stages of shrinkage there are also various *types* of linear change which can be physically measured on a specimen, mainly drying and autogenous. Both of these types can occur during either shrinkage stage. In addition to drying and autogenous shrinkage, the concrete is also subjected to volume reductions due to thermal changes and carbonation reactions. Both thermal and carbonation shrinkage are noted here, though they are not as

significant as the other two and their full analysis is outside the scope of this work. The shrinkage types are mapped in Figure 2.1 and will be further described in the following sections.

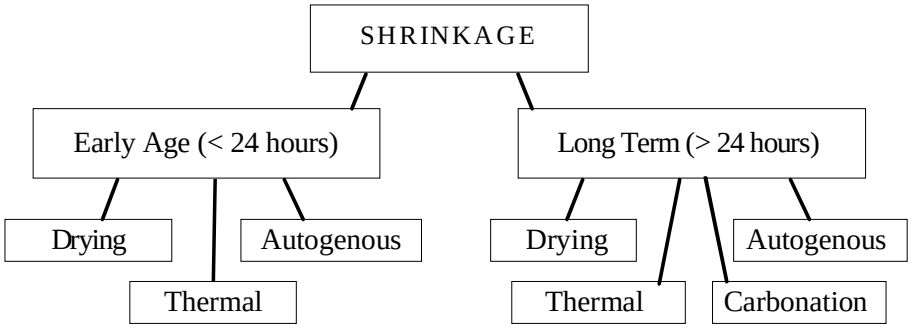

Figure 2.1. Diagram of shrinkage stages and types.

2.1 Shrinkage Stages

2.1.1 Early Age Shrinkage

The exact definition of "early age" changes depends on the context and time frame of the measurements. In this work early age shrinkage is defined as the volume changes occurring immediately after concrete placing up to the age of about 24 hours. This includes the time when the concrete is fluid or liquid, then the transition period when it is undergoing early stiffening by the formation of a skeletal frame, and finally the initial hardening when the concrete is rigid and the formwork or molds can be removed. For high strength concrete, the rigid or hardening period usually starts about 12 hours after mixing and the early age shrinkage rate is minimal at the onset of this phase. "Plastic shrinkage" refers to the volume changes occurring during the very first hours within the early age reactions, while the concrete is still fresh in the liquid and skeleton formation stages. The breakdown of these early age phases is shown in Figure 2.2.

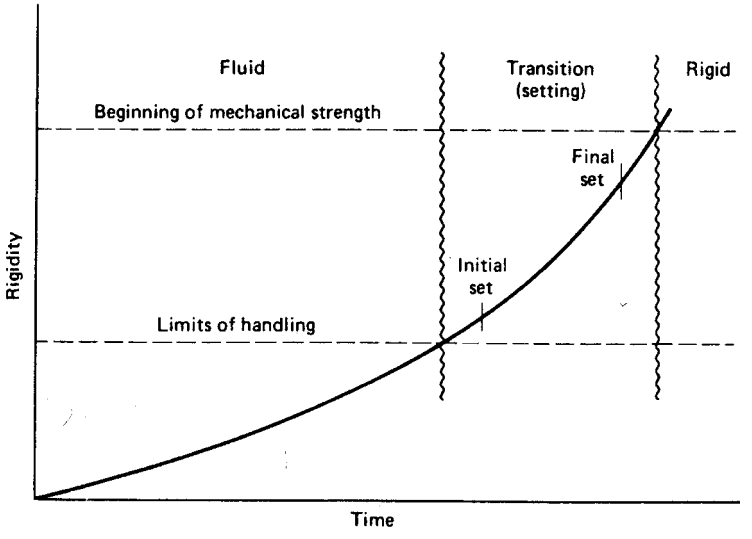

Figure 2.2. Early age shrinkage phases: liquid, hardening transition with setting, and rigid hardening. [Mehta & Monteiro 1993]

Shrinkage of concrete is due to the movement or loss of water. As water is lost to either evaporation (drying shrinkage) or internal reactions (autogenous shrinkage), tensile stresses are generated. These stresses pull the cement paste closer together which registers as a volume reduction. During the early ages shrinkage is even more critical since the concrete still has not gained much strength. Even the smallest stress during the early age can have large resulting shrinkage strains.

The internal capillary system in the hydrated paste also affects the concrete shrinkage. In summary, any changes to the paste will result in a variation in the total concrete shrinkage during both the early and late ages. The stages of the early age reactions are elaborated on in the next sub-sections.

2.1.1.1 Liquid Phase

Immediately after the concrete is mixed it is still a liquid. During this liquid concrete phase there is no structure to hold the body firmly in place. Any movement due to applied stresses will be immediately corrected by a shift in the position of the body. For instance, in a fluid mixture the larger aggregate particles may settle and excess bleed water will move to the concrete surface.

2.1.1.2 Skeleton Formation Phase

After the cement and water have begun to react, a skeleton will form as a result of the hydration products. This typically occurs a couple hours after the mixing of the concrete.

During this skeletal phase the setting time will also occur due to the stiffening of the concrete. The setting time can be delayed by either the surrounding environment or by additions to the concrete which affect the chemical reactions. It has been shown by Justnes et al. [2000] that setting time of pastes increased with an increased w/c ratio. Other admixtures, such as some superplasticizers, may also have a secondary affect of retarding setting. This has been shown by other VTT research [Holt & Leivo 1996] and is detailed in Table 2.1. Brooks et al. [2000] also showed that setting time of high strength concrete is affected by increasing amounts of mineral admixtures, such as silica fume, fly ash, ground granulated blast-furnace slag and metakaolin. His research found that setting time was not affected by using a shrinkage reducing admixture (SRA) alone but the SRA combined with mineral admixtures such as silica fume had a delayed setting time.

Table 2.1. Delay of concrete setting time with addition of melamine-based superplasticizer. w/c = 0.45 in all mixtures. [Holt & Leivo 1996]

SP Dosage (%)	Setting Time (hr:min)	
	White Cement	Gray Cement
0	4:10	3:40
0.5	4:20	3:50
1.0	6:00	4:30
1.5	7:30	5:00

The setting time is also highly dependent on the concrete's surrounding environment and specifically the temperature. This was also demonstrated in a VTT research project on drying shrinkage [Holt & Leivo 2000] and is shown in Table 2.2.

Table 2.2. Influence on concrete final setting time due to change of curing temperature.

Temperature (°C)	Setting Time (hr:min)
5	11 +
20	5:30
30	4:20

2.1.1.3 Hardening Phase

Once the skeleton is well established the concrete often has sufficient strength during the early ages to resist additional stresses. The rate of additional drying or autogenous shrinkage will be slowed as the concrete can withstand these driving forces. This point when the concrete can usually withstand the drying shrinkage forces is approximately 2 hours after the initial setting time. Work by Kronlöf and others [1995] at VTT noted this phenomena and it was validated by Holt [2001] as shown in Figure 2.3 for a concrete subjected to a drying environment. In some cases if there is not enough strength to resist the forces than cracking will occur.

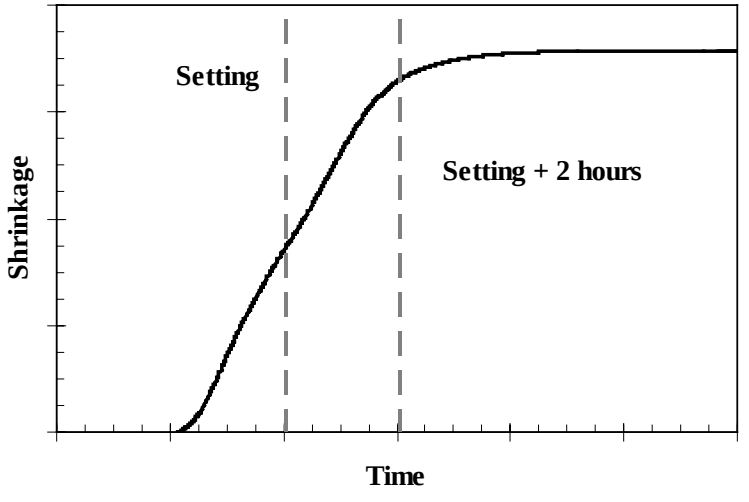

Figure 2.3. End of early age drying shrinkage due to hardening of concrete after initial setting time. [Holt 2001]

Once the concrete has hardened it will still continue to have volume changes for a very long period as the cement is still slowly reacting. The progress of a cement reacting until it reaches its full potential is referred to as the *degree of hydration*, α. This is depicted in Figure 2.4 for cement paste, where the cement particles are continuing to react with each time step (left to right). [Kronlöf 1999] As the hydration proceeds the porosity, or empty voids, within the paste are consumed. The pores will have a smaller diameter and there will be a decrease in the total volume of pores, as shown in Figure 2.5 [Young 1974]. This typically leads to decreased permeability and increased strength and durability of the cement paste.

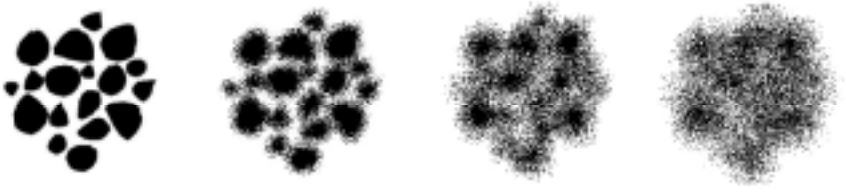

Figure 2.4. Typical advancement of cement paste hydration with time (left to right), resulting in decreased porosity. [Kronlöf 1999]

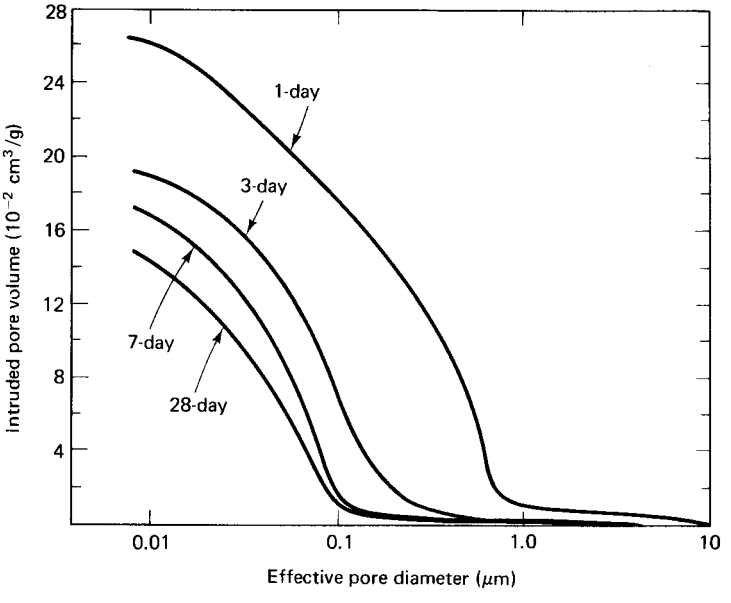

Figure 2.5. Mercury intrusion porosimetry curves for portland cement paste, showing pore diameters and volume with hydration. [Young 1974]

For normal strength concretes (~ 5,000 psi or 35 MPa) the ultimate hydration of α approaching 1, or 100%, is reached after many years. In high strength concrete the hydration may not be able to continue due to a lack of water, which is necessary for the complete cement reaction. In such a case the degree of hydration may only proceed until α is << 1 (i.e. α_{max} = 0.5 at a w/c = 0.21). [Powers 1968]

2.1.1.4 Relation to Other Processes

The shrinkage of concrete in the early stages can be examined in the same terms as ceramic manufacturing. Ceramics, like concrete, are created from gels consisting of a very small fraction of suspended solids. These gels undergo a phase transformation where the material loses its fluidity and appears as an elastic solid. This is attributed to either drying or internal chemical reactions. Drying during the "plastic" stage involves liquid transfer through the pores due to evaporation. The internal reaction is called "syneresis" which is the action of "bond formation or attraction between particles inducing contraction of the network and expulsion of liquid from the pores." [Brinker et al. 1990] Many of the same principles of gel shrinkage during drying are the same as concrete behavior: where the cement paste loses water and contracts. In both situations an internal capillary pressure creates stresses to induce volume changes. Syneresis of gels is analogous to autogenous concrete shrinkage where water is not allowed to evaporate from the specimen. The driving forces are dependent on internal chemistry, temperature, and other conditions such as sample size.

2.1.1.5 Tensile Strain Capacity

Early age shrinkage is a concern because it is during the early hours, immediately after casting, that concrete has the lowest strain capacity and is most sensitive to internal stresses. Work by Byfors in Sweden [1980] and Kasai in Japan [1972] has shown that concrete has the lowest tensile strength in these early hours. An example from Kasai [1972] is given in Figure 2.6, where the lowest point is reached at about 10 hours and then the tensile strain capacity again increases. Some other current research is focused on developing methods to quantify these magnitudes of concrete stresses within the first hours for various shrinkage loading. [Emborg 1989, Bjøntegaard 1999, Hedlund 1996]

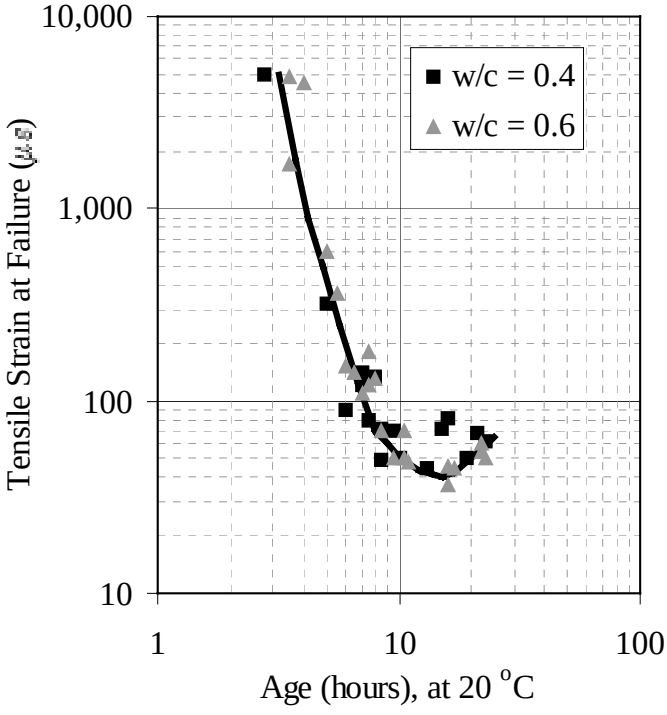

Figure 2.6. Decreasing tensile capacity during early ages. [after Kasai 1972]

Early age shrinkage can result in cracks that form in the same manner as at later ages. Even if the early resulting cracks are internal and microscopic, further shrinkage at later ages may merely open the existing cracks and cause problems. It is suggested by VTT and others that if the early age shrinkage magnitude exceeds 1000 με (1 mm/m) there is a high risk of cracking. [Uno 1998] This corresponds to the American Concrete Institute guidelines [ACI 209, 1997] of an expected shrinkage of about ¼ to ½ inch of movement in 20 feet, or 400 to 1000 με.

2.1.1.6 Driving Forces

The driving forces affecting early age shrinkage can be strongly influenced not only by material properties but also by the concrete's surrounding environment. For both autogenous and drying cases the environment should be monitored to account for shrinkage variations due to temperature, wind and relative humidity.

In the case of drying, all of these factors severely alter the amount of water evaporating from the concrete surface and thus the ultimate shrinkage amount.

2.1.2 Long Term Shrinkage

Long-term shrinkage has been well measured and accounted for in concrete practice for many years. It is generally measured from the starting point of 24 hours after the time of concrete mixing or placing; at the time of mold or formwork removal. It is measured on standardized prismatic specimens as a length change over time, according to standards such as ASTM C157 or RILEM CPC 9.

Drying shrinkage can continue for many years, though it is generally expected that about 80% of the laboratory-measured shrinkage occurs within about 3 months. The duration of shrinkage is dependent on the concrete's size and shape since they control the rate of moisture loss. The size and shape are often considered together as the volume-to-surface area ratio. Larger specimens will shrink for longer periods but the ultimate magnitude may be lower. This extended period is in accordance with the CEB-FIP model code predictions, as given by Equation 1 [1990].

$$\varepsilon_S(t,t_0) = \varepsilon_{S0}[\beta_S(t) - \beta_S(t_o)] \qquad (1)$$

where: ε_{SO} = basic shrinkage coefficient, = $\varepsilon_1 \times \varepsilon_2$,
ε_1 = factor depending on the environment,
ε_2 = factor depending on, h_o,
h_0 = notional thickness, depending on specimen size and ambient humidity,
β_S = factor for shrinkage development with time, depending on h_o,
t = concrete age, adjustable if temperature is different from 20 °C, and
t_0 = age when drying starts.

A high volume-to-surface ratio will usually result in lower shrinkage magnitudes, as shown in Figure 2.7. [Mindess & Young 1981] Also shown here is the example of a T-beam compared to a solid beam with the different volume-

to-surface ratios. If the two beams have equal widths and heights, the T-beam will dry more rapidly and will exhibit slightly less ultimate shrinkage since it has the lower volume-to-surface ratio. The faster drying is attributed to the shorter diffusion path for water to travel to reach an equivalent relative humidity through the cross-section.

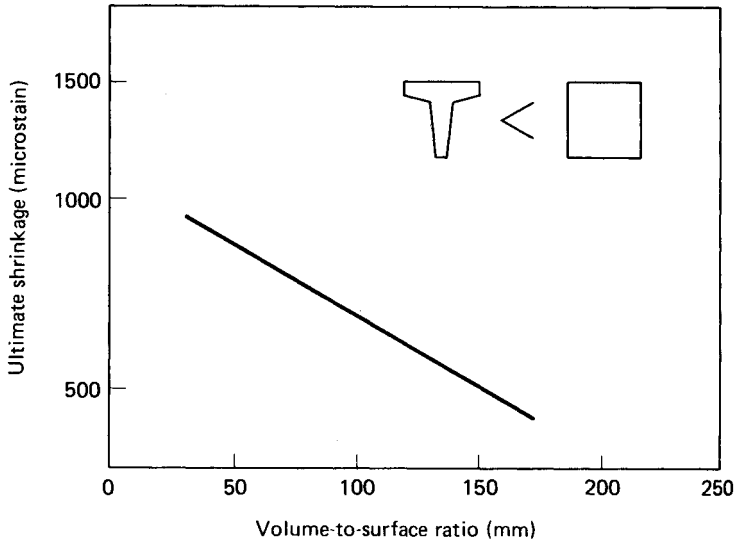

Figure 2.7. Effect of volume-to-surface ratio on the drying shrinkage of concrete. [Mindess & Young 1981]

When concrete is restrained by reinforcing, the subgrade, or other structural elements the concrete shrinkage will not be able to proceed freely. This long term "restrained shrinkage" will be less than the "free shrinkage" of an unrestrained sample. It can be measured by a ring-test that exerts restraint on a concrete donut by an interior metal ring of high rigidity. Ring tests generally will induce cracking and allow for the comparison of various concrete mixtures. A restrained ring test is not standardized but must be designed for each case to model a specific type of restraint. [Holt 1998, Grzybowski & Shah 1990]

There is also a concern with stress relaxation of concrete when addressing the early age reactions. *Stress relaxation* is the loss of stress over time with a constant level of strain in the concrete. The strain is generated by shrinkage

forces but during the early ages it is difficult to account for any mechanisms providing a means of stress relaxation.

There is no correlation between the magnitudes of early age and long term shrinkage. The shrinkage occurring during these two stages should be taken together as the "total shrinkage" for a concrete. In some cases, such as poor curing conditions with rapid drying, the first day's shrinkage can easily exceed the long-term measurements. This is demonstrated in Figure 2.8 for various environmental conditions during the first day. [Holt 2001] The long-term shrinkage due to drying was equivalent in all cases, though the first day had a significant change to the magnitude of "total shrinkage" and thus affected the expected cracking.

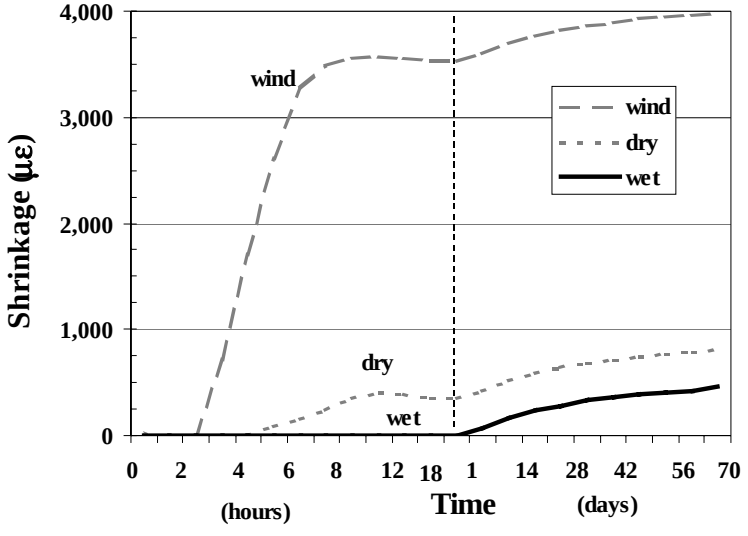

Figure 2.8. Accumulation of early age and long term shrinkage, with various curing environments during the first day. Wind = 2 m/s (4.5 mph), dry = 40% RH, wet = 100% RH. [Holt 2001]

It has also been shown that the first day curing conditions do not affect the shrinkage occurring at later ages. Figure 2.9 is an example of such testing, where the first day had both wet and dry curing (autogenous and drying shrinkage). After 1 day of curing the slabs were again stored in different curing conditions of wet or dry. The slabs with either type of curing during the first day had equivalent amounts of drying shrinkage at a later time. This proves that the

magnitude of additional drying shrinkage starting at 1 day is unaffected by the curing conditions of the early age. [Holt 2001]

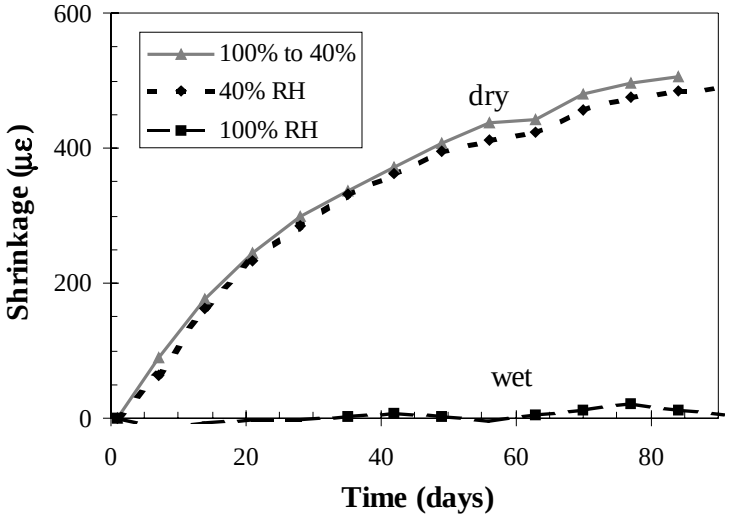

Figure 2.9. Variation in long term shrinkage depending on first day curing conditions. (wet = 100% RH, dry = 40% RH). [Holt 2001]

2.2 Shrinkage Types

Concrete volume change is an unavoidable phenomenon resulting from the materials *drying* in their exposed environment as well as their *autogenous*, or internal, reactions. Shrinkage is most often evaluated over a long time period of months or years, with the earlier plastic state changes deemed insignificant. In the next sub-sections thermal expansion and carbonation will be briefly addressed before getting into more details on the mechanisms of drying and autogenous shrinkage.

2.2.1 Thermal

Thermal dilation refers to the volume changes that occur when concrete undergoes temperature fluctuations. It is often referred to as thermal expansion, which is the portion resulting when the concrete temperature is rising. Dilation can occur due to heating or cooling, in both the early and late ages. When the

temperature is increasing the concrete will expand, followed by contraction with cooling. Thermal expansion causes problems when the rate of temperature change is too severe and when gradients exist over the concrete's cross-section.

During early ages the concrete temperature is changing due to cement hydration. As a general rule, this early heat of hydration is about 5 to 8 °C (10 - 15 °F) of adiabatic temperature rise per 45 kg of cement. [Kosmatka & Panarese 1988] Thus a mortar mixture will have much greater amount of heat generated compared to a concrete mixture since it is richer in cement. The heat rise typically occurs in the first 12 hours as long as no extreme retarding conditions exist. The next stage where the concrete is cooling results in a contraction or shrinkage. Some of the thermal expansion is elastic since the concrete will return to its original dimensions upon subsequent cooling. But any non-elastic portion will result in early age shrinkage.

The gradient resulting from uneven temperatures will cause strains and may result in cracking. During the early ages, differential temperatures within a concrete specimen cause thermal strains as the exterior surface will have a different temperature (due to environmental exchanges) than the interior. The gradient develops when temperature equilibrium cannot be reached, thus generating stresses and risking cracking. This become even more of a risk with massive concrete structures (i.e. > 1 meter thick) since it takes much longer to obtain a temperature equilibrium.

Each concrete has a "thermal dilation coefficient" which is dependent on the individual material properties (such as aggregate and w/c). During early ages the thermal dilation coefficient is changing very rapidly as the concrete grains strength. Research by Hedlund [1996] in Sweden has provided early age measurements of the thermal coefficients of concrete with time, as shown in Figure 2.10. These tests are supplemented with results obtained by Weigler, and Alexanderson [Byfors 1980], providing even higher values in the first hours. The thermal dilation coefficient reaches a platform of approximately 12 με/°C (12 x 10^{-6}/°C) after 24 hours. For comparison, the thermal expansion coefficient of water at 23 °C is 237 με/°C and even much greater for water vapor . [Kell 1967]

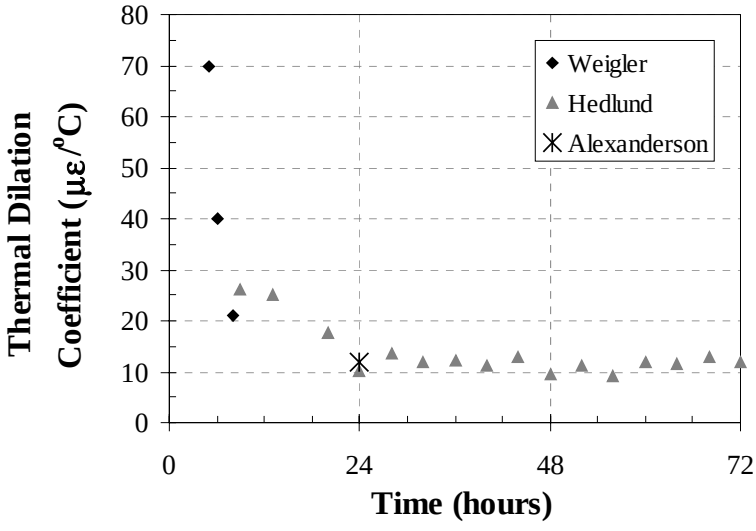

Figure 2.10. Early age thermal dilation coefficients for concrete. [Hedlund 1996, Byfors 1980]

In the later ages, thermal dilation is typical a result of temperature fluctuations in the surrounding environment. Again, the concrete may crack if the rates of expansion or contraction are too severe. These changes are somewhat dependent on the amount of free water in the concrete since the water needs to expand during ice formation with freezing. Thermal expansions can also be a problem if the concrete is restrained in any manner and there is no space for the volume change to occur, such as a large restrained slab without joints.

Later age thermal dilation is a measure of how much the concrete will have a reversible volume change with temperature fluctuations. The typical values of the thermal dilation coefficient for mature concrete are from 6 to 12 με/°C. [Mehta & Monteiro 1993] Typical values for mature concrete made from Finnish materials (cement and aggregate) are given in Table 2.3. [Jokela et al. 1980] These are in agreement with Hedlund's predictions at the age of 24 hours.

Table 2.3. Coefficient of thermal expansion for mature concrete made from Finnish materials. [Jokela et al. 1980]

Aggregate-Cement Ratio	Coefficient of Thermal Expansion (με/°C)
Cement Paste	18.5
1	13.5
3	11.2
6	10.1

2.2.2 Carbonation

Carbonation occurs when cement paste in the hardened concrete reacts with moisture and carbon dioxide in the air, in accordance with Equation 2. [Mehta & Monteiro 1993] This results in a slight shrinkage and a reduction in the pH of the concrete. Lowering the pH can be detrimental to other forms of deterioration, primarily corrosion of reinforcing steel. The corrosive rust can cause expansion, cracking and spalling of the concrete. [Kosmatka & Panarese 1988]

$$H_2CO_2 + Ca(OH)_s \rightarrow CaCO_3 + 2H_sO \qquad (2)$$

The amount of carbonation is dependent on the concrete density and quality but is usually limited to 2 cm (0.8 in) of depth on the exposed surface. The amount is dependent on the age and the surrounding environmental conditions.

Carbonation is generally considered a durability issue that takes a long time, in the order of many years, to affect a concrete structure. Therefore, it is outside the scope of this work and will not be discussed further here.

2.2.3 Drying

Drying shrinkage refers to the reduction in concrete volume resulting from a loss of water from the concrete. As the water is lost the concrete will shrink. Initially, free water escapes to the concrete surface as bleed water, as the heavier aggregate particles settle. This bleed water can evaporate off the surface to the surrounding environment. Once the bleed water has disappeared the concrete

will still be subjected to drying and excess water will be pulled from the interior of the concrete mass. The most common situation resulting from drying shrinkage at early ages is the appearance of surface cracking. [Mindess & Young 1981] There can also be a problem with internal stresses or cracking due water suction into the formwork and/or sub-base material.

The drying mechanisms causing shrinkage are dependent on the internal pore spaces. The description of the various pore sizes is diagramed in Figure 2.11 along with the solid particles of the hydrated cement paste. The capillary voids are the spaces once occupied by excess water that was removed during the cement hydration reactions. In Figure 2.11 the most prominent size of capillary voids will shift towards the smaller size of 0.01 μm (from 1 μm) when the paste has a denser microstructure.

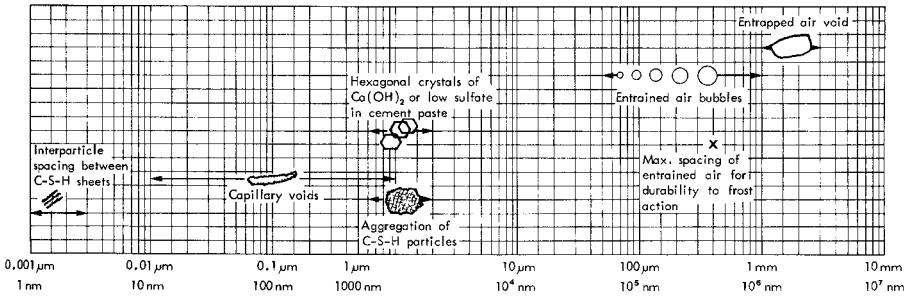

Figure 2.11. Distribution of solids and pores in hydrated cement paste. [Mehta & Monteiro 1993]

A cement paste's *microstructure* is the portion of the concrete which cannot be viewed naturally (< 200 μm) and is examined with the use of microscopes. With equivalent amounts of cement in a paste mixture, the microstructure will become denser as the w/c is lowered. [Mehta & Monteiro 1993] Therefore, it is expected that high strength concrete will have a denser microstructure composed of smaller pores and a lower total pore volume compared a standard mixture. This improvement in the cement paste's microstructure leads to reduced permeability and thus improved durability characteristics.

A finer microstructure also can result from altering the concrete ingredients, such as including silica fume. Silica fume, or microsilica, refines the pore

structure by subdividing the larger pores but maintaining nearly the same total pore volume. [Lea 1998]

When concerned with drying of concrete, the larger pores are the first ones to lose their internal water. This is demonstrated by Koenders [1997] in Figure 2.12.

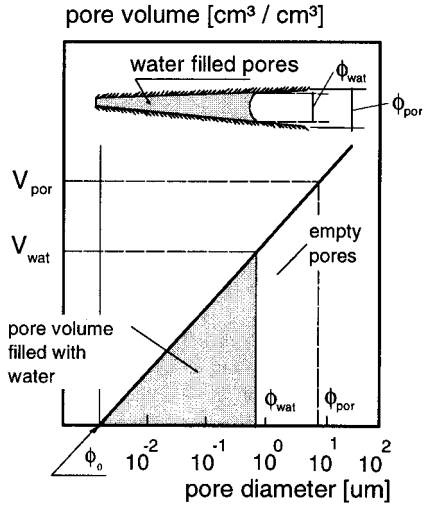

Figure 2.12. Schematic representation of the pore size distribution with emphasis on the state of the pore water within the total pore volume. [Koenders 1997]

The interaction of the pore spaces and internal water is influenced by the moisture movement, such as rising bleed water. During drying of fresh concrete the evaporation rate can exceed the amount of bleed water rising to the concrete surface. The free surface from which extra water is lost will then migrate into the concrete body as evaporation continues. The loss of internal water causes the drying shrinkage. Powers [1968] has clearly stated how the water surface is changing and how this relates to the pore spaces:

> "the liquid surface become converted to myriad curved surfaces (menisci), which are concave between the particles. Since the fluid pressure on the convex side of a meniscus is less than on the concave side, that is, less that the pressure of the atmosphere, the difference constitutes a motive force in

addition to gravity driving the topmost particles downward. The curvature of the water surface is limited by the dimensions of the interstitial spaces among the particles at the surface."

This phenomenon is shown in Figure 2.13 for two cement particles at the surface of a paste subjected to drying. [Radocea 1992] In this case the evaporating water (W) exceeds the bleed water moving to the surface from within the concrete. This generates stress and causes the meniscus to be lowered with the increasing the capillary pressure.

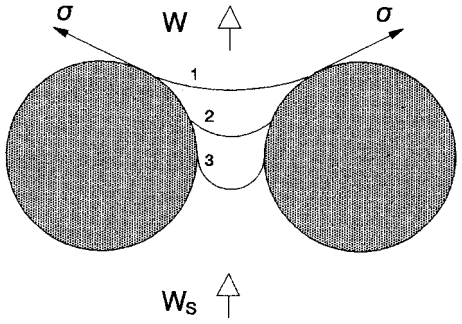

Figure 2.13. Stresses pulling the water meniscus lower between two cement particles due to moisture transfer and capillary pressure development. [Radocea 1992]

The amount of pore water pressure, or suction, which will be generated in the concrete paste is due to the capillary forces. In turn, the capillary force is a function of the radius of curvature of the resultant meniscus between the water and air. This suction, s, is given by the Laplace equation (Equation 3) [Janz 2000]:

$$s = \frac{2\sigma}{r} \tag{3}$$

where: s = suction pressure (Pa),
σ = surface tension of air-water interface (~0.074 N/m), and
r = meniscus radius (m).

As the diameter of the capillary decreases, the capillary pressure (and therefore the shrinkage) increases accordingly. [Czernin 1980] The capillary pressure is on the order of 10 to 100 MPa due to the moisture changes. [Scherer 1999]

Another useful relation for interpretation of the effect of the pore sizes is given by Kelvin's equation (Equation 4). [Janz 2000] Here the relative humidity existing within a body is correlated to the size of the capillary pore. It is shown that as the pore size decreases the internal relative humidity quickly drops, which will in-turn induce stress and shrinkage. The Kelvin relation is graphically shown in Figure 2.14, with a logarithmic scale on the x-axis for the pore radius and an assumed temperature of 20°C (68°F).

$$\ln \phi = -\frac{2\sigma M}{\rho R T r} \tag{4}$$

where: ϕ = relative humidity,
M = molecular weight of water (18 kg/Kmol),
ρ = density of water (998 kg/m^2),
R = gas constant (8,214 J/(Kmol°K),
T = temperature (°K), and
r = pore radius (m).

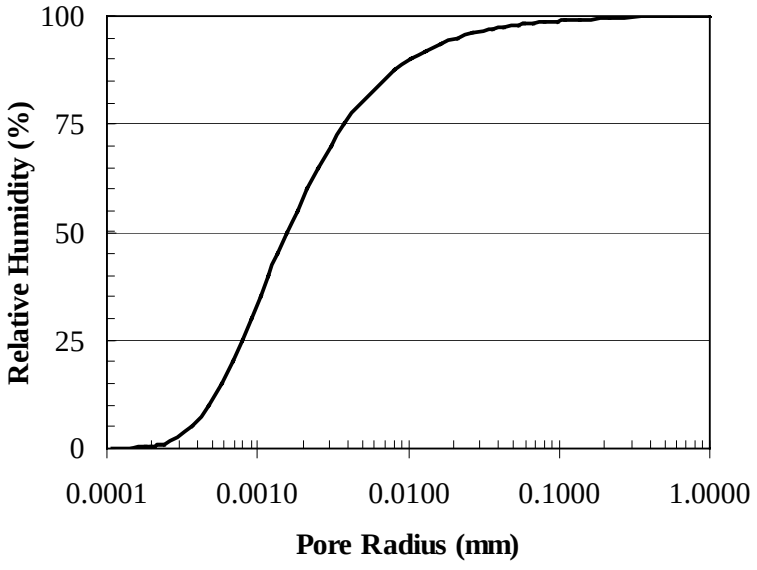

Figure 2.14. Relation of relative humidity dependence on empty pore radius, based on Kelvin's equation at T = 20 ℃.

The Laplace and Kelvin equations can be combined to show the relation between the relative humidity and the pressure, as given in Equation 5. [Janz 2000] This is also graphically depicted in Figure 2.15, where the pressure drastically increases with a decrease in humidity. This is useful when understanding how a change in internal humidity of the concrete will create greater stresses within the system. It is these stressed which lead to shrinkage.

$$\ln \phi = \frac{sM}{RT\rho} \tag{5}$$

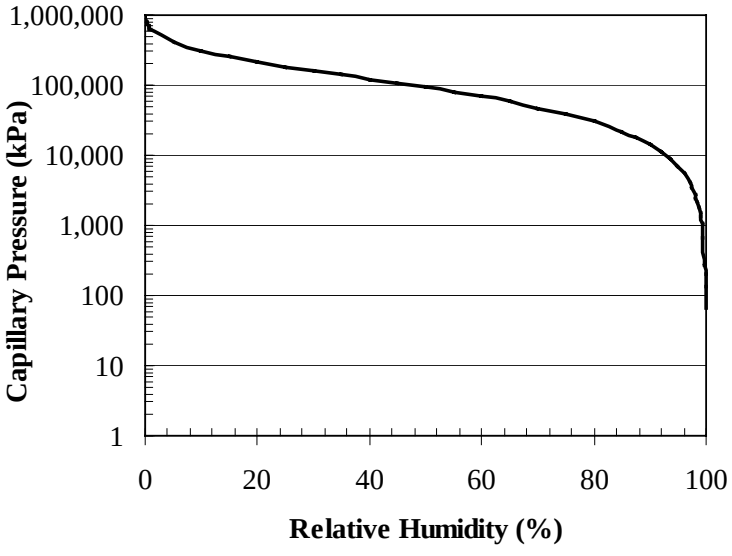

Figure 2.15. Relation of relative humidity and pressure (suction) based on combination of Laplace and Kelvin equations.

A final measure of the amount of stress induced by emptying pores can be shown by a rise in capillary water height. This capillary water height is a function of the pore radius, as given by Washburn [1921] in Equation 6. As the radius decreases the capillary water height increases drastically. This again means there is an increase in stress and thus shrinkage.

$$h = \frac{2\sigma \times \cos\alpha}{r \times \rho \times g} \tag{6}$$

where: h = height of capillary rise,
α = contact angle between the water surface and pore wall, and
g = acceleration due to gravity.

Drying shrinkage magnitudes are highly dependent on the amount of water lost and the rate of evaporation. If the bleeding rate exceeds the evaporation rate this excess water will act as a curing blanket. In this case there will be no drying shrinkage since there is enough water on the surface to allow for evaporation without drawing extra water from the internal capillary pores.

Shrinkage is typically measured on a linear scale, with the conversion of directional measurements to total volume change given in Equation 7. Linear drying shrinkage values are on the order of 500 to 1000 με (0.5 to 1 mm/m) over a long duration but can exceed 5000 με (5 mm/m) during some cases, included accelerated drying during early ages.

$$VolumeChange = 1 - \left(1 - \frac{shrinkage}{length}\right) \tag{7}$$

Part of the long term drying shrinkage can be reversible, in that the concrete will swell upon subsequent re-wetting.

2.2.4 Autogenous

2.2.4.1 Definitions and History

Autogenous shrinkage of cement paste and concrete is defined as the macroscopic volume change occurring with no moisture transferred to the exterior surrounding environment. It is a result of chemical shrinkage affiliated with the hydration of cement particles. [Japan 1999]

A graphic depiction of a sealed concrete's composition change due to the cement hydration reactions is given in Figure 2.16 [Japan 1999]. This bar graph related how the autogenous shrinkage is a portion of the chemical shrinkage. While the chemical shrinkage is an *internal* volume reduction, the autogenous shrinkage is an *external* volume change. It is therefore possible to measure autogenous shrinkage as a linear change on a concrete slab or other similar arrangement.

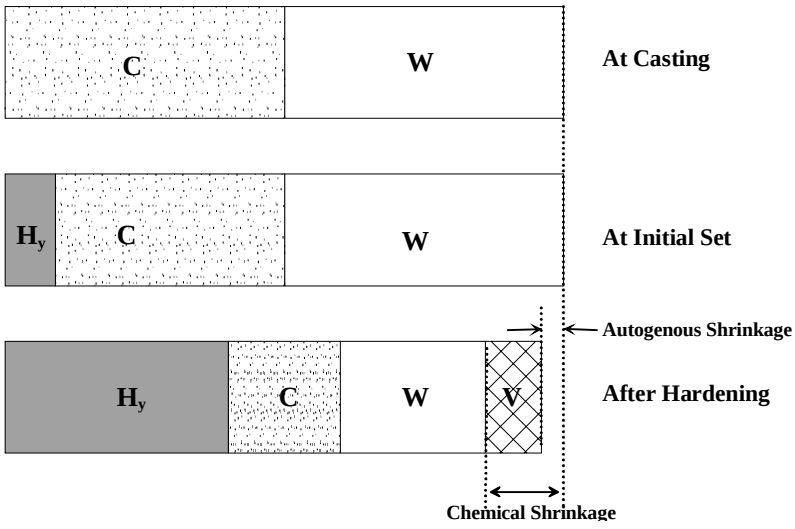

Figure 2.16. Reactions causing autogenous and chemical shrinkage. [Japan 1999] C = unhydrated cement, W = unhydrated water, H_y = hydration products, and V = voids generated by hydration.

The factors influencing the magnitude of autogenous shrinkage are often disputed. It is agreed that autogenous shrinkage cannot be prevented by casting, placing or curing methods, but must be addressed when proportioning the concrete mixture. It appears that the internal components or ingredients have the most significant influence, as will be discussed in upcoming paragraphs. This volume change has been given a variety of labels, some of which include: autogenous deformation, chemical shrinkage (both total and external), volume contraction, Le Chatelier shrinkage, bulk shrinkage, indigenous shrinkage, self-desiccation shrinkage, and autogenous volume change. [Justnes et al. 1996]

Autogenous shrinkage has only recently been documented and accurately measured. It was first described in the 1930's [Lyman 1934] as a factor contributing to the total shrinkage, which was difficult to assess. In these earlier days autogenous shrinkage was noted to occur only at very low water-to-cement ratios that were far beyond the practical range of concretes. But with the development and frequent use of modern admixtures, such as superplasticizers and silica fume, it is much more realistic to proportion concrete susceptible to autogenous shrinkage. Today we often have greater structural demands for high strength and high performance concretes. This leads engineers and designers to specify concrete with lower w/c ratios, much beyond the limitations of the

1930's. Even though many strength and durability aspects are now improved with these specifications, the risk of autogenous shrinkage is greater.

Autogenous shrinkage occurs over three different stages, as described in Section 2.1.1 and Figure 2.2, within the first day after concrete mixing: liquid, skeleton formation, and hardening. After the hardening stage the concrete shrinkage can be measured using more standard long term measuring practices. During the first day it is necessary to clearly define the mechanisms that are generating the autogenous shrinkage in these three stages.

2.2.4.2 Liquid Stage

Immediately after mixing water and cement, a chemical shrinkage change will occur due to the reduction in volume of the reaction products. In this early phase while the concrete is still liquid the autogenous shrinkage is equivalent to chemical shrinkage. The definitions of chemical shrinkage and the descriptions of the mechanisms driving it will be described in Section 2.2.5.

2.2.4.3 Skeleton Formation Stage

The point when autogenous shrinkage changes from being a function of chemical shrinkage versus self-desiccation is a function of the degree of cement hydration. *Self-desiccation* is defined as the localized drying of the concrete's internal pores and will be further described in the next stage (Section 2.2.4.4). At the point when a skeleton is formed due to the stiffening of the paste the concrete can resist some of the chemical shrinkage stresses. Soon after this initial skeleton formation the concrete will set, as earlier described in Section 2.1.1. During this stage the capillary pressure will start to develop and may cause shrinkage. This pressure mechanism works as the water, or meniscus, is moving between the pores. As the water is lost from subsequently smaller pores, the water meniscus will continue to be pulled into the capillary pores and will generate more stress on the capillary pore walls. This is similar to the phenomena described by Radocea in Figure 2.13 (Section 2.2.3) for drying shrinkage and it again causes a contraction in the cement paste.

The changes occurring during the skeleton formation are demonstrated in Figure 2.17 [Acker 1988] and were experimentally confirmed by Norwegian research

[Justnes at al. 1996]. As described in the previous paragraphs, when the concrete is still liquid immediately after mixing the autogenous shrinkage is proportional to the degree of hydration (section AB in the figure). This means the autogenous shrinkage is due only to chemical changes. Once a skeleton has formed the chemical shrinkage becomes more and more restrained (Section BC). Beyond point C the material is rigid and autogenous shrinkage is comprised of less and less chemical shrinkage. The further volume reductions are only due to self-desiccation. [Boivin et al. 1999] This changes during the hardened stage where the shrinkage is a result of a lowering internal relative humidity will be described in Section 2.2.4.4.

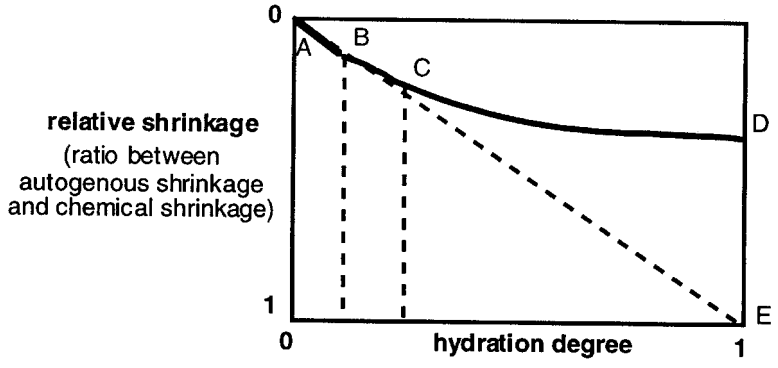

Figure 2.17. Schematic evolution of autogenous shrinkage as a function of hydration degree. [Acker 1988]

These changes in the driving force of autogenous shrinkage over time have also been well documented by Norwegian researchers Hammer [1999] and Justnes et al. [1996]. The Norwegians have simultaneously conducted volumetric tests of chemical shrinkage (bottle test)[1] and autogenous shrinkage (thin rubber membrane test)[1] on cement paste, as shown in Figure 2.18. Here it can clearly be seen that once a skeleton starts to form at approximately 5 hours the autogenous shrinkage diverges from the chemical shrinkage. But during the very early hours the autogenous shrinkage can be fully attributed to the chemical changes due to cement hydration. This will be further discussed in Section 2.2.5.

[1] Test procedures are elaborated on in Sections 2.3 and 5.

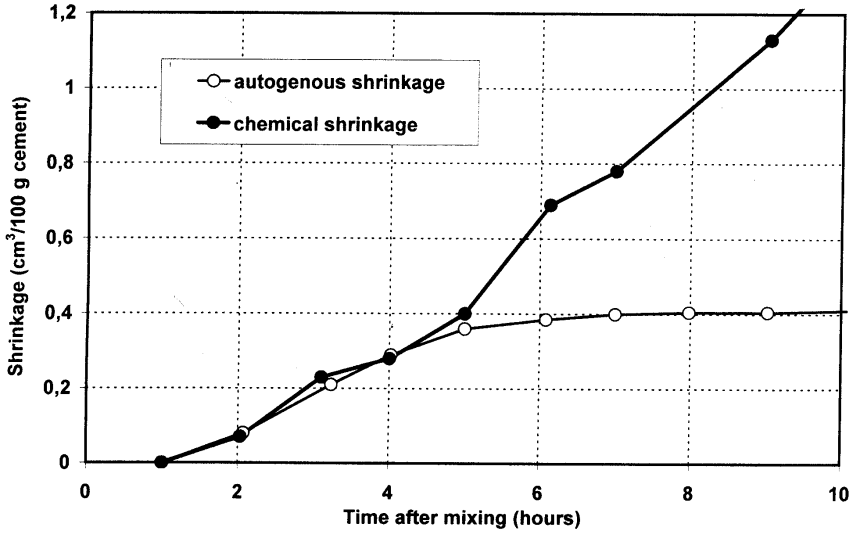

Figure 2.18. Chemical shrinkage by bottle test and volumetric autogenous shrinkage by thin rubber membrane test. Cement paste with water-to-binder ratio of 0.40 and 5% silica fume. [Hammer 1999]

2.2.4.4 Hardened Stage

Once concrete has hardened with age (> 1+ day), the autogenous shrinkage may no longer be a result of only chemical shrinkage. During the later ages the autogenous shrinkage can also result from self-desiccation since a rigid skeleton is formed to resist chemical shrinkage. Self-desiccation is the localized drying resulting from a decreasing relative humidity. The lower humidity is due to the cement requiring extra water for hydration.

In a high strength concrete with a low w/c ratio, the finer porosity causes the water meniscus to have a greater radius of curvature. These menisci cause a large compressive stress on the pore walls, thus having a greater autogenous shrinkage as the paste is pulled inwards.

Self-desiccation occurs over a longer time period than chemical shrinkage and does not begin immediately after casting. It is only a risk when there is not enough localized water in the paste for the cement to hydrate; thus the water is drawn out of the capillary pore spaces between solid particles. This would

typically begin after many hours or days in high strength (low w/c ratio) concretes. At later ages, a strong correlation exists between internal relative humidity and free autogenous shrinkage, as shown in work by Baroghel-Bouny (Figure 2.19). [1996]

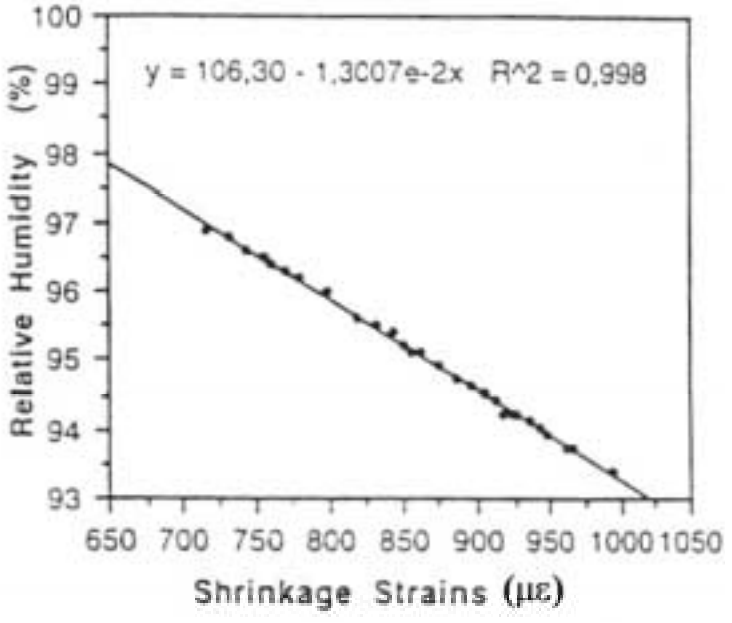

Figure 2.19. Correlation between free autogenous shrinkage strains and internal RH of the materials, measured at T = 21 °C, from 28 days. [Baroghel-Bouny 1996]

Historic research by Powers & Brownyard [1948] showed that autogenous shrinkage due to self-desiccation occurs when the w/c ratio is below 0.42, since all mixing water is consumed at this ratio. This w/c limit can vary from 0.36 to 0.48 [Taylor 1997], depending on the cement type, but the most common ratio cited in literature is 0.42. [Neville 1978, Mindess & Young 1981] The lower values (i.e. 0.38) assume there is an unrestricted supply of water available during curing. When the w/c ratio is much lower than 0.42 and can no longer gain curing water, the cement will seek extra water from the internal pores and thus lower the relative humidity.

Recently, these guidelines of greater long-term autogenous shrinkage occurring at lower w/c ratios have been supported by French research [Baroghel-Bouny

1996]. Baroghel-Bouny has shown that with a decreasing w/c ratio the 28-day autogenous shrinkage of cement paste increases, as shown in Figure 2.20. Tazawa and Miyazawa [Tazawa & Miyazawa 1995c] attribute this to the denser paste microstructure.

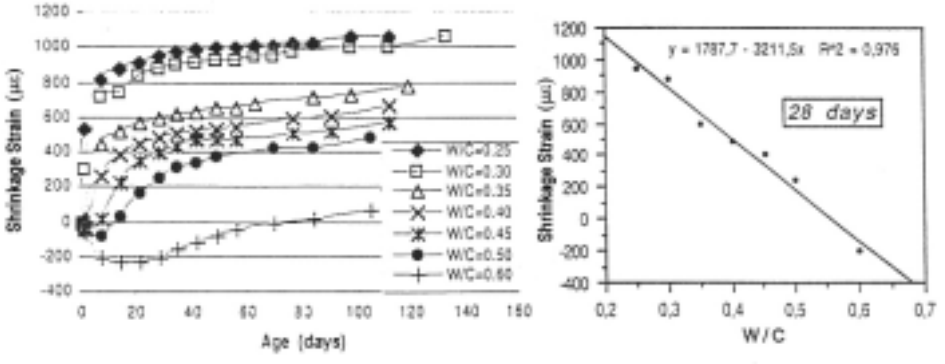

Figure 2.20. Correlation between autogenous strain and w/c ratio for cement pastes aged to 28 days. [Baroghel-Bouny 1996]

The use of mineral admixtures, such as silica fume, may also refine the pore structure towards a finer microstructure. If there is a finer pore structure the water consumption will be increased and thus the autogenous shrinkage due to self-desiccation will be increased. On the other hand, research by Kinuthia et al. [2000] has shown that the mineral admixture Metakaolin may reduce the autogenous shrinkage caused by self-desiccation by improving the particle size distribution and causing expansion that compensates shrinkage.

Work by Igarashi et al. [1999] has shown that adding aggregate to a mixture will decrease the amount of autogenous shrinkage. This seems reasonable, since the aggregates are rigid and cement paste is the portion of the mixture responsible for the shrinkage. His tests showed concrete shrinkage 30 to 45% less than the shrinkage corresponding to pastes at the age of a few days.

The draft European Standard prEN 1992-1 [Eurocode 2001] is the first to include a method for predicting long term autogenous shrinkage strain, as given by Equation 8. The strain is based on the cement type and compressive strength of the concrete.

$$\varepsilon_{cs} = \beta_{cc}(t)\varepsilon_{cs,\infty} \tag{8}$$

where: $\varepsilon_{CS,}$ = autogenous shrinkage strain,
$\beta_{CC}(t)$ = factor found using Equation 9,
$\varepsilon_{CS,\infty}$ = $2.5\,(f_{C'} - 10) \times 10^{-3}$, and
$f_{C'}$ = characteristic compressive cylinder strength of concrete at 28 days.

$$\beta_{cc}(t) = \exp\left\{ s\left[1 - \left(\frac{28}{t/t_1} \right)^{1/2} \right] \right\} \tag{9}$$

where: s = coefficient depending on the type of cement (s = 0.20 for rapid hardening high strength cements, 0.25 for normal and rapid hardening cements, and 0.38 for slowly hardening cements),
t = age of concrete (days), and
t_1 = 1 day.

In a high strength concrete element there will be no variation in the autogenous shrinkage magnitude over the cross-section or depth. Since the porosity is low and no excess curing water can infiltrate high strength concrete, the internal water will be evenly distributed after concrete hardening and reaching temperature equilibrium. The loss of internal water will be localized on a microscopic scale in the capillary pores and will not register as a change in autogenous shrinkage magnitudes. This is much different than drying shrinkage, where the amount of shrinkage is dependent on the moisture gradient across the element generated by uneven evaporation.

The measuring methods for autogenous shrinkage investigate the changes occurring in either cement paste, mortar or concrete. The material changes can be measured linearly, volumetrically or gravimetrically. Information regarding the shrinkage measuring methods is detailed in Section 2.3.

2.2.5 Chemical

2.2.5.1 Volumetric Changes

As earlier described, autogenous shrinkage is fully attributed to chemical shrinkage during the very first hours after mixing. The chemical shrinkage is a result of the reactions resulting between cement and water, which lead to a volume reduction.

Cement is the ingredient in concrete providing the chemical reactions to bind the mass. The basic reactions of cement clinker are well understood and generally defined by the following symbolic equations of the clinker phases [Paulini 1992, Lea 1998]:

C_3S: $2\,C_3S + 6\,H \rightarrow C_3S_2H_3 + 3\,CH$ (10)

C_2S: $2\,C_2S + 4\,H \rightarrow C_3S_2H_3 + CH$ (11)

C_3A: $C_3A + 6\,H \rightarrow C_3AH_6$ (12)

C_4AF: $C_4AF + 2\,CH + 10\,H \rightarrow C_3AH_6 + C_3FH_6$ (13)

Since chemical shrinkage is based merely on the volumes of initial and final products, it is possible to calculate it based on molecular weights. The general equation (Equation 14) for chemical shrinkage is given below. The complication with this calculation is that it is often difficult to know the exact volume of various components within the concrete without doing elaborate tests.

$$CS = \frac{(V_c + V_w) - V_{hy}}{V_{c_i} + V_{w_i}} \times 100 \quad (14)$$

where: CS = chemical shrinkage,
V_{Ci} = volume of cement before mixing,
V_C = volume of hydrated cement,
V_{Wi} = volume of water before mixing,

V_W = volume of reacted water, and
V_{hy} = volume of hydrated products.

Based on Boyles equation, Paulini [1996] has theoretically modeled the individual cement clinker components which influence the autogenous shrinkage (Figure 2.21). Paulini's model shows C_2S swelling during the first day, while all other components are shrinkage. This is likely due to the surface reactions of the C_2S and its polymorphic behavior. Paulini [1990] also attributed the swelling behavior to the presence of retarding agents, which slow the setting time. For the other components, C_3A reacts extremely fast during the first hours, while C_3S and C_4AF are much slower and gradual over many days.

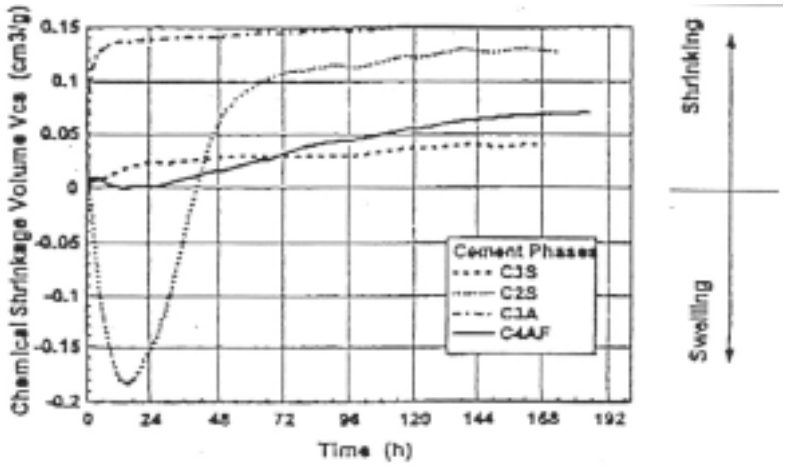

Figure 2.21. Model of cement composition influence on chemical shrinkage. [Paulini 1996]

Another way to view the chemical reactions is to mathematically examine the product volumes based on weight and density. As seen in Equations 10 to 13, each of the four cement clinker compounds requires water for reacting. These processes are exothermic and result in a decreased volume of the reaction products. This volume reduction, or chemical shrinkage, begins immediately after mixing of water and cement and the rate is greatest during the first hours and days. The magnitude of chemical shrinkage can be determined using the molecular weight and densities of the compounds as they change from the basic to reaction products. Table 2.4 shows the sample calculations for the C_3S

reaction, which is based on similar work by Paulini [1992] and Justnes at al. [1999].

Table 2.4. Reaction of C_3S during cement hydration.

	Mol. Wt. (g/mol)	Density (g/cm^3)	Mol. Vol. (cm^3/mol)	
2 C_3S	456.630	3.130	145.884	
6 H	108.089	0.998	108.284	
Basic Total	564.719		254.172	= V_b
$C_3S_2H_3$	342.443	2.630	130.207	
3CH	222.275	2.230	99.675	
Reaction Total	564.719		229.882	= V_r
			24.290	= V_s

The difference in the molecular volume of the basic (V_b) and reaction (V_r) products give the volume of shrinkage, V_s. Then it is necessary to relate the shrinkage volume to the original solid mass of the basic product (Equation 15):

$$V_{cs} = \frac{V_s}{M} = \frac{24.290}{456.630} = 0.0532 \text{ cm}^3/\text{g}, \quad \text{for } C_3S \tag{15}$$

All four of the individual phases can be calculated in the same manner. Then each factor is used in a full equation to predict chemical shrinkage of cement. Table 2.5 gives the 4 chemical shrinkage values for each cement phase. [Paulini 1992] These are then used in Equation 16 to estimate the total amount of chemical shrinkage, using the percentage of each phase.

Table 2.5. Chemical shrinkage values for individual cement phases. [Paulini 1992]

Chemical Shrinkage (cm^3/g)	
C_3S	0.0532
C_2S	0.0400
C_4AF	0.1113
C_3A	0.1785

$$V_{CS\text{-}TOTAL} = 0.0532\,[C_3S] + 0.0400\,[C_2S] + 0.1113\,[C_4AF] + 0.1785\,[C_3A] \quad (16)$$

From both of these examples of Paulini modeling or mathematical calculations, it is shown that the cement chemistry will affect the autogenous shrinkage due to the varying chemical shrinkage in the very early ages. For instance, if a cement has a high a C_3A content it is expected that there will be greater shrinkage than a comparable cement with lower C_3A. Some compounds also work together, such as C_2S and C_3S. Cement with high C_2S content usually has a corresponding lower C_3S content. This combination of a higher C_2S and lower C_3S would result in an overall lower shrinkage than the reference cement.

Chemical shrinkage of cement paste is not affected by the w/c ratio. [Gangé et al. 1999] The w/c ratio and cement fineness will only affect the rate of the chemical shrinkage. The final magnitude of the shrinkage as the degree of hydration approaches 100% will only be influenced by the chemical composition of the cement.

It must be noted that Equations 10-13 were given as the very general approximations for the clinker reactions though they are known to be much more complex [Lea 1998, Taylor 1997]. Some of the reactions could be elaborated on and are described further in the Modeling work (Section 4).

In the above calculations there are also some discrepancies in literature regarding the densities used for the reaction products. For instance, $C_3S_2H_3$ has a density ranging from 2.44 to 2.63 g/cm^3. The discrepancies are due to the difficulties in measuring pure compounds. The assumed densities for various compounds are given in Appendix A, with their corresponding references.

2.2.5.2 Hydration

Another factor related to the chemical shrinkage of cement paste is the amount of the reaction that has occurred, known as the *degree of hydration*. It is understood that the chemical reactions begin immediately after mixing cement and water, but the actual chemistry of the cement can vary the amount of chemical shrinkage that has taken place. Since the autogenous shrinkage

deviates from the chemical shrinkage at some point (as shown by Hammer in Figure 2.18, Section 2.2.4.3), it is important to identify which clinker components will have reacted up to that point.

The 4 cement clinker compounds have different hydration rates when contacting water at the start of the mixing process. These degrees of hydration for both individual pure clinker compounds and for portland cement are presented by Lea [1998] and shown as Figures 2.22 and 2.23, respectively. The figures have different time scales on the x-axis and both represent degree of hydration on the y-axis, with 1 (or 100%) being the maximum.

When the individual clinker compounds, such as C_3A, are reacting in the presence of gypsum (C-S-H) the degree of hydration is much lower as a result of the early ettringite formation. This is seen in Figure 2.22 for the two different C_3A curves, where the gypsum contributes to the growth of ettringite crystals that block the hydration of C_3A. [Viirola & Raivio 2000] In Figure 2.23 the gypsum is included in the reaction of the portland cement so the amount of C_3A hydration is again lowered. The change in ultimate hydration of C_4AF from 40% to 90% in Figure 2.23 compared to 2.22 is also attributed to the presence of gypsum and the ettringite crystal growth.

For interpretation of chemical shrinkage at early ages, a combined figure of these two representations of hydration would be desirable. Figure 2.22 provides a time scale for the hydration to approach 90% while Figure 2.23 provides earlier time measurements (< 1 hour) and a better representation of C_4AF hydration. This will be further addressed in the Modeling section of this work. (Section 4)

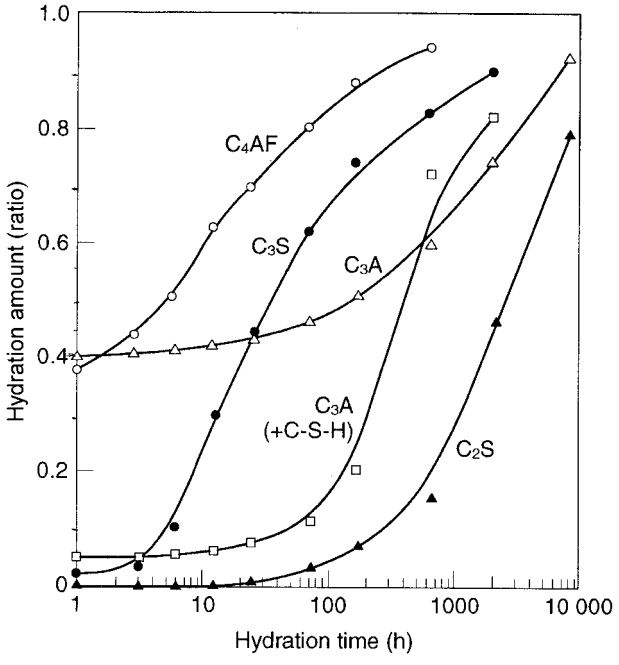

Figure 2.22. Typical hydration kinetics of pure clinker minerals (C_3A with and without added gypsum) - paste hydration at ambient temperature. Ratio of 1 = 100% hydration. [Lea 1998]

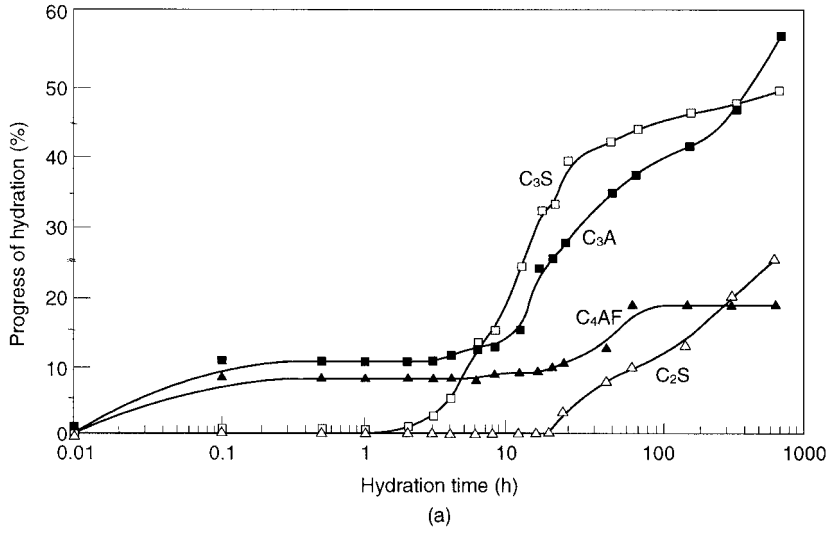

Figure 2.23. Hydration kinetics of an ordinary portland cement (paste hydration at ambient temperature). [Lea 1998]

Finally, the rate of chemical shrinkage will be affected by the fineness of cement. The hydration of a finer cement will proceed fast while a coarsely ground cement will have a slower hydration rate. This is due to the availability of water to infiltrate and react with the raw cement components. A cement's fineness will not affect the final magnitude of chemical shrinkage.

2.2.6 Total

Total shrinkage should be taken as the sum of each individual volume change due to carbonation, thermal expansion, drying and autogenous deformations. Since much of the thermal expansion is reversible at later ages, it is usually not included in the ultimate amount of total shrinkage. In practice, design codes are using an ultimate shrinkage value that is likely a measure of only the long term drying shrinkage. This is erroneous, since the early age shrinkage can sometimes equal or even exceed the standard long-term test. In addition, for high strength concrete where there is a w/c under approximately 0.42 there is a high probability of autogenous shrinkage contributing to the ultimate shrinkage.

In normal strength concrete where the w/c is greater than 0.42 autogenous shrinkage is often not detected. This is because the concrete has enough water to allow full hydration. In exposed concretes (slabs, floors, etc.), any excess water needed can often be obtained by re-absorption of bleeding or curing water since the high paste permeability permits water transfer. In some cases autogenous shrinkage can be eliminated [Radocea 1992] or swelling can be detected rather than shrinkage [Whiting et al. 2000], due to the imbibition of the curing water. This swelling would also offset the unavoidable chemical shrinkage that is always present. If curing water is not available or the w/c ratio is less than about 0.42 there are the risks of immediate harmful early age shrinkage.

It has been reported [Tazawa & Miyazawa 1995b] that the total shrinkage is composed of more and more autogenous shrinkage rather than drying shrinkage as the w/c ratio becomes smaller. (Figure 2.24) This means that at a low w/c all of the total shrinkage is attributed to autogenous deformation rather than drying shrinkage. All drying shrinkage measured on a standard beam would be a result of autogenous shrinkage. Figure 2.24 shows that at a w/c ratio of 0.40 the autogenous shrinkage is 40% of the total shrinkage magnitude, while at a w/c ratio of 0.23 it is equivalent to 80%.

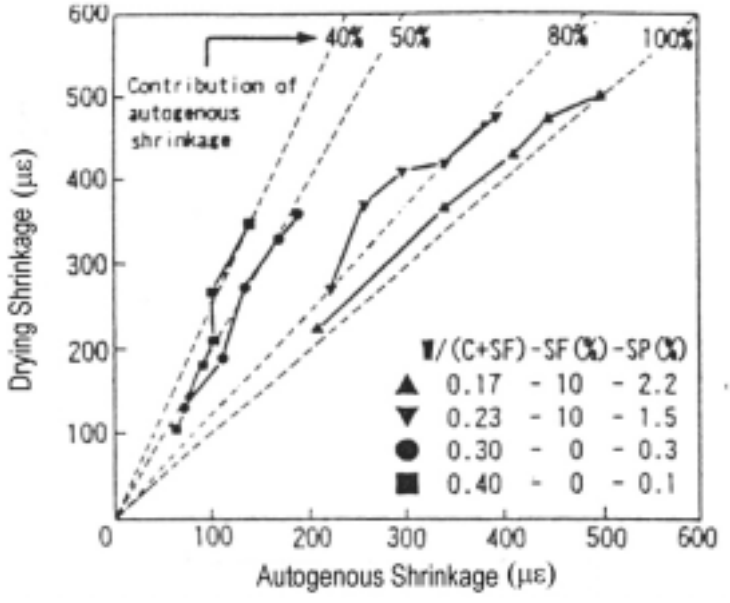

Figure 2.24. Ratio of drying to autogenous shrinkage with lowering w/c ratio. [Tazawa & Miyazawa 1995b]

It is understood that autogenous shrinkage cannot be avoided but in most cases it is assumed to be so small that it is deemed insignificant. In actuality, the exact proportion of these two shrinkage types, autogenous and drying, to the total shrinkage amount is still unknown in most cases, especially at early ages and in high-strength or high-performance concretes.

2.3 Measuring Methods

2.3.1 Early Age Shrinkage

Early age shrinkage measurements provide a challenge due to the difficulty in making accurate measurements of the concrete prior to demolding. The shrinkage must be measured immediately after casting in a mold which permits constant readings without disturbing the concrete.

ASTM C827 is the only standardized test to measure early age shrinkage of concrete. This method involves placing a steel ball on the surface of a fresh concrete cylinder and manually measuring the vertical displacement. This test

method is limited as only vertical movement can be measured, which is primarily a function of settlement. The actual horizontal contraction is not measured. This test is applicable for more fluid concretes that are filling a cavity, such as grout, and also shotcrete. The precision is specified at 2.5 mm and is recorded in 5-minute intervals.

There is no standardized method of measuring early age length change as there is for long term shrinkage (ASTM C157). The most practical measures of length change are done on a concrete slab simulating field situations such as floors or facades. These tests have been developed by work at VTT, the Technical Research Centre of Finland [Kronlöf et al. 1995, Leivo & Holt 1997, Holt & Leivo 1996], as well as others in Scandinavia and Japan [Radocea 1992, Mak et al. 1999, Bjøntegaard 1999, Hammer 1999, Tazawa & Miyazawa 1995a,b,c]

In these slabs both vertical (settlement) and horizontal shrinkage are measured, along with evaporation and capillary pressure. The slab holds 7.3 liters (0.25 ft^3) of concrete and the maximum aggregate size can be 32 mm. A temperature profile is also taken at 2 different depths, along with a simultaneous measure of setting time on a separate sample. Within the slab, a change in internal capillary pressure is the primary indicator of the start of autogenous shrinkage. The early age measurements begin immediately after concrete placing (approximately 30 minutes) and continue for 24+ hours. The horizontal shrinkage is measured by LVDTs over a length of 200 mm. More details about the slab test arrangement and data analysis methods can be found in the Procedures, Section 5.

Jensen and Hansen have devised a method for measuring linear autogenous shrinkage of cement paste. [Jensen & Hansen 1995] This method uses sealed soft plastic tubes that are partially fixed to a rigid frame. A transducer monitors the change in tube length over time, starting soon after casting but it does not allow for volumetric estimations.

If autogenous shrinkage measurements are done on cement paste alone, they can also be done using a flexible rubber membrane test. [Justnes et al. 1996, Hammer 1999] This method seals a sample in a thin latex membrane (condoms are typically used) and then takes the mass over time when the sample is continuously submerged in water. A schematic sketch is given in Figure 2.25. It is similar to the weighing methods for measuring chemical shrinkage (as

described in the next section) except the sample is encased and not allowed excess water for hydration. Therefore the autogenous shrinkage during the early ages is equivalent to the chemical shrinkage, but at later ages is due to self-desiccation.

The rubber membrane method is very sensitive since it can have no excess air pockets within the membrane. If there is any bleeding the membrane can stretch to form pockets of the excess water. This pooled water will later be re-absorbed after skeleton formation and will then register as a weight change, or autogenous deformation. [Bjøntegaard 2000] If the test is done with mortar rather than paste, there is the risk of breaking the rubber membrane with sharp aggregate particles and getting entrapped air. This trapped bleed water and air would yield to misevaluation of the shrinkage. [Gangé et al. 1999] If this test method is used it is critical that the sample be only cement paste and it should be continuously rotated to prevent pooling of bleed water. Otherwise the sample should be very stiff (with no workability) and non-segregating.

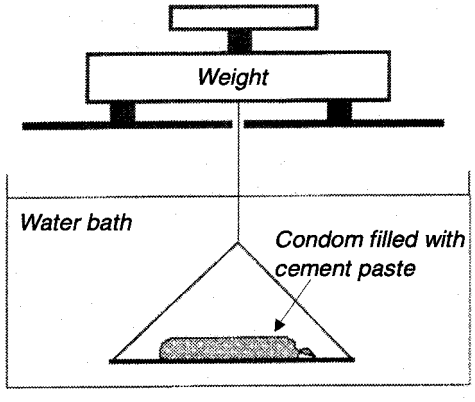

Figure 2.25. Flexible rubber membrane (condom) test for measuring theoretical autogenous shrinkage. [Bjøntegaard 2000]

2.3.2 Chemical Shrinkage

Le Chatelier [1900] was the first to report measurements of chemical shrinkage in cement by measuring the volume contraction of paste in a glass beaker connected to a water-filled tube. He assumed the contraction was due only to the contraction of the water. At a water-to-cement ratio of 0.40 he established the

amount of non-evaporable water to be dependent on the cement chemistry, as follows in Equation 17. In this equation the chemical shrinkage, CS, is given as ml/100 g cement and the cement clinker compounds are entered as percentages of the total cement content. With this equation normal portland cement has a chemical shrinkage of about 6 ml per 100 g cement, or approximately 9% of the volume of the hydrated products. [Gangé et al. 1999]

$$CS = 0.266(C_3S) + 0.194(\frac{C_2S}{0.982}) + 0.510(C_3A) + 0.097(C_4AF) + 0.149(CaSO_4) \qquad (17)$$

Another method to estimate chemical shrinkage was provided by Powers [1935] based on the individual shrinkage of the 4 clinker minerals: C_3S, C_2S, C_3A and C_4AF. As earlier noted, Power's & Brownyard's model [1948] showed that autogenous shrinkage occurs only below a w/c of 0.42 since all mixing water is consumed at this ratio. Powers theoretically calculated that 0.23 g of water would fully react with 1 gram of cement to get a chemical shrinkage of 5.9 ml/100 g of cement, which was in agreement with Le Chatelier's work. [Gangé et al. 1999]

Both of these methods by Le Chatelier and Powers have recently been elaborated on by many researchers [Tazawa & Miyazawa 1995a, Paulini 1992, Justnes et al. 1996, Gangé et al. 1999]. The early methods are now more easily investigated with modern technology allowing for more precise measurements of clinker minerals and their reaction products.

There have been two methods used to directly measure chemical shrinkage: dilatometry and weighing reduced buoyancy. Both of these methods include an external water source in contact with the cement paste sample. This is different than autogenous shrinkage tests previously described since then the samples were sealed to prevent moisture exchange with the surrounding environment.

The dilatometry test procedure follows Le Chatelier's principle where an Erlenmeyer flask containing a diluted cement paste sample is connected to a pipette from which the dropping water level is monitored. (Figure 2.26) It is a simple test procedure often used [Tazawa & Miyazawa 1995a] but requires manual reading from the pipette. The cement paste must be diluted to provide a high enough permeability for water to penetrate and saturate all of the capillary

pores. [Gangé et al. 1999] There is also the risk of faulty readings due to the fit of the pipette through a rubber stopper in the bottle top.

The weight method (reduced buoyancy) is a bit easier in the sense that it can be continuously measured and logged by computer. It was developed based on Archimedes principle that a water-submerged sample will register a volume reduction by a weight increase. The mass of the cement paste or mortar sample will lower as the cement hydration proceeds. This method has been applied by many researchers and is shown in Figure 2.27 [Boivin et al. 1999, Geiker & Knudsen 1982, Paulini 1992]. An excellent correlation between the two chemical shrinkage measuring methods has been shown in tests by Boivin et al. [1999].

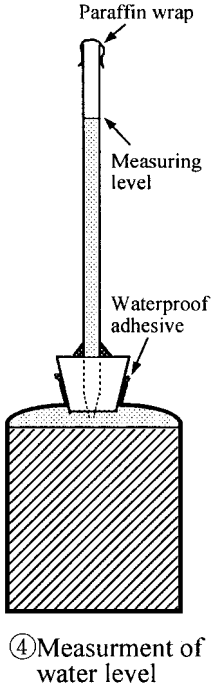

Figure 2.26. Dilatometry test arrangement. [Japan 1999]

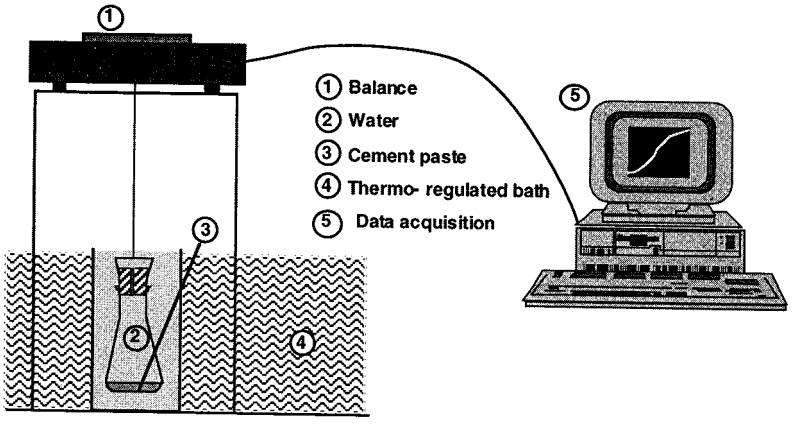

Figure 2.27. Reduced buoyancy test arrangement. [Boivin et al. 1999]

2.4 Autogenous Shrinkage - Summary

Autogenous shrinkage is defined as an external volume change occurring when no moisture is transferred to the surrounding environment. The existing explanations of autogenous shrinkage are based on the theories of cement hydration. In the very early stages after mixing the cement is consuming water and the hydration products require a smaller volume than the individual compounds. This reaction is termed *chemical shrinkage* and cannot be avoided in any cement paste. The rate and ultimate amount of chemical shrinkage are highly dependent on the cement type.

Autogenous shrinkage is also governed by the Kelvin and Laplace relations, showing how the capillary pressure forces the water meniscus farther between the pores and thus pulls the paste pore walls closer together. This shrinkage stress is dependent on the microstructure density and porosity, which are influenced by the materials used (such as silica fume, superplasticizer, etc.) and mixture proportions (such as w/c ratio).

In this work “early age” refers to the 24-hour period following concrete mixing. When measuring the chemical shrinkage it may be necessary to examine results over a longer time period (i.e. 72 hours) to more clearly see the trends resulting from material parameter adjustments.

At later ages the contribution of chemical shrinkage to autogenous shrinkage will slow as the concrete stiffens and can resist the shrinkage stresses. Still the autogenous shrinkage will continue as the cement tries to obtain extra water for hydration from the pore cavities. This internal drying resulting from the lowering internal relative humidity is termed *self-desiccation* and has been well measured by other researchers. It is already possible to predict long term autogenous shrinkage (due to self-desiccation) and account for it in design.

Currently there is a lack of knowledge regarding the contribution of chemical to autogenous shrinkage during the first day. There have been early age measurements of chemical shrinkage but the results are typically interpreted in reference to the ultimate value. Autogenous shrinkage has only been measured following standard long-term length change procedures (ASTM C157) and there is no established test method to assess early age length change. This is little, if

any, numeric results of autogenous shrinkage during the first hours after casting and no attempts have been made to correlate the chemical reactions to the autogenous deformations.

This work aims at explaining the phenomena driving early age autogenous shrinkage with respect to the chemical shrinkage and other mixture parameters.

3. Materials

The majority of tests in this work were done using cement paste or mortar, comprised of typical Finnish materials. The exact material properties are described in the following sub-sections.

3.1 Aggregate

3.1.1 Appearance and Size

Aggregate consisted of Finnish clean natural granite, with a density or dry rodded unit weight of 2670 kg/m^3 (167 lbs/ft^3). The fine aggregate was natural sand and the coarse aggregate had rounded particles. Absorption was approximately 0.1% and the material was batched in an air-dried state. One standard gradation was used for the mortar mixtures as given in Table 3.1, where the maximum aggregate size was 2 mm (0.08 in). The graphic depiction of the gradual increase in aggregate size fractions for the mortar gradation is given in Figure 3.1.

Table 3.1. Gradation of Finnish aggregate used in mortar mixtures.

Size (mm)	% Passing
4	100
2	96.3
1	67.8
0.5	41.6
0.25	29.0
0.125	11.6

One set of tests on the autogenous shrinkage of concrete had a maximum aggregate size of 10 mm. The gradation for this test is presented in Table 3.2 and again had an even distribution of size fractions (as was shown by Figure 3.1 for the mortar). The low amount of filler (< 0.125 mm) was used since the concrete mixtures had a high amount of cement.

Table 3.2. Gradation of Finnish aggregate used in concrete mixtures.

Size (mm)	% Passing
10	100
8	91.2
4	57.2
2	32.7
1	19.8
0.5	8.7
0.25	4.5
0.125	1.0

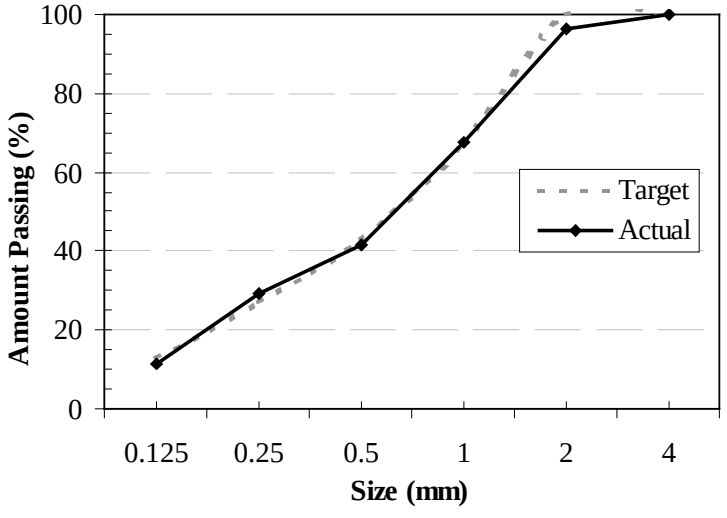

Figure 3.1. Gradation of Finnish aggregate used in mortar mixtures.

3.1.2 Absorption

The rate of water absorption was tested following Winslow's test method [1987] where a sample is suspended under water and continuously weighed until saturation at approximately 24 hours. The test was performed on 5 samples of size 5 to 10 mm aggregate with an oven dry weight of 420 g. A representative test result is shown in Figure 3.2 as a percentage of total water absorption with time (on a log scale). The test showed that over 60% of the water was absorbed

within the first 30 minutes, corresponding to the start of early age slab testing. Since the total absorption is also so low (0.1%), it is assumed that the remaining amount of water which would be absorbed by the aggregate would have an insignificant effect on the water amount available during the early age testing.

In the tests performed in this work the typical test specimen was cement paste or mortar with a maximum aggregate size of 2 mm. Therefore the aggregate absorption after 30 minutes becomes even less significant with these finer aggregate particles since there is a much greater surface area-to-volume ratio.

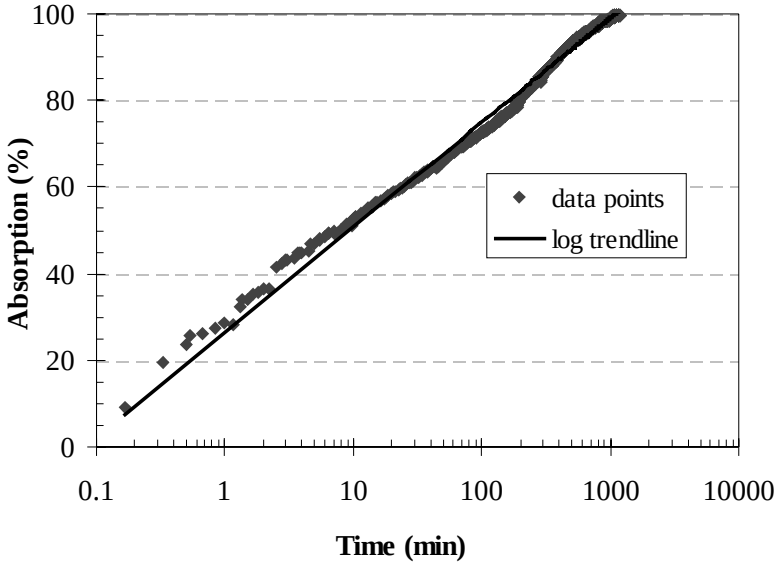

Figure 3.2. Winslow absorption of Finnish aggregate, maximum size = 10 mm.

3.2 Cement

The majority of tests in this work were done using Finnish rapid hardening cement since it is typically used in structural applications requiring high strength and/or high performance. The chemical shrinkage tests also used other Finnish cements to evaluate the variation in reaction rates and magnitudes due to the cements' chemical composition. In a few tests American cements were used for comparison.

3.2.1 Finnish Cements

Most of autogenous shrinkage testing was focused on using rapid setting cement, which is comparable to Type III cements in the USA. Rapid cement is commonly used for high strength and/or high performance products, such as in pre-cast facade manufacturing. The two most common hydraulic gray cements in Finland are named “Yleis” and “Rapid”, both of which are from either the Lappeenranta or Parainen manufacturing plants. Both of these cements are classified as “CEM IIA” and are made from the same clinker. The clinker is ground to two different levels, as shown by their Blaine fineness values, to vary the speed of reaction. The Yleis cement then has 15% inert material added, as blast furnace slag and limestone. There is also a slightly different amount of gypsum added to regulate the setting time. “Pika” is the third type of Finnish gray cement, which provides a higher strength, but it was not used in this work.

The other two cements often used in Finland are sulphate resistant (SR) cement and Danish white cement. The white cement is commonly used in architectural pre-cast facades. Table 3.3 provides the chemical breakdown of the three clinkers most commonly used in Finland, with Yleis and Rapid clinker only differing in how they are ground for the Blaine fineness. [Heikkilä 2000] Throughout this report these three will be referred to as “Finnish cements” though this actually means “used in Finland” since the white cement is produced in Denmark.

Table 3.3. Finnish clinker chemical composition and fineness. [Heikkilä 2000]

Compounds & Bogue	Cement Types and Composition (%)		
	Gray Yleis/Rapid	SR	White
CaO	65	65	71
SiO_2	21	21	26
Al_2O_3	4.5	3	2
Fe_2O_3	3	4.5	0.5
MgO	2	2	0.5
$K_2O + Na_2O$	0.5	0.3	-
SO_3 (gypsum)	3.5	3.3	2.2
C_3S	68	75	67
C_2S	10	5	23
C_3A	8	1	4
C_4AF	8	14	1
Blaine (m^2/kg)	380 / 440	330	400

The Finnish gray cement used in this work had a higher C_2S content than is normal for Finnish material. In most cases the range of C_2S is 5 to 8% and the Finnish cement manufacturers try to keep this level as low as possible. It is the goal of these manufacturers and the cement users to have faster reacting cement with higher early strength and therefore the C_2S is reduced. In this case with a higher C_2S, the cements' C_3S content in-turn decreases to a level slightly lower than normal. Another observation is the low 1% level of C_3A in the Finnish SR cement. It is expected that the normal level may be slightly higher than this reported value.

3.2.2 American Cements

American cements were obtained from various manufacturers around the United States using the recommendations of the Portland Cement Association. These materials were chosen based on the cements having a large range of C_3A contents (11, 6 and 4%). It was expected that there would be a good variation in the chemical shrinkage due to the cement chemistry. It was also anticipated that there would be no variation in the shrinkage due to the alkali (Na_2O) content or

Blaine fineness of the three cements since they are quite similar. The percentages of compounds and chemistries of the American cements used are shown in Table 3.4. In this work the American cements are referred to as “high”, “med” and “low”, corresponding to their C_3A amounts.

Table 3.4. Three American cement chemical compounds, percentages of each item.

Compounds & Bogue	Cement Types and Composition (%)		
	Hig Type I	Medium Type II	Low Type II / V
Source	New York	S. Carolina	Oregon
CaO	61.9	65.0	63.9
SiO_2	19.1	21.0	22.1
Al_2O_3	5.8	5.0	4.1
Fe_2O_3	2.2	4.1	3.9
MgO	2.4	1.2	2.9
Na_2O	0.45	0.30	0.44
SO_3 (gypsum)	3.6	2.5	2.1
C_3S	54.8	58.5	53.7
C_2S	13.5	16.1	22.7
C_3A	11.5	6.3	4.4
C_4AF	6.8	12.4	11.7
Blaine (m^2/kg)	369	382	386

3.3 Admixtures

In some cases chemical admixtures were added to the concrete mixtures to improve the mixture characteristics. This mainly included the use of superplasticizers to aid workability of the mixtures. The primary superplasticizer (SP) used was Rheo-Build, which is naphthalene-based, made by Masterbuilders Inc., and was provided by Finnsementti Oy in Finland. In one set of chemical shrinkage tests another superplasticizer was tested, SSP2000, which is polycarboxylate-based. SSP2000 is distributed by Grace Construction Products and sold by Finnsementti Oy in Finland. One test of concrete autogenous

shrinkage used a naphthalene-based superplasticizer, Superparmix, which is also sold by Finnsementti Oy.

A shrinkage-reducing admixture (SRA) was also used in one set of chemical shrinkage tests. The SRA used was Peramin, sold by the Perstorp Construction Chemicals company from Sweden. This chemical works by reducing the capillary tension of the pore water and can reduce long term drying shrinkage 20 - 50%. [Engstrand 1997]

No air entraining chemicals or mineral admixtures were used in any tests. In most cases the target fresh mixture properties were a slump of 50 mm and an air content of 3 %.

3.4 Water

Fresh clean tap water was used in all cases, which was at 20 ºC (68 ºF).

3.5 Mixture Designs

3.5.1 Chemical Shrinkage

The mixture designs used when testing chemical shrinkage of cement pastes and mortars are detailed in Tables 3.5 to 3.16. Mixtures in bold denote ones that are used in both the chemical and autogenous shrinkage tests.

Table 3.5. Mixture designs for pastes used in chemical shrinkage tests about Finnish cement types.

w/c	Chemical		Cement	Cement	Water
	(%)	Type	Type	(kg/m^3)	(kg/m^3)
0.25	1	Naph. SP	Rapid	1700	425
0.25	1	Naph. SP	White	1700	425
0.25	1	Naph. SP	SR	1700	425

Table 3.6. Mixture designs for pastes used in chemical shrinkage tests about American cement types.

w/c	Chemical		Cement	Cement	Water
	(%)	Type	Type	(kg/m^3)	(kg/m^3)
0.30	-	-	US – High	1560	470
0.30	-	-	US – Med.	1560	470
0.30	-	-	US - Low	1560	470

Table 3.7. Mixture designs for pastes used in chemical shrinkage tests about use of superplasticizer in gray cement.

w/c	Chemical		Cement	Cement	Water
	(%)	Type	Type	(kg/m^3)	(kg/m^3)
0.30	1	Naph. SP	Rapid	1560	470
0.30	-	-	Rapid	1560	470

Table 3.8. Mixture designs for pastes used in chemical shrinkage tests about use of superplasticizer in white cement.

w/c	Chemical		Cement	Cement	Water
	(%)	Type	Type	(kg/m^3)	(kg/m^3)
0.30	1	Naph. SP	White	1560	470
0.30	-	-	White	1560	470

Table 3.9. Mixture designs for pastes used in chemical shrinkage tests about use of different superplasticizer types.

w/c	Chemical		Cement	Cement	Water
	(%)	Type	Type	(kg/m^3)	(kg/m^3)
0.25	1	Naph. SP	Rapid	1700	425
0.25	1	SSP2000 SP	Rapid	1700	425

Table 3.10. Mixture designs for pastes used in chemical shrinkage tests about use of a shrinkage-reducing admixture.

w/c	Chemical		Cement	Cement	Water
	(%)	Type	Type	(kg/m^3)	(kg/m^3)
0.30	1	Naph. SP	Rapid	1560	470
0.30	-	-	Rapid	1560	470
0.30	1	SRA	Rapid	1560	470

Table 3.11. Mixture designs for pastes used in chemical shrinkage tests about effect of altering w/c ratio and no superplasticizer.

w/c	Chemical		Cement	Cement	Water
	(%)	Type	Type	(kg/m^3)	(kg/m^3)
0.30	-	-	Rapid	1560	470
0.35	-	-	Rapid	1440	505
0.40	-	-	Rapid	1340	535

Table 3.12. Mixture designs for pastes used in chemical shrinkage tests about effect of altering w/c ratio and superplasticizer.

w/c	Chemical		Cement	Cement	Water
	(%)	Type	Type	(kg/m^3)	(kg/m^3)
0.20	1	Naph. SP	Rapid	1860	370
0.25	1	Naph. SP	Rapid	1700	425
0.30	1	Naph. SP	Rapid	1560	470

Table 3.13. Mixture designs for paste and mortar used in chemical shrinkage tests about effect of aggregate restraint.

w/c	Chemical		Cement	Cement	Water	
	(%)	Type	Type	(kg/m^3)	(kg/m^3)	
0.35	-	-	Rapid	1440	500	Paste
0.35	-	-	Rapid	780	275	Mortar

Table 3.14. Mixture designs for mortars used in chemical shrinkage tests about use of Finnish cements.

w/c	Chemical		Cement	Cement	Water
	(%)	Type	Type	(kg/m^3)	(kg/m^3)
0.30	-	-	Rapid	915	275
0.30	-	-	Yleis	915	275
0.30	-	-	White	915	275
0.30	-	-	SR	915	275

Table 3.15. Mixture designs for mortars used in chemical shrinkage tests about effect of w/c and no superplasticizer.

w/c	Chemical		Cement	Cement	Water
	(%)	Type	Type	(kg/m^3)	(kg/m^3)
0.30	-	-	Rapid	915	275
0.35	-	-	Rapid	780	275
0.40	-	-	Rapid	685	275

Table 3.16. Mixture designs for mortars used in chemical shrinkage tests about effect of w/c and superplasticizer.

w/c	Chemical		Cement	Cement	Water
	(%)	Type	Type	(kg/m^3)	(kg/m^3)
0.25	1	Naph. SP	Rapid	1095	275
0.30	1	Naph. SP	Rapid	915	275
0.35	1	Naph. SP	Rapid	780	275
0.40	1	Naph. SP	Rapid	685	275

3.5.2 Autogenous Shrinkage

The mixture designs used when testing autogenous shrinkage of the cement pastes, mortars and concretes in the slab test are detailed in Table 3.17. The bold mixtures signify those that were also tested for chemical shrinkage.

Table 3.17. Mixture designs for autogenous shrinkage tests.

Type	w/c	SP	Cement Type	Cement (kg/m^3)	Water (kg/m^3)
Paste	**0.35**	-	Rapid	1440	505
Mortar	**0.30**	-	Rapid	915	275
Mortar	**0.35**	-	Rapid	780	275
Mortar	**0.40**	-	Rapid	685	275
Mortar	0.45	-	Rapid	915	275
Mortar	**0.30**	1%	Rapid	915	275
Mortar	**0.30**	-	Yleis	915	275
Mortar	**0.30**	-	White	915	275
Mortar	**0.30**	-	SR	915	275
Concrete	0.30	5%	Rapid	545	165
Concrete	0.35	2%	Rapid	505	165

4. Modeling

4.1 Chemical Shrinkage of Cement Pastes

The reaction of water and cement results in a decreased volume of the reaction product. This process was explained with Equations 10-13 in Section 2.2.5 for the basic cement clinker compounds reacting to form products with a decreased volume.

In literature there is typically only one reaction presented for C_3A, as listed in Equation 12 in Section 2.2.5 and repeated below. In reality this phase is undergoing 3 different changes in reaction products, with 2 reactions actual occurring prior to the basic one (Equation 18 and 19, before 12). The extra two reactions [Taylor 1997, Lea 1998] as well as the basic one are shown by the following equations:

$$C_3A + 3C\bar{S}H_2 + 26H \rightarrow C_6A\bar{S}_3H_{32} \quad (18)$$

$$C_6A\bar{S}_3H_{32} + 2C_3A + 4H \rightarrow 3C_4A\bar{S}H_{12} \quad (19)$$

$$C_3A + 6H \rightarrow C_3AH_6 \quad (20)$$

When estimating the chemical shrinkage during the early ages it is beneficial to account for these three different C_3A reactions. Each of the reaction products has a very different magnitude of chemical shrinkage, so to make an accurate estimate of early age shrinkage it is necessary to know the reaction rates of these products. Existing models in literature to predict chemical shrinkage do not account for these three different C_3A reactions. Therefore a model is presented here for the C_3A reactions and rates that will be used in the analysis of the test results in this work.

The assumption in this modeling that these reactions follow in such progressive steps is over-simplified because it assumes that all of the gypsum ($\bar{S}$ present in $C\bar{S}H_2$) will first react to form ettringite ($C_6AS_3H_{32}$) before the monosulphate (C_4ASH_{12}) reaction proceeds with the remaining C_3A. In reality these reactions

can occur simultaneously but without constant microscopic tracking it is not possible to identify the amount of each product that is occurring over time.

The first reaction of C_3A shown in equation 18 begins immediately after water contacts the cement and proceeds for the first hours. The C_3A is reacting with gypsum, which is almost always added to cement at about 5% by dry weight to regulate the setting time. [Lea 1998] The amount of gypsum is regulated by cement manufacturers and in these calculations is assumed to be consumed by 12 hours. The reaction product of the C_3A and gypsum is ettringite, $C_6AS_3H_{32}$, which has a much lower density than either the C_3A or gypsum.

Once the gypsum is consumed, the reaction proceeds as given by Equation 19, where the ettringite combines with extra C_3A and water to produce monosulphate, C_4ASH_{12}. Again, once all of the ettringite is consumed the production of monosulphate also ends. At this point the "basic" reaction remains, as given by Equation 12. In reality this phase may never be reached if the initial reactions of ettringite and/or monosulphate are not expired. It is therefore critical to consider these three individual C_3A reactions independently when evaluating the total magnitude of chemical shrinkage. The same calculations are presented in Tables 4.1 and 4.2 for ettringite and monosulphate, as were used for C_3S in Table 2.4 in Section 2.2.5. Table 4.3 then reveals the updated version of Table 2.5 (Section 2.2.5) and the final values used in forthcoming modeling. Assumptions made about the compound densities are provided in Appendix A.

Table 4.1. Reaction producing ettringite, $C_6A\bar{S}_3H_{32}$, during cement hydration.

	Mol. Wt. (g/mol)	Density (g/cm^3)	Mol. Vol. (cm^3/mol)	
C_3A	270.190	3.001	90.033	
3 $C\bar{S}H_2$	516.509	2.320	222.633	
26 H	468.385	0.998	469.229	
Basic Total	1255.084		781.896	= V_b
$C_6A\bar{S}_3H_{32}$	1255.084	1.780	705.103	
Reaction Total	1255.084		705.103	= V_r
			76.793	= V_s

$$V_{cs} = \frac{V_s}{M} = \frac{76.793}{270.190} = 0.2842 \quad \text{cm}^3\text{/g}, \quad \text{for } C_6A\bar{S}_3H_{32} \tag{21}$$

Table 4.2. Reaction producing monosulphate, C_4ASH_{12}, during cement hydration.

	Mol. Wt. (g/mol)	Density (g/cm^3)	Mol. Vol. (cm^3/mol)	
$C_6A\bar{S}_3H_{32}$	1255.084	1.780	705.103	
2 C_3A	540.380	3.001	180.067	
4 H	72.059	0.998	72.189	
Basic Total	1867.523		957.359	= V_b
$3C_4A\bar{S}H_{12}$	1867.523	1.990	938.454	
Reaction Total	1867.523		938.454	= V_r
			18.905	= V_s

$$V_{cs} = \frac{V_s}{M} = \frac{18.905}{1255.084} = 0.0151 \quad \text{cm}^3\text{/g}, \quad \text{for } C_4A\bar{S}H_{12} \tag{22}$$

Table 4.3. Final chemical shrinkage values for individual cement phases.

Chemical Shrinkage (cm^3/g)	
C_3S	0.0532
C_2S	0.0400
C_4AF	0.1113
C_3A – Ettringite	0.2842
C_3A Monosulphate	0.0151
C_3A - Extra	0.1785

4.2 Degree of Hydration for Compounds

To more accurately predict the chemical shrinkage at any time, it would be necessary to know which reaction phase is occurring at that specific point in the

hydration process. Then it would be possible to predict which of the four clinker phases is contributing the most to the chemical shrinkage magnitude at any given time. For this interpretation, the rate of chemical shrinkage is assumed to proceed along the same path as shown by the hydration rates of individual compounds.

The basic representations of cement and clinker degrees of hydration were given in Section 2.2.5 by Figures 2.22 and 2.23. Figure 2.22 for clinker hydration allowed the hydration to progress to nearly 100% at 10,000 hours while the portland cement representation including gypsum (Figure 2.23) limited hydration to 60% at the age 1,000 hours. The cement hydration figure also provided extra data of the hydration during the first hour, which is beneficial to this work when interpreting early age reactions. Therefore, a combination of these two figures was developed (Figure 4.1) which would account for the early ages and full hydration.

When combining the figures the C_4AF reaction represented in the cement hydration (Figure 2.23) was used since its degree of hydration will remain low when in the presence of gypsum and the other clinker minerals. The C_3A reaction was taken with gypsum (+C-S-H) from Figure 2.23 for clinkers. In this figure, the modeled dormant period occurring from about 0.5 hours to about 2 hours is too “flat” with no reactions taking place. In actual chemical shrinkage hydration it was seen that there are more steady reactions occurring but in Figure 4.1 they are assumed to follow the past work from Figure 2.22 and 2.23.

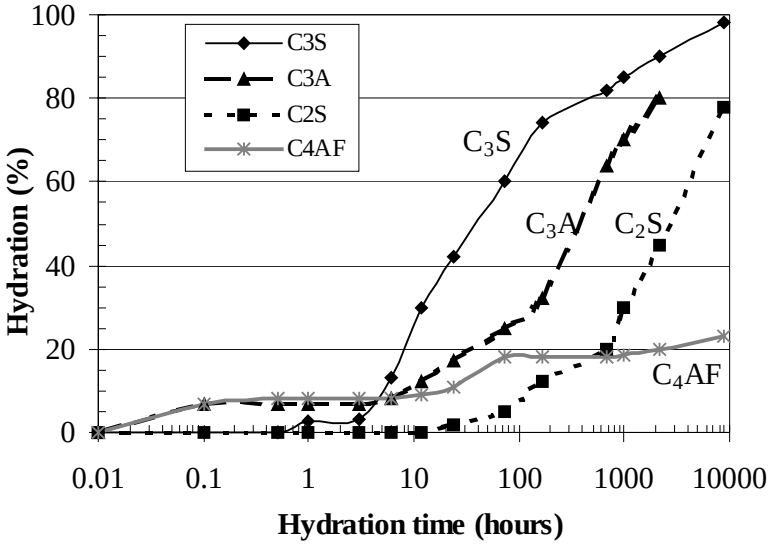

Figure 4.1. Combination of Figures 2.22 and 2.23 for cement degree of hydration of individual clinker compounds. (after [Lea 1998])

For the early age shrinkage analysis, some additional assumptions needed to be drawn when determining which reaction phase was occurring at various times. It was assumed that the amount of gypsum, SO_3 (or $\overline{S}$) added to each cement during clinker processing was based on the desire to achieve a final set of the cement paste at 12 hours. If this is true and all of the gypsum is then consumed in the first 12 hours, it would also be true that the ettringite reaction would stop at approximately 12 hours. After 12 hours the C_3A reaction proceeds as monosulphate conversion until all of the initial ettringite is consumed. After this point, the reaction would continue in the final reaction of the basic product.

In each of these stages it is possible to determine what amount of C_3A is remaining based on the chemical reaction equations (12, 18, and 19) and the molecular weights. If the amount of C_3A remaining is known then it can be graphically shown on the degree of hydration curves of Figure 4.1. For the estimates of chemical shrinkage, the amount of C_3A consumed at each of these stages will indicate which shrinkage magnitude (from Table 4.3) to use for the three different phase reactions.

To predict the amount of C_3A remaining for hydration after each change of the phase reactions, the following calculations are made. The calculations use 100 grams of Finnish gray cement with the chemical composition given in Table 4.4.

Table 4.4. Composition of cement for C_3A hydration calculations.

Compound	Amount (%)	Weight (g/mol)
C_3A	8	270.19
$\overline{S}$	3.5	80.063

To determine the amount of C_3A consumed by this first reaction of ettringite formation, the amount of $\overline{S}$ will be the limiting factor. In 100 g of cement, there would be 3.5 g of $\overline{S}$, which is equivalent to 0.44 mol available for the reaction in equation 1. For this reaction to proceed, it takes 3 CSH_2 to react with 1 C_3A. Therefore 0.015 mol of C_3A are consumed, which is equivalent to 3.94 grams. Finally, of the original 8 grams of C_3A, 49.2% have been consumed by the initial ettringite reaction. There would be 4.06 grams remaining to react in the second stage of monosulphate formation. These math steps are shown in Equations 22 and 23.

$$\frac{3.5g_{\overline{S}}}{80.063^{g}/_{mol}} = 0.044mol_{\overline{S}} \times (\frac{1mol_{C_3A}}{3mol_{\overline{S}}}) = 0.015mol_{C_3A} \times 270.19^{g}/_{mol} = 3.94g \text{ of } C_3A \tag{23}$$

$$\frac{3.94g}{8g} \times 100\% = 49.2\% \text{ of } C_3A \text{ used in ettringite reaction} \tag{24}$$

From the first basic C_3A reaction in Equation 18, it was seen that 1 mol of C_3A produced 1 mol of $C_6AS_3H_{32}$. In the second reaction (Equation 19) this 1 mol of $C_6AS_3H_{32}$ took an additional 2 mol of C_3A to form monosulphate. Therefore, the 0.015 mol of $C_6AS_3H_{32}$ produced above (Equation 22) needed 0.029 mol of C_3A to fully react, which was equivalent to 7.87 grams of C_3A. This exceeded the amount of C_3A that was remaining from the first reaction. The total amount of C_3A to have full monosulphate hydration was 11.81 grams, which was 148%

of the original amount. Again, these math steps are shown in Equations 24 and 25.

$$0.015mol_{C_3A} = 0.015mol_{C_6AS_3H_{32}} \times \frac{2mol_{C_3A}}{1mol_{C_6AS_3H_{32}}} = 0.029mol_{C_3A} \times 270.19\,{}^{g}\!/_{mol} = 7.87g \quad (25)$$

of C_3A

$$\frac{3.94g + 7.87g}{8g} \times 100\% = 148\% \text{ of } C_3A \text{ needed for full monosulphate reaction} \quad (26)$$

Since the monosulphate reaction occurs beyond 100% of the available C_3A, the "basic" reaction of Equation 12 would never according to this simplified model. Each cement type has different levels of when these percentages switch and which reaction governs. These calculations of the various shrinkage amounts of C_3A over time can be combined with the estimates of hydration degrees (Figure 4.1) to graphically depict the anticipated chemical shrinkage with time. This depiction is presented in Figure 4.2 for Finnish gray cement clinker. The total chemical shrinkage is the sum of the individual clinker compounds at each time interval.

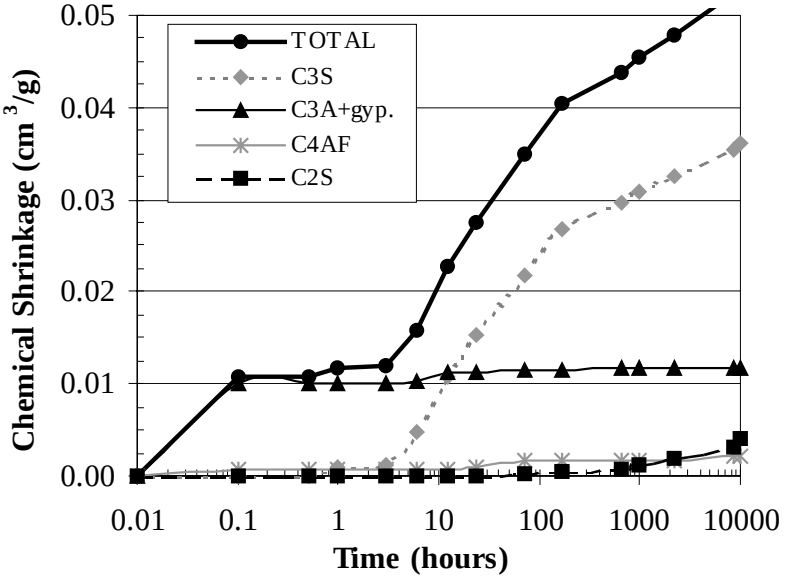

Figure 4.2. Amount of chemical shrinkage dependent on cement clinker composition, for Finnish gray cement.

In viewing these calculations, the earlier oversimplified assumption of the three progressive C_3A reactions must be kept in mind. These three different stages were split in this case to allow a generalized interpretation of the reactions. At least from this simple presentation it is possible to see the variation in the degree of cement reaction based on the C_3A content. The variation in these percentages of reacted C_3A for different cements will be addressed in the Results, Section 6.1.

5. Test Procedures

In this study shrinkage at early ages was measured by two methods: chemical shrinkage bottle tests and full autogenous shrinkage slab tests. The basic parameters of these tests were described in Section 2.2 and further details are provided here following the basic mixing and placing test procedures.

5.1 Mixing and Placing

Cement paste and mortar were mixed following normal VTT practices. Depending on the amount of material needed, the cement and other materials were mixed in either a 1 or 20 liter (0.04 or 0.70 ft^3) Hobart mixer. The 1-liter mixer is shown in Figure 5.1 mixing a small paste amount.

Figure 5.1. Mixing 1 liter of cement paste in a Hobart mixer.

When making cement paste, the water was first added to the bowl and then mixing began. The cement was slowly added to the water while mixing to prevent clumps forming. For mortar mixtures, the aggregate and cement were

combined in the bowl. Initial mixing started and then the water was added. Mixing continued for 3 minutes before placing in both cases.

Sampling, making specimens and consolidating the mixtures were done following Finnish standards SFS 5283 and SFS 5341 [Betonistandardit 1992]. Summaries of these Finnish test standards are located in Appendix C. Consolidation was done by placing the test mold on a vibrating table.

In some cases the mixtures' slump and air content were measured in accordance with SFS 5284, 5285 and SFS 5287 standards (Appendix C) [Betonistandardit 1992] to verify they were within the desired range. No tests included air-entraining agents so the target air content was 3%, as is standard in most mixtures. The slump varied from 0 to 100 mm depending on which type of mixture was being tested. It was preferable to have a very low slump for mixtures being tested in the chemical shrinkage test arrangement. The low workability was needed to prevent segregation and mixing with the container water.

5.2 Slab Test

5.2.1 Test Arrangement

The early age shrinkage testing method was developed by the Concrete and Stone Materials group at VTT, the Technical Research Centre of Finland. Various research programs measuring early age drying shrinkage on these slabs were conducted from 1995-2000. These previous projects included autogenous measurements in about 20% of the tests. In many cases there was no autogenous shrinkage present because the mixtures investigated were not high strength concretes (i.e. w/c > 0.40). VTT's work has been used to establish guidelines and equipment parameters for the current autogenous testing program.

The early age shrinkage test equipment was modified from a previous arrangement [Kronlöf et al. 1995]. The slab apparatus allows for continuous measurement of horizontal and vertical displacement as well as evaporation and internal capillary pressure. Figure 5.2 shows a schematic of the VTT test arrangement and Figure 5.3 is a picture of the test underway. In Figure 5.3 a

hood is placed around the mold to provide an environment with no moisture transfer and a stable 100% RH for the measurement of autogenous shrinkage.

The equipment is usually used to measure shrinkage for the first 24 hours, but measurements can be continued for many days if desired. The equipment is assembled as two separate molds to simultaneously evaluate drying and autogenous shrinkage.

The setting time of the concrete was measured by an automatic penetration test developed by Luigi Giazzi in Milano, Italy (Penetrometro automatico recistratore), similar to ASTM C403. The benefit of this test arrangement is that it allows for continuous measurement with time. The setting time is indicated by rapidly increasing the penetration resistance. The test sample is in autogenous (non-drying) conditions and can have a maximum aggregate size of 2 mm. The thickness of the penetration test sample was 30 mm. The calibration of the Penetration Test equipment can be found in Appendix B.

The following sub-sections elaborate on the various equipment components of the actual slab test.

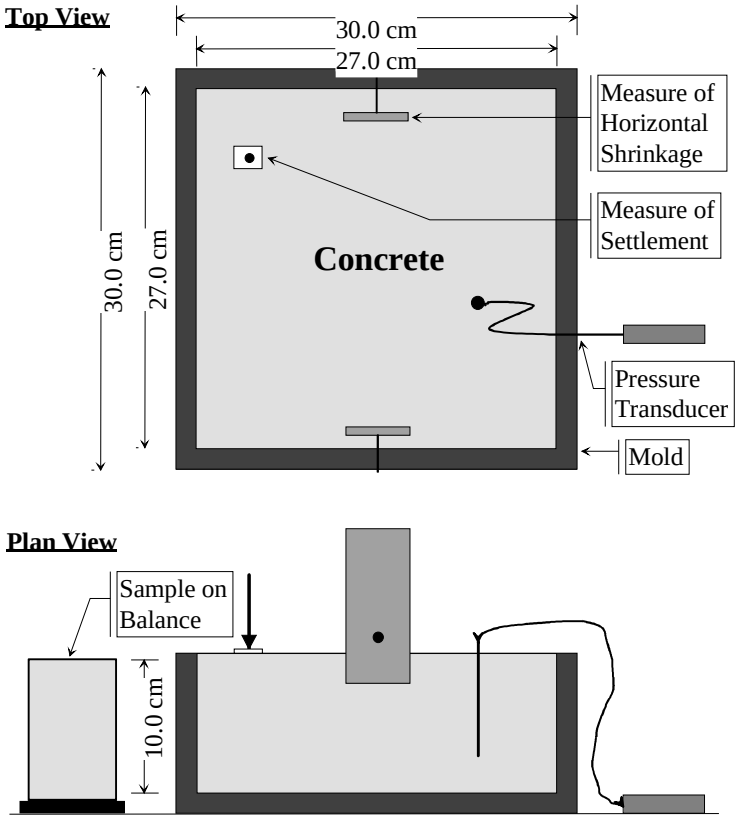

Figure 5.2. Schematic of VTT early age shrinkage test arrangement.

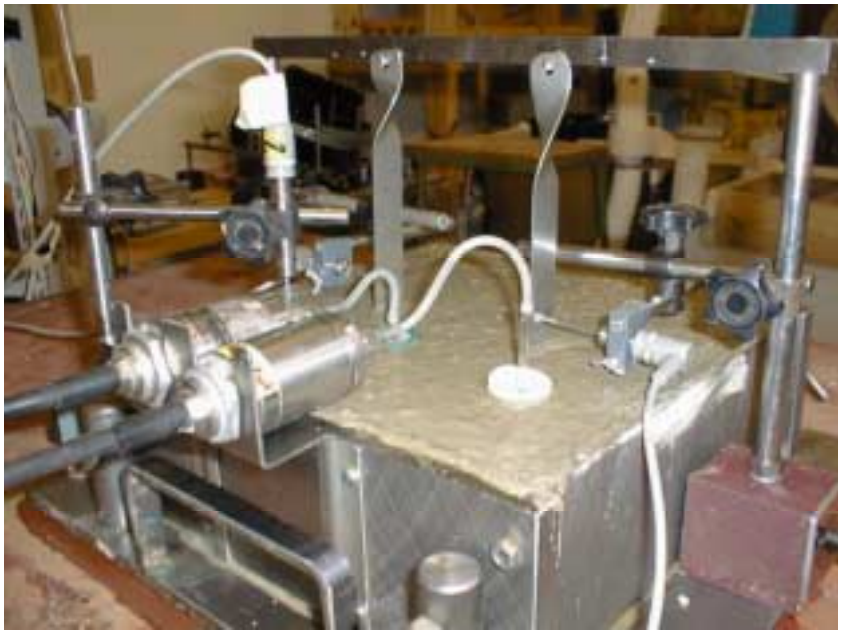

Figure 5.3. Picture of early age shrinkage test underway at VTT.

5.2.1.1 Mold

The mold was designed for a concrete specimen as large as possible so that the greatest amount of shrinkage could be detected over the span. One of the primary limiting factors was the weight of the hardened specimen. It was necessary to be able to lift and maneuver the concrete and mold before and after testing. The dimensions were also limited by the desire to have an uncracked specimen under normal conditions. The final arrangement had the dimensions of 100 mm deep, by 270 mm wide and 270 mm long.

Initially the mold was made of wood but this mold was replaced after development testing at VTT (prior to 1996). The problems with the wood molds included their deformation due to water absorption, fixings becoming loose, and service life being shorter. Plastic or PVC was not chosen because of its similar "soft" nature. After this development testing (May 1996) the mold was re-constructed of stainless steel. Prior to each test the mold was double lined with plastic. An interior layer of talc powder was included to allow easy movement of the plastic layers. The plastic ensured no friction between the concrete and mold.

5.2.1.2 Encasing Hood

In observing autogenous shrinkage it was necessary to prevent evaporation from the concrete. This was achieved by placing a stiff plastic hood around the concrete specimen and test equipment. The encasing hood was slightly larger than the mold base size and has a slanting roof of 35 cm at the center height. Moist towels were placed inside the hood to maintain a moist environment (100% RH) and prevent evaporation from the concrete surface.

Another method used to provide addition autogenous conditions was to cover the surface of the concrete with a thin sheet of plastic to prevent drying. Prior to using plastic, other liquid materials were tried but these changed the surface properties (i.e. surface tension, paste properties, etc.) of the concrete. These materials include oil, curing compound, or a constant water layer, such as suggested in ASTM C827.

5.2.1.3 Capillary Pressure

The internal capillary pressure development was measured in the middle of the concrete specimen by a pore pressure transducer, Type KP-2A (Sokki Kenkyujo Co., Ltd., Japan). It was incorporated after work by Whitman [1976] and Radocea [1992] showing that rising pressure induces stresses in the concrete capillary pores which results in shrinkage of the body. Two transducers were used to measure pressure build-up in the concrete and have specifications of a measuring capacity of 200 kPa with a non-linearity of 2%. The calibrations of the two transducers are given in Appendix B. From the calibrations the actual precision was found to be 1 kPa. For reference, in the early age test arrangement a typical capillary pressure measurement was 50 kPa, which corresponds to 0.5 bars or 7.25 psi.

5.2.1.4 Settlement

Soon after placing fresh concrete it can settle due to gravity and consolidation. In the slab test this vertical deformation was measured by a linear variable differential transformer (LVDT) placed perpendicular to the concrete surface. The LVDT measures an electrical output proportional to the position of a solid core in a cylindrical shaft. The lightweight core and shaft are not in contact with

each other and work by a series of inductors. The two settlement LVDTs were manufactured by Hottinger Baldwin Messtechnik GMBH and were of Type W2AK. Their measuring range is ± 2 mm with linear deviation of 0.2%. Calibrations for the two LVDTs used to measure settlement are given in Appendix B. From the calibrations the measuring precision was found to be 2 μm (0.002 mm/m), though the equipment specifications had noted a precision of 5 με.

The LVDT was supported by a small metal mesh that was heavy enough to not float on the concrete's bleed water yet light enough to not sink farther into the concrete. The concerns with the settlement gauge were that it needed to be positioned perfectly vertical and was in a location representative of the whole specimen. If the gauge was placed too close to the vertical walls the concrete may have a lower settlement magnitude due to edge restraint. The limit for the proximity of the gauges to the mold edges was determined to be 30 mm, as shown in Figure 5.4. This figure also shows how the test arrangement was improved by lining the mold walls with the double plastic and talc. This was noted in Section 5.2.1.1 where the lining helped eliminate the friction caused by the walls and provided a more uniform displacement measurement over the whole slab.

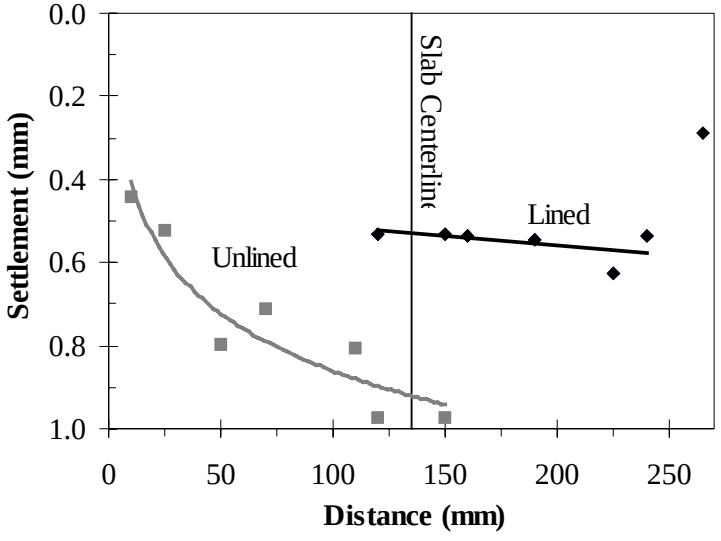

Figure 5.4. Distance of settlement gauges from mold walls.

5.2.1.5 Horizontal Shrinkage

The horizontal displacement of the concrete starts soon after the settlement is complete and internal pressure begins to develop. It is often measured at a depth considered representative of the whole concrete depth. The exact method of measuring varies and only the details of the basic VTT arrangement will be explained here. The other main method [Japan 1999, Hammer 1999, Radocea 1997] has the measuring gauges placed through the mold's sidewalls as shown in Figure 5.5. The method in Figure 5.5 is limited to measurements beginning after the setting time and there is a risk of friction between the gauge plug and the mold walls.

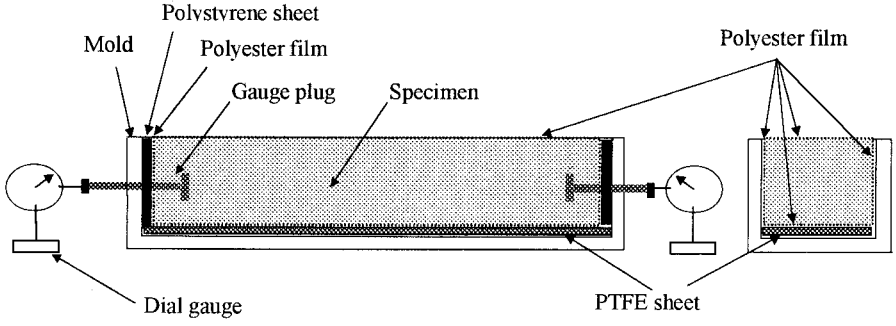

Figure 5.5. Alternative method for measuring horizontal shrinkage at early ages through mold walls. [Japan 1999]

In this work the horizontal shrinkage arrangement included two vertical metal supports being suspended from 15 cm above the concrete specimen. On each support an LVDT was attached 3 cm above the concrete surface, as shown in Figure 5.6. The four horizontal shrinkage LVDTs were similar to those used for measuring settlement, but were slightly smaller, of Type W1E/0. Their measuring range is ± 1 mm with a linear deviation of 0.2%. Calibrations for the four LVDTs used to measure horizontal shrinkage are given in Appendix B. From the calibrations the measuring precision was found to be 5 με (0.005 mm/m), though the equipment specifications had noted a precision of 10 με.

The metal strip supports were hung from a bar with pivots to allow for horizontal movement. The supports were embedded a depth of 2 cm into the concrete. This depth was chosen when originally using the arrangement to

measure drying shrinkage, which is greatest at the concrete surface. In the autogenous case there is no variation in shrinkage magnitude over the concrete cross-section so the embedded depth was not altered. The problem with this method is that the settling concrete may exert some force on the metal strip at the concrete surface due to the metal friction. When the gauge tries to move with the shrinking mass, the forces could infringe on the measurement of the actual displacement experienced by the body. This was accounted for by zeroing the horizontal shrinkage data measurements after concrete placement and settlement, as will be described in Sections 5.2.3 and 6.3.

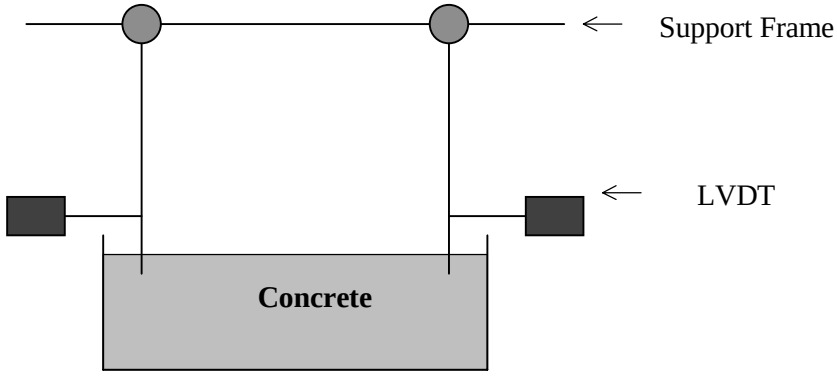

Figure 5.6. Horizontal shrinkage measuring method, with gauges suspended from above.

5.2.2 Test Implementation

Early age testing in the slab arrangements began approximately 30 minutes after water addition to the concrete mixing process. The fresh concrete was placed in the 270 x 270 x 100 mm steel mold and consolidated by an exterior vibrating table. After assembling the measuring devices, a laboratory computer program (LabTech) was used to log the results. Data interpretation was done using Excel spreadsheets. Autogenous shrinkage samples were observed during the first 24 hours following casting while encased in a hood with a moisture source to maintain 100% RH. If cast, companion drying shrinkage slabs were exposed to ambient air conditions (T = 20 °C and RH 40%) alongside the autogenous specimens. The setting time was measured in a separate specimen by an Italian Penetration Test arrangement.

5.2.3 Interpreting Data

As earlier explained, shrinkage results from both the chemical reactions and the development of capillary pressure within the concrete. As the chemical reactions proceed the capillary pressure develops simultaneously. The capillary pressure causes the water menisci, forming at the concrete surface (when drying) or in the pore-to-gel interfaces, to penetrate into the pore spaces and pull the pore walls closer. As the pressure increases the pulling forces on the paste accumulates and facilitates shrinkage.

The early age slab tests began 30 minutes after mixing but during the first hour movements, such as settlement, are accommodated by liquid flow of the concrete. Once the concrete has started to form a skeleton, any stresses (such as capillary pressure) will result in strains to the concrete body. This transition point in the concrete as it changes from the liquid to skeletal formation phase can be identified by the change in capillary pressure (suction).

During the first hour the internal pressure is a measure of the free water in the concrete mixture. The pressure is positive (greater than atmospheric) at the start of the test but becomes a negative pressure (less than atmospheric) due to capillary suction with the cement paste hydration. At the age of approximately two hours the suction increases and has a slight platform as it is measuring the pressure of the gel product formed in the cement paste. At this point the horizontal shrinkage measurement is accurate and not influenced by settlement so the clear measurement is started. The change of pressure leading to the start of clear horizontal shrinkage is shown in Figure 5.7.

As the capillary pressure continues to develop due to the chemical reactions and moisture movement, the horizontal shrinkage follows the same increasing path. This is demonstrated in Figure 5.8 as the horizontal shrinkage parallels the pressure development. Such behavior is the same for both drying and autogenous shrinkage measurements and has been previously documented in VTT literature [Kronlöf et al. 1995, Holt & Leivo 1996, Leivo & Holt 2001].

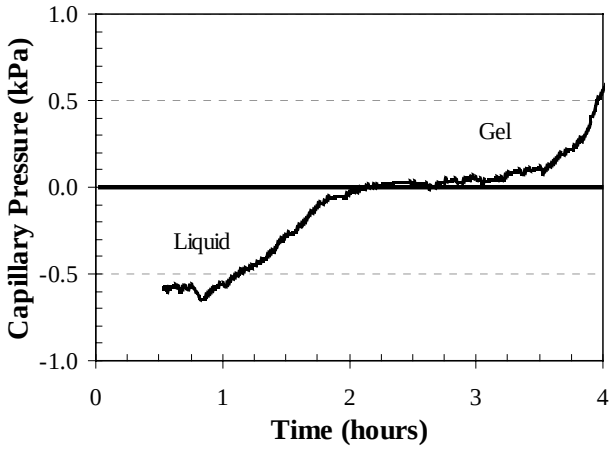

Figure 5.7. Early change of capillary pressure from measuring liquid water to gel in concrete paste.

The early age horizontal shrinkage due to drying will continue at a high rate until approximately 2 hours after the initial setting time, as was earlier shown in Figure 2.3 (Section 2.1.1.3). Near this 2-hour point the concrete has gained enough strength to resist some of the additional stresses. This drying shrinkage behavior and has been previously explained by Leivo and Holt and may be the same in the autogenous shrinkage case. [2001]

The progress of shrinkage and its dependence on the development of capillary pressure can be clearly demonstrated with the next sequence of 3 graphs. This series is taken from result of concrete drying shrinkage tests with various levels of wind. In this series of tests the concrete had 300 kg/m^3 of Finnish gray cement, w/c = 0.63, maximum aggregate size of 10 mm and no chemical admixtures. As the wind speed increased, the amount of evaporation from the concrete surface increased, thus the pressure (capillary suction) developed earlier. The increase of wind, evaporation and pressure ultimately led to a greater amount of early age drying shrinkage. Figure 5.9 shows the evaporation rate increasing with the increase of wind speed. Figure 5.10 shows the corresponding capillary pressure levels at the 3 different wind speeds. Notice that the pressure developed earlier at the higher wind speeds where there is greater evaporation. Finally, Figure 5.11 shows the amount of horizontal drying shrinkage at these 3 environmental conditions, with the greatest shrinkage resulting from earlier pressure development.

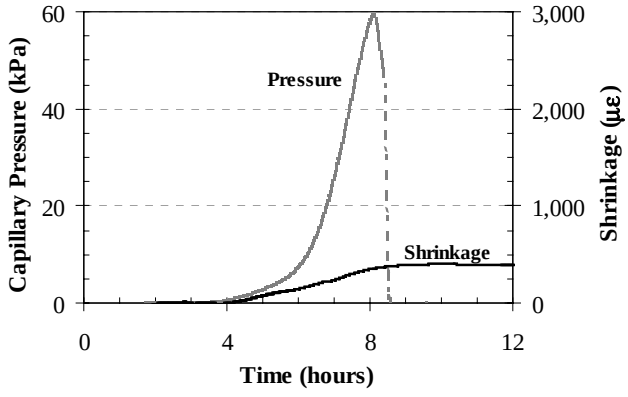

Figure 5.8. Horizontal shrinkage development following capillary pressure, for a concrete subjected to drying at early ages.

When evaluating the pressure the key item to interpret as a shrinkage indicator is the time when the pressure starts to develop. It is not possible to predict the amount of shrinkage based on the magnitude of the capillary pressure, since the point when the pressure stops rising is a fault of the transducer measuring method. This "break-through" pressure occurs in a localized area because the paste is non-homogeneous. The break results when air penetrates the transducer, as the surrounding water menisci cannot find stable positions in the region adjacent to the outer surface of the pressure gauge. [Radocea 1992] Therefore, in Figure 5.10 it is most important to note that the pressure starts earlier with the varying wind speeds. The peak pressures and the duration these pressures are sustained cannot be correlated to the amount of resulting shrinkage.

The variation in the starting time of pressure is dependent on the internal paste. In the case of autogenous shrinkage, the paste will have a uniform change in properties since there is no uneven moisture distribution due to moisture loss as there is for drying shrinkage. Therefore the capillary pressure within the concrete or paste will be uniform throughout the sample cross-section. There will be no capillary pressure variation with depth, which has been verified in numerous tests during this work. Figure 5.12 shows an example of the pressure measured at 30 and 60 mm deep in an early age autogenous shrinkage test. In both transducers the rise of capillary pressure starts at the exact same time of 2 hours and the pressure increases at the same rate. This verifies that there is no variation in capillary pressure over the depth of the sample cross-section.

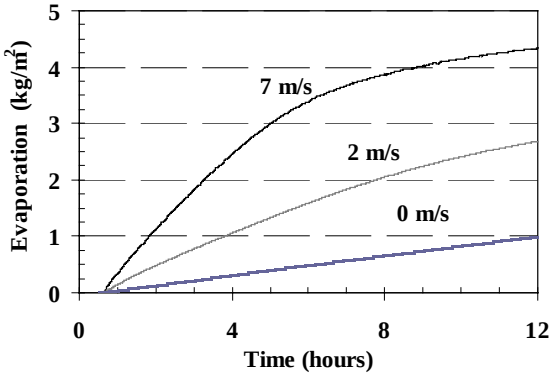

Figure 5.9. Early age evaporation from a slab due to drying with 3 wind speeds.

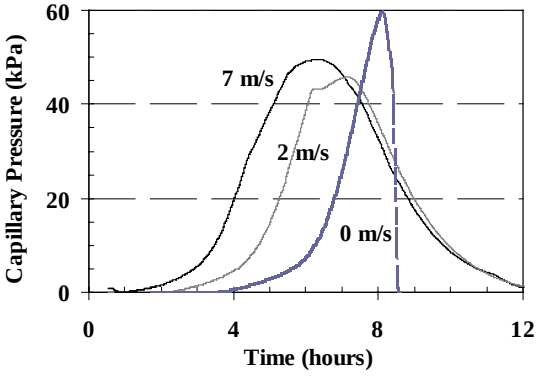

Figure 5.10. Early age capillary pressure development with 3 wind speeds.

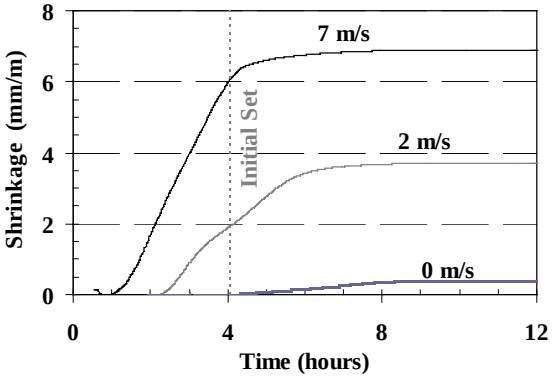

Figure 5.11. Early age horizontal drying shrinkage levels with 3 varying wind speeds.

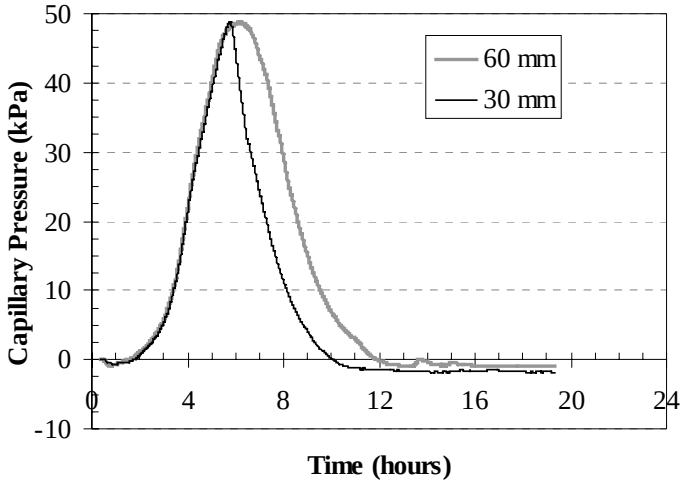

Figure 5.12. Capillary pressure at 30 and 60 mm deep in early age autogenous shrinkage slab.

Similar to the distribution of capillary pressure, there should be no variation in horizontal autogenous shrinkage with depth. The cement paste will have uniform chemical shrinkage reactions over the cross-section and the resulting autogenous shrinkage will not vary with depth. For this reason it is also acceptable to measure the autogenous shrinkage near the surface of the concrete and expect it to be representative of the whole sample depth.

5.3 Chemical Shrinkage Tests

5.3.1 Test Arrangement and Implementation

Chemical shrinkage was tested using the buoyancy method similar to Boivin et al. [1999], Geiker & Knudsen [1982], and Paulini [1992], as shown in Figure 2.27 (Section 2.3.2). A 100 gram sample of fresh cement paste or mortar was placed in a 0.2-liter glass jar. The sample thickness was approximately 20 mm. Work by Boivin et al. [1999] has established this maximum thickness limit in the dilatometry test method and it was applied here as well. This limit allows for full infiltration of extra water to the sample at representative w/c ratios. The thickness of the sample in the chemical shrinkage test prevents testing of

concrete mixtures where the maximum aggregate size is greater than three times the thickness.

The sample was vibrated and then the jar was filled with distilled water and tightly sealed with a flexible rubber lid. The jar was suspended in a mesh basket in a distilled water bath which was at a constant 20ºC. The bath included a double bucket system with oil over the water surface as well as lids to prevent evaporation. The weight was continuously logged on a balance with a maximum measuring range of 6100 g and a precision of 0.01 g. This precision corresponds to a chemical shrinkage precision of 0.1 mm^3/g, which is about 0.5% of the measuring range expected in the forthcoming chemical shrinkage tests.

The chemical shrinkage test method was periodically calibrated with a solid steel weight in the jar to ensure no weight change over time. Figure 5.13 shows the test arrangement, without the lids covering the inner bucket so the jar containing the concrete can be viewed in the water.

Figure 5.13. Side view of a chemical shrinkage test underway.

5.3.2 Interpreting Data

The chemical shrinkage test uses Archimedes principle: a volume reduction of a water-submerged sample will register as a weight increase. The chemical shrinkage was measured for the first 3 days after mixing the materials and placing the concrete sample in the jar under water. The early age results occurring in the first day were examined but it was also necessary to continue the test a couple extra days to get a "leveling" of the curves. This was beneficial when trying to compare mixtures, such as different cement types or w/c ratios. After 72 hours the variation in the chemical shrinkage amounts were more pronounced than at 24 hours and the rate had slowed, as shown in the example of Figure 5.14. In this case the test was done on two mortars with different amounts of superplasticizing chemical.

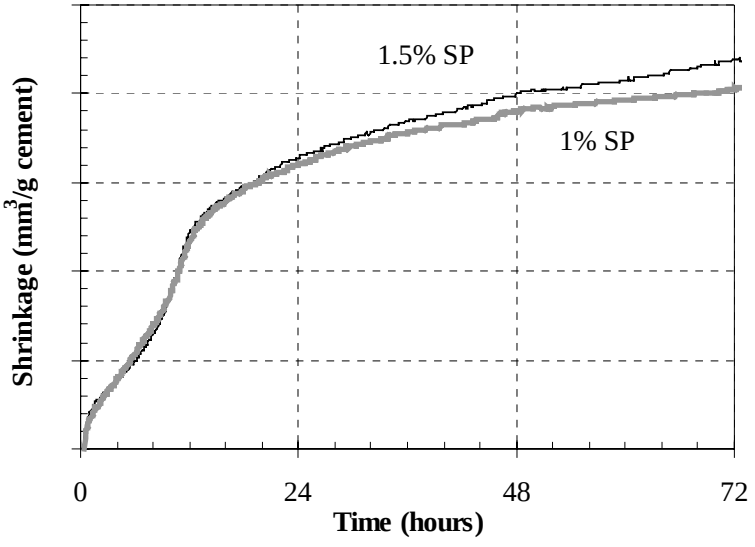

Figure 5.14. Sample chemical shrinkage results of mortars, where it was beneficial to continue testing until 72 hours (x-axis) to see variation in mixtures.

The amount of volume reduction due to chemical shrinkage is given as mm^3 per gram of cement in the original mixture. The change of weight in the sample is divided by the density of water to be converted to volume, as shown in Equation 26.

$$CS = \frac{W}{\delta} \div M \tag{27}$$

where: CS = chemical shrinkage (mm^3/g of cement)
W = change in weight of the sample under water (g),
δ = density of water = 0.9982 g/cm^3, and
M = original mass of cement in the sample (g).

6. Results and Discussion

In this investigation on early age autogenous shrinkage of concrete it was first necessary to evaluate the chemical shrinkage and determine how it was contributing to the autogenous deformations. The chemical shrinkage was initially predicted for various Finnish and American cements based on the model presented in Section 4. The chemical shrinkage was then measured for both pastes and mortars before correlating these values to the actual autogenous shrinkage measured in the slab test arrangement. The final section of the results addresses how autogenous shrinkage should be predicted and minimized based on the chemical shrinkage and other contributing factors.

6.1 Predictions of Chemical Shrinkage

The first step in understanding autogenous shrinkage is to predict the amount of volume change resulting from the chemical reactions of the cement paste. This can be done using Paulini's equation [1992] for estimating chemical shrinkage based on a cement's compositions, presented in Section 2.2.5.1 as Equation 16. These values are given in Table 6.1 for the three Finnish and American cements tested. From these values the general rule that cement with a higher C_3A content will have greater chemical shrink is upheld. It is expected that the American "high" cement (with a high C_3A content) and the Finnish gray cement would have the greatest chemical shrinkage in a bottle test.

Table 6.1. Estimates of chemical shrinkage based on Equation 16 from Paulini [1992].

	Cement	C_3A Content (%)	Estimated $CS_{Paulini}$ (mm^3/g)
Finnish	Gray	8	63.4
	White	4	53.1
	SR	1	59.3
American	High	11.5	62.7
	Medium	6.3	62.6
	Low	4.2	58.2

The amounts of chemical shrinkage in Table 6.1 are the ultimate values expected and assume the C_3A shrinkage term is only due to the final stage reactions (Equation 12). It does not include the greater shrinkage magnitude due to ettringite formation, which was twice as high, detailed in Section 4.1. Therefore, to more accurately predict the chemical shrinkage over time the point at which the C_3A reaction phases switch are calculated as a percentage of the C_3A hydration. This was shown in Section 4.1 for the Finnish gray cement with 3.5% gypsum and 8% C_3A.

Table 6.2 shows the calculated amount of C_3A (%) which has hydrated at the point when the phase reactions are changing from ettringite, to monosulphate, and then to the final basic phase. If the percentage is > 100% then the phase will not continue to the next step.

Table 6.2. Phase change points of Finnish cements, based on hydration degree (%) for C_3A reaction.

Finnish Cement	Compound (%)				Gypsum	Theoretical C_3A Consumption	
						Ettringite	Monosulphate
	C_3S	C_2S	C_3A	C_4AF	SO_3 (%)	Reaction (%)	Conversion (%)
Gray	68	10	8	8	3.5	49	*148*
White	67	23	4	1	2.2	62	*186*
SR	75	5	1	14	3.3	*371*	*1114*

From Table 6.2 it is seen that the Finnish gray and white cements have 49 and 62%, respectively, of the C_3A consumed when all of the gypsum has reacted to form ettringite at 12 hours (following Equation 18). After this point the reaction continues in the second phase (Equation 19) as ettringite converts to monosulphate with the excess C_3A. The reaction will never proceed to the final reaction phase of the basic product (Equation 12) since the amount of C_3A needed is greater than 100% of the available amount (148% and 186% for the gray and white cements, respectively).

In the case of the Finnish SR cement, 371% of C_3A is needed in order to consume all gypsum and form ettringite. There is not enough C_3A in the SR

cement for this to occur and therefore the reaction will not proceed to monosulphate formation in this simplified model.

Using these hydration amounts, it is possible to estimate the total amount of chemical shrinkage expected for each cement. As earlier stated, it is assumed that the chemical shrinkage proceeds in the same manner as the degree of hydration curve (Figure 4.1 in Section 4.2). The above calculations of the percentage of C_3A existing at each phase change allow the chemical shrinkage rate curves to be adjusted for the various phases. For instance, since the ettringite has a much greater chemical shrinkage than monosulphate (Table 4.3) there will be a greater chemical shrinkage at the early ages if the reaction converts the C_3A to ettringite at a low percentage. This is seen in Figure 6.1 for the three Finnish cements. The gray cement has the fastest reaction during the early ages because it is quickly converting to ettringite with high shrinkage.

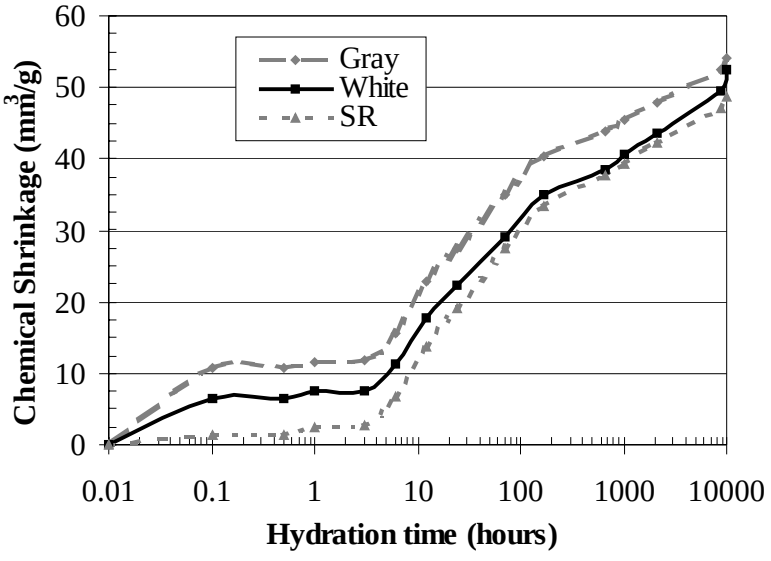

Figure 6.1. Predicted amounts of chemical shrinkage for Finnish cements with time.

The same calculations can be made for a few representative American cements and can be found in Table 6.3 and Figure 6.2. As noted in Section 3.2.2 these cements were chosen based on their varying levels of C_3A. Again, the cement with the lowest percentage of C_3A consumed for full ettringite formation has the

highest chemical shrinkage in the early ages. After a longer period the amounts become more equivalent. With the American cements there is also no transition to the final reaction phase since all of the C_3A would be consumed by the formation of monosulphate.

Table 6.3. Phase change points of American cements, based on hydration degree (%) for C_3A reaction.

American Cement	Compound (%) C_3S	C_2S	C_3A	C_4AF	Gypsum SO_3 (%)	Theoretical C_3A Consumption Ettringite Reaction (%)	Monosulphate Conversion (%)
High	55	13	11.5	6.8	3.6	35	*106*
Medium	59	16	6.3	12.4	2.5	45	*134*
Low	54	23	4.2	11.7	2.1	56	*169*

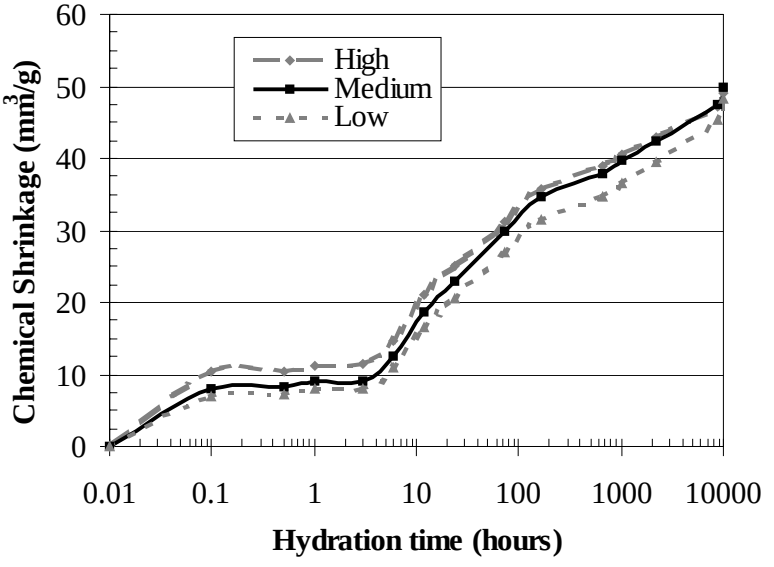

Figure 6.2. Predicted amounts of chemical shrinkage with time for three American cements with varying C_3A content.

Based on the chemical shrinkage rates of Figure 6.1 and 6.2 for the 6 cements, the ultimate chemical shrinkage could again be predicted for the age of 415 days (10,000 hours) as given in Table 6.4. The only difference between these

predictions and the ones given earlier in Table 6.1 is that now the chemical shrinkage due to the C_3A was separated into the three different phases. The shrinkage due to ettringite in the first 12 hours will be much greater than the value used to obtain the Table 6.1 values. But then the shrinkage due to monosulphate (12+ hours) will be very low, so the values in Table 6.3 are a combination of these two factors. The calculations earlier using Paulini's terms (Table 6.1 and last column of Table 6.4) used only the final C_3A stage reactions that had a lower shrinkage term than ettringite (see Table 4.3). The revised values for chemical shrinkage presented in the second-to-last column of Table 6.4 are from 2 to 28% lower than the values predicted earlier by Paulini's equation.

Table 6.4. Predicted ultimate chemical shrinkage based on degree of hydration graphs and estimates from Paulini equation (as given in Table 6.1).

	Cement	C_3A Content (%)	Estimated CS_∞ (mm^3/g)	Estimated $CS_{Paulini}$ (mm^3/g)
Finnish	Gray	8	54	63.4
	White	4	52	53.1
	SR	1	49	59.3
American	High	11.5	49	62.7
	Medium	6.3	50	62.6
	Low	4.2	48	58.2

The ultimate chemical shrinkage value was predicted at the age of 415 days from the hydration graphs. For comparison to actual chemical shrinkage test values, it is helpful to note the estimated shrinkage at earlier ages. Table 6.5 lists the chemical shrinkage values at 3, 12 and 72 hours in addition to the ultimate value at 10,000 hours. The values predicted using Paulini's estimates are also presented in Table 6.5, as seen earlier in Table 6.1. From the new estimates of early age shrinkage in Table 6.5, it is seen that the 12-hour chemical shrinkage value is 30 - 40% of the ultimate value, while the 72 hour value is about 60% of the ultimate.

Table 6.5. Predicted early age chemical shrinkage based on degree of hydration graphs and then compared to Paulini's estimates (from Table 6.1).

Cement		Estimated CS_{Holt} (mm^3/g)				Est. $CS_{Paulini}$ (mm^3/g)
		3 hours	12 hours	72 hours	Ultimate	Ultimate
Finnish	Gray	12	23	35	54	63.4
	White	8	18	29	52	53.1
	SR	3	14	28	49	59.3
American	High	11	21	31	49	62.7
	Medium	9	19	30	50	62.6
	Low	8	17	27	48	58.2

The reason that the Finnish cements have greater estimates of chemical shrinkage than the American cements is because of their higher C_3S content (see Table 6.2 versus 6.3). The C_3S does not have the greatest shrinkage amount of the various components (see Table 4.3) but because there is nearly 10% more C_3S in the Finnish cements than the American cements it will play a greater role in determining the ultimate chemical shrinkage.

The chemical shrinkage amounts predicted by Figures 6.1 and 6.2 at the age of 0.1 to 1 hour are 15 to 20% of the ultimate shrinkage. This very early chemical shrinkage is attributed to the quick ettringite reactions. This amount of shrinkage in the first hour would have no effect in hardened concrete since the paste is fluid enough to prevent development of stresses. There is also a platform during this time period of 0.1 to 1 hour on the graphs, though it is not actually measured as a dormant period in laboratory chemical shrinkage tests. This is a fault of the existing hydration models presented in Section 2.2.5.2 (Figures 2.22 and 2.23).

It must also be noted that the chemical shrinkage values of concrete or pastes made with gray and SR cement could be expected to be slightly higher in the general Finnish market. As noted in Section 3.2.1, the C_2S content is usually lower in Finnish gray cements compared to the cement samples used in this work. This would result in the C_3S content being higher and thus the shrinkage being greater. In SR cement the C_3A content may be higher and thus the shrinkage would again be greater for average Finnish material.

6.2 Measurements of Chemical Shrinkage

To support the chemical shrinkage amounts given in Table 6.5 the bottle test based on dilatometry was used, as described in Section 5.3. One main purpose for conducting chemical shrinkage tests was to compare the results to the values estimated by the modeling equations. The second major goal of doing chemical shrinkage tests was to try and establish a correlation between the chemical and autogenous shrinkage during the early ages. In theory, the chemical shrinkage is the primary driving force to the autogenous shrinkage so it was beneficial to compare their magnitudes during the first hours. When conducting the chemical shrinkage tests, it was also critical to note the rate of shrinkage in addition to the ultimate magnitudes.

The repeatability of the chemical shrinkage test was verified prior to the detailed test program. The sample mixture used in the test was repeated four times on different days and is shown in Figure 6.3. In this repeatability test the mixture was a mortar made of Finnish gray cement with no chemical admixtures and a w/c = 0.35. The corresponding shrinkage values taken from the graph are given in Table 6.6 at the ages of 12, 24 and 72 hours.

Some statistical values are also given in the table to help assess the test repeatability. The error in the measurements was calculated within the 90% probability range and it was under 2% at 24 and 72 hours. The coefficients of variation (within 50% probability) in this particle set of measurements were also calculated to be about 1% at 24 and 72 hours, which is within the accepted range. Test D was only tested until 18 hours and is not included in the statistical analysis.

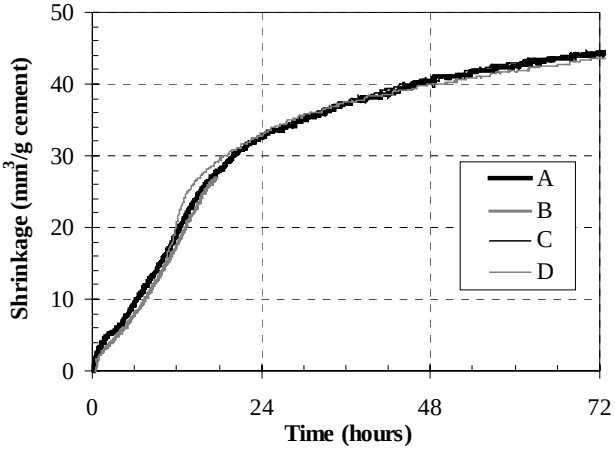

Figure 6.3. Repeatability of chemical shrinkage test on mortar made of 780 kg/m^3 Finnish gray cement with a w/c = 0.35.

Table 6.6 Early age chemical shrinkage values at 12, 24 and 72 hours of repeatability test from Figure 6.3.

	Chemical Shrinkage (mm^3/g)		
Test	12 hr CS	24 hr CS	72 hr CS
A	19.1	32.5	44.2
B	19.3	33.0	44.6
C	20.5	33.0	43.6
Average	19.6	32.9	44.1
SD	0.8	0.3	0.5
Variation (%)	4.0	0.9	1.1
Error (± %)	6.6	1.6	1.9

6.2.1 Cement Pastes

In the first set of tests only cement pastes were investigated, so there were no aggregates present in the mixtures. The mixture proportions for these tests can be found in Table 3.6. Figure 6.4 shows the variation in the three main types of Finnish cements: Rapid gray, white and sulphate resistant (SR). In this figure the x-axis is extended to 72 hours to allow a view of the "platform" magnitude of shrinkage. The early age reactions are magnified in Figure 6.5 for the first 24

hours. As predicted in the earlier calculations, the gray cement had greater chemical shrinkage than the white cement, while the SR cement has the least amount of all three pastes.

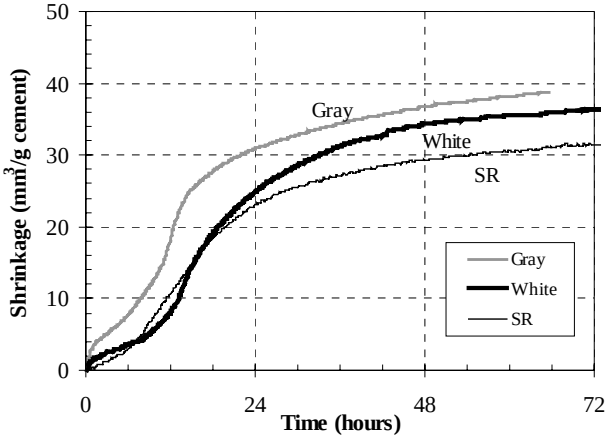

Figure 6.4. Volumetric shrinkage of 3 pastes with various Finnish cement types in chemical shrinkage test, with w/c = 0.25, superplasticizer and equivalent water amount of 425 kg/m^3.

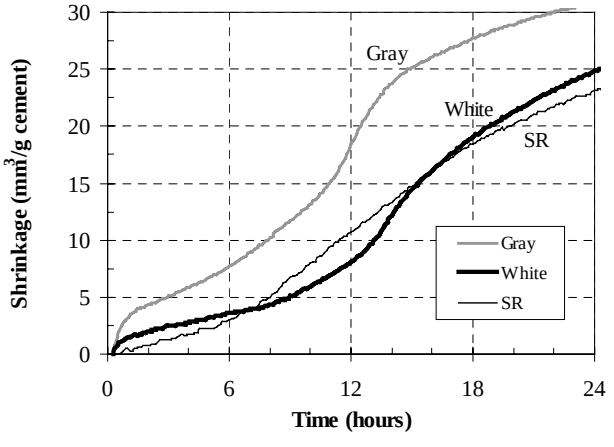

Figure 6.5. Volumetric shrinkage of same 3 pastes as Figure 6.4, but shorter x-axis time scale.

In Figure 6.5 it can be seen that the rates of chemical shrinkage for the gray and white cement pastes are changing during the time period of 10 to 14 hours. This

is due to the inclusion of 1% naphthalene-based superplasticizer in the mixtures. The superplasticizer is added at the low w/c ratios to improve the pastes' workability. The improved workability is achieved by the chemical admixture providing particle repulsion leading to an improved dispersion of the cement particles. [Lea 1998] This has the secondary effect of a more efficient hydration [Lea 1998] and in this work it also results in an increase in the chemical shrinkage reaction rate during the early hours. The chemical shrinkage rate change is more evident in the gray and white cements, while the SR cement's rate is steadier.

Similar tests were done on pastes made from three different American cements: high, medium and low aluminate contents. The mixture proportions for these tests can be found in Table 3.6. These chemical shrinkage test results are presented in Figure 6.6. All three pastes showed equivalent chemical shrinkage during the first 12 hours and then the rates changed. The paste made with the "high" aluminate cement continued at a faster shrinkage rate until about 24 hours and thus it had the greatest amount of chemical shrinkage. This greater shrinkage for the "high" cement is in agreement with predicted values from Table 6.4. It was expected that the paste made with "low" aluminate cement would have the least amount of shrinkage but that was not the case. The paste with "medium" aluminate cement had slightly lower shrinkage than the "low" cement paste though they were quite similar.

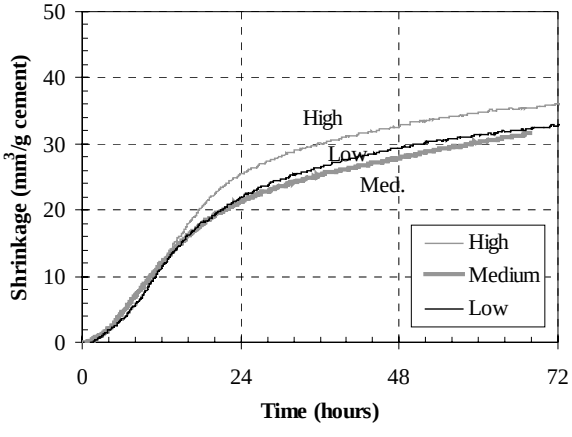

Figure 6.6. Volumetric shrinkage of three American cement pastes in chemical shrinkage test, with w/c = 0.30 and water amount of 470 kg/m^3.

The next set of tests was done when the paste included admixture chemicals. A paste's chemical shrinkage variation with and without superplasticizer (SP) is given in Figure 6.7 for Finnish gray cement at a w/c ratio of 0.30. The mixture proportions for these tests can be found in Table 3.7. Again it is shown that the mixture containing the superplasticizer had a change in the rate of chemical shrinkage in the period of around 12 hours, while the non-superplasticized mixture had a more steady shrinkage rate. Eventually the magnitudes will reach an equivalent level.

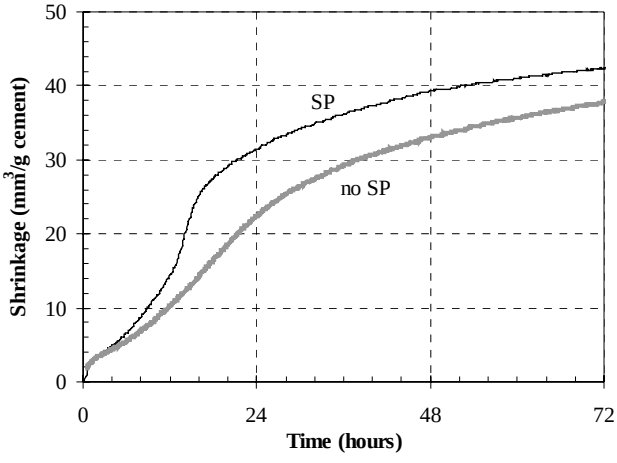

Figure 6.7. Volumetric shrinkage of Finnish gray cement paste in chemical shrinkage test, with and without 1% superplasticizer, w/c ratio = 0.30 and equivalent water amount of 470 kg/m^3.

When the same test is done on white cement there is a different result, as shown in Figure 6.8. The mixture proportions for these tests can be found in Table 3.8. The combination of white cement and superplasticizer has a great delay in the start of the chemical shrinkage. The basic white mixture with no chemical admixture has a greater shrinkage during the first day but with time becomes less than the superplasticized mixture. This is the opposite of the gray cement paste and demonstrates how the chemical shrinkage is difficult to predict. The combination of this particular superplasticizer and white cement lowered the early age chemical shrinkage (< 24 hours) compared to the gray cement and superplasticizer combination. The white cement and superplasticizer combination would then be a better choice for use when considering the first day

shrinkage magnitude and the lower risk of cracking since it has a slower rate of chemical shrinkage.

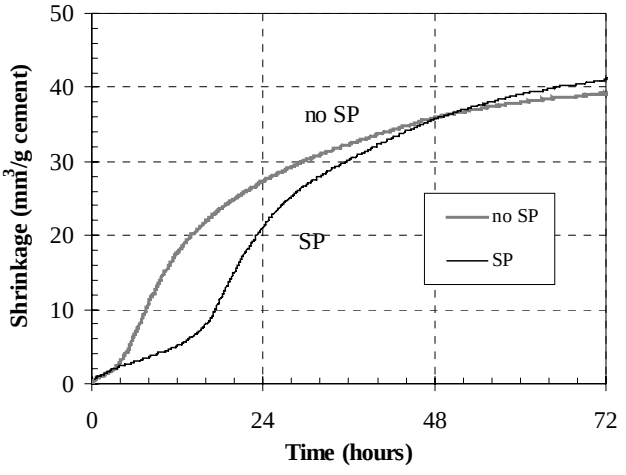

Figure 6.8. Volumetric shrinkage of Finnish white cement paste in chemical shrinkage test, with and without 1% superplasticizer, w/c ratio = 0.30 and equivalent water amount of 470 kg/m^3.

To verify the chemical shrinkage rate change with the addition of superplasticizer, further tests were done with other chemical admixtures. In Figure 6.9 the test was repeated using a synthetic polycarboxylate-based superplasticizer, SSP2000 (referred to as "polymer"). The mixture proportions can be found in Table 3.9. The test supported the previous explanation when the superplasticizer again altered the shrinkage rate at 12 hours. The test also demonstrated that the adjustment of the shrinkage rate was not due to the actual chemistry of the admixture. It was a concern that the naphthalene-based superplasticizer (containing sulphate) may have contributed sulphur to the gypsum reaction and altered the chemical shrinkage. [Mannonen 1996] But the independence of sulphur was verified by testing with the SSP2000 superplasticizer. This admixture is based on polymers and has no sulphur, yet it provided the same improved dispersion with the changing shrinkage rate.

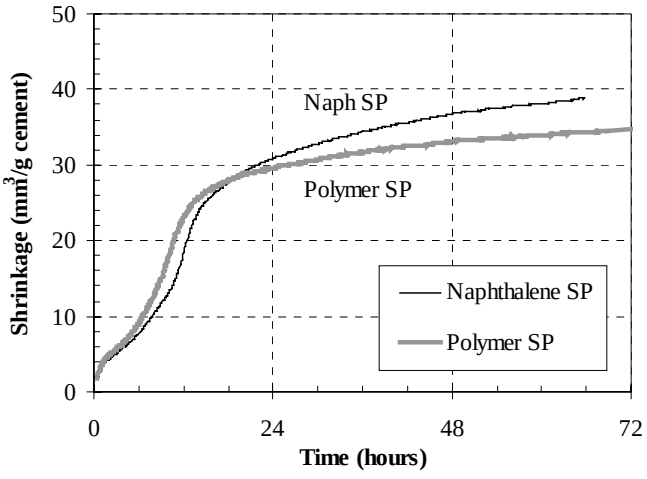

Figure 6.9. Volumetric shrinkage of Finnish gray cement paste in chemical shrinkage test, with 1% of two different superplasticizers: naphthalene- and polycarboxylate- (polymer) based. w/c ratio = 0.25 and equivalent water amount of 425 kg/m^3.

Another chemical admixture, a shrinkage reducing admixture (SRA), was also used to investigate how it affected the early age chemical shrinkage reactions. As described in Section 3.3, the SRA works by decreasing the capillary tension of the pore water and it does not include any internal superplasticizers. Figure 6.10 shows the variation in shrinkage with and without superplasticizer and the SRA. The mixture proportions for these tests can be found in Table 3.10. Again the rate of shrinkage changed at about 12 hours but it was not as pronounced as the superplasticized mixture. Even though the paste with SRA had a slightly quicker reaction, the final magnitude was the same as the basic, non-superplasticized, mixture. SRA had no effect in reducing the chemical shrinkage of the paste during the early ages.

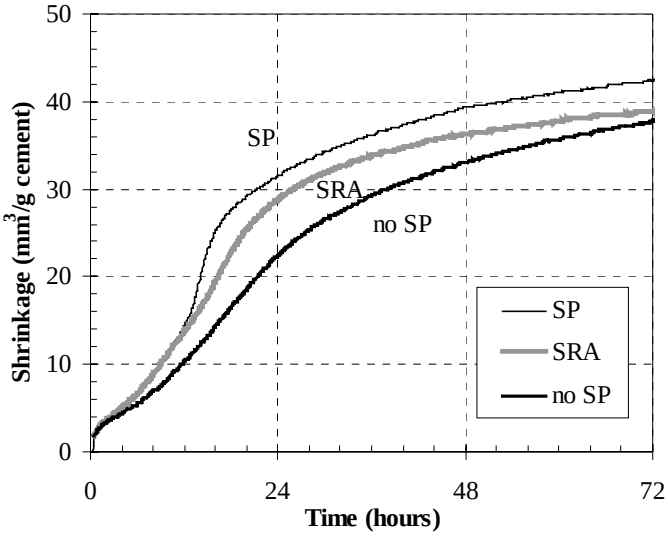

Figure 6.10. Volumetric shrinkage of Finnish gray cement paste in chemical shrinkage test, and with shrinkage reducing admixture (SRA) with and without 1% superplasticizer (SP), w/c ratio = 0.30 and equivalent water amount of 470 kg/m^3.

A final set of tests was done with the cement pastes where the w/c was altered from 0.40 to 0.20. In these tests the cement amount increased from 1,340 to 1,860 kg/m^3 (2260 to 3135 lb/yd^3). It was expected that the chemical shrinkage should be equivalent during the early ages since the shrinkage is measured in terms of mm^3 of shrinkage per gram of cement. As the cement amount changes the shrinkage would still be equivalent. This theory proved true for cement pastes at the higher w/c ratios (0.40 to 0.30) containing no superplasticizer, as shown in Figure 6.11. The mixture proportions for these higher w/c ratios can be found in Table 3.11.

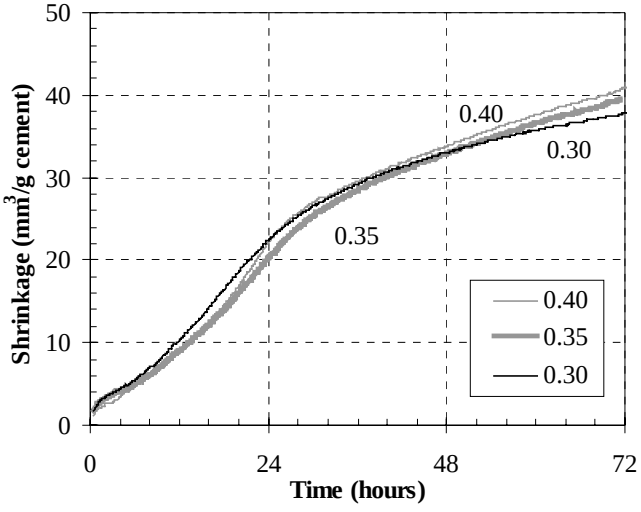

Figure 6.11. Volumetric shrinkage of Finnish gray cement paste in chemical shrinkage test, with varying w/c ratio and no superplasticizer.

The same set of tests was also done at slightly lower w/c ratios (0.30 to 0.20) and then included the basic naphthalene-based superplasticizer (Figure 6.12) The mixture proportions can be found in Table 3.12. Again the chemical shrinkage was equivalent during the very first (0-12) hours, but then there was divergence of the shrinkage magnitudes.

At the very low w/c ratio of 0.20 the high rate of shrinkage ends slightly earlier than at the higher ratios of 0.25 and 0.30 and does not reach the same maximum value. From this point the rate becomes much more level and the total chemical shrinkage is lower than at a higher w/c ratio. This is due to the lack of water within the cement paste, which does not allow for full hydration. The cement paste microstructure has already become so dense that excess water cannot infiltrate from the surrounding water bath.

Recall that Powers [1968] had calculated that the lowest possible w/c ratio for a cement paste to achieve full hydration is about 0.40 to 0.45. Therefore, a fully hydrated cement paste with a w/c ratio of 0.42 would have an average ultimate chemical shrinkage of 50 mm^3/g of cement (from Table 6.5). When the w/c ratio is lowered to 0.20 the paste can only hydrate to 47%, corresponding to a limiting level of chemical shrinkage of approximately 24 mm^3/g of cement. In the paste

with w/c = 0.20 of Figure 6.12 the chemical shrinkage is following this trend, where there is a lack of water for hydration to continue and the shrinkage begins to platform near 25 mm^3/g of cement at the early age of 20 hours. The shrinkage can still continue by removal of water from internal pores (lowering the RH) but this shrinkage proceeds at a much slower rate.

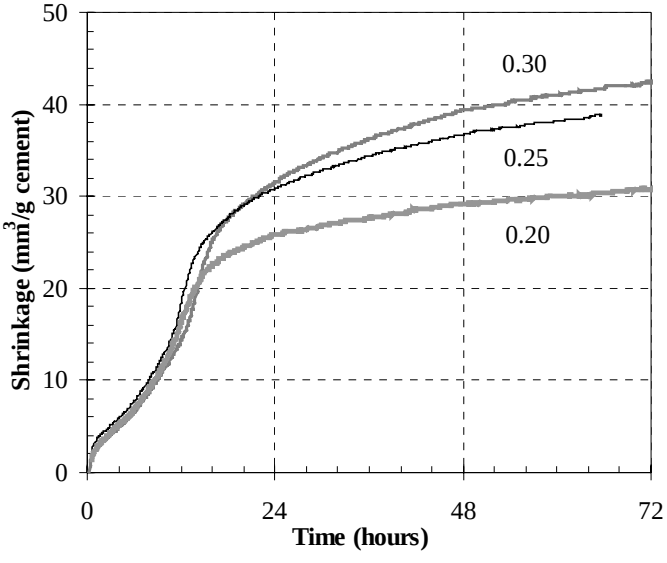

Figure 6.12. Volumetric shrinkage of Finnish gray cement paste in chemical shrinkage test, with varying w/c ratio, superplasticizer and equivalent water amount of 195 kg/m^3.

6.2.2 Mortars

After the testing of cement pastes, the chemical shrinkage tests progressed to testing of some mortars. In these cases aggregate was included in the mixture with a maximum size of 2 mm. The mixture proportions can be found in Table 3.13. A comparison of the chemical shrinkage of a cement paste and mortar is given in Figure 6.13. The mortar mixture included 45% aggregate compared to the paste mixture and had a lower workability. It was not possible to test the chemical shrinkage of concrete mixtures due to their aggregate size being larger than allowed for the sample thickness in the bottle test.

The results in Figure 6.13 show that the chemical shrinkage was larger in the mortar mixture compared to the paste mixture. This was due to the better dispersion of cement due to the grinding action of the aggregates. During mixing the aggregates will break up any cement clumps and provide a better dispersion of the cement. In the mortar there may also be an improved ability for the water to infiltrate throughout the mass via the transition zone (around aggregate particles) connecting to the surface. The transition zone of weaker cement paste along the aggregate edges provides a path for the exterior water to mitigate into the sample and speed the cement hydration with excess water. After 7 days the test results still showed the mortar exceeding the paste's chemical shrinkage, though it is expected that after a much longer time period the chemical shrinkage amounts would be equal.

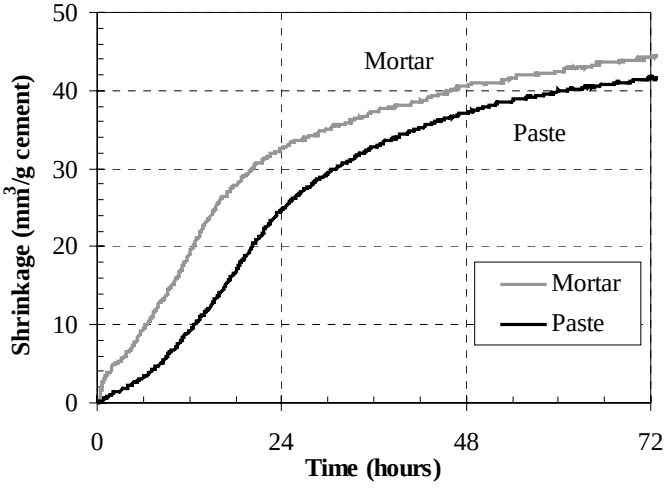

Figure 6.13. Volumetric shrinkage of Finnish gray cement paste and mortar in chemical shrinkage test, with equivalent w/c ratio of 0.35.

Similar to the results seen in the pastes, the comparison of mortars made with various cement types also showed various magnitudes of chemical shrinkage. The mixture proportions can be found in Table 3.14. Figure 6.14 shows the repeated test of mortars made from Finnish gray cements, white cement and SR cement at a w/c of 0.30. In this figure the mortar with gray cements again had much greater shrinkage than the SR cement, which is similar to results in Figure 6.4 and in-line with the calculated values reported in Table 6.5.

Also in Figure 6.14, mortar made from both Finnish Rapid and Yleis gray cements were tested. This was done to determine if there was any variation in the amount of chemical shrinkage depending on the fineness of the cement and inclusion of inert filler to the cement. Recall from the Materials descriptions (Section 3.2) that these two cements are derived from the same clinker and the only differences between them are their Blaine fineness, the amount of gypsum and the extra inert material added to the Yleis clinker.

The figure shows that the mortar made from Finnish Rapid cement has an increase in the reaction rate at approximately 12 hours. The higher rate of chemical shrinkage occurs in the Rapid cement for a longer period than the mortar made with Yleis cement and thus the final magnitude of shrinkage is greater. This is as expected, with the finer ground and pure Rapid cement having improved hydration but risking greater early age chemical shrinkage. It is expected that the mortars made with the Yleis cement would always have a slower early age and lower final amount of shrinkage since it is composed of 15% inert material, which is not contributing to the early age shrinkage.

The mortar with white cement also had greater shrinkage than the SR cement mortar and a magnitude nearly equivalent to the Yleis gray cement mortar. This is in agreement with the predictions based on chemistry as well as the fineness levels. The White cement is ground coarser than the Rapid cement but finer than the SR and their shrinkage magnitudes reflect the idea that the paste made of finer cement will shrink faster. Even though the rates during the first day were changing at different points for the Yleis and white cement mortars, their shrinkage magnitudes were the same after 24 hours.

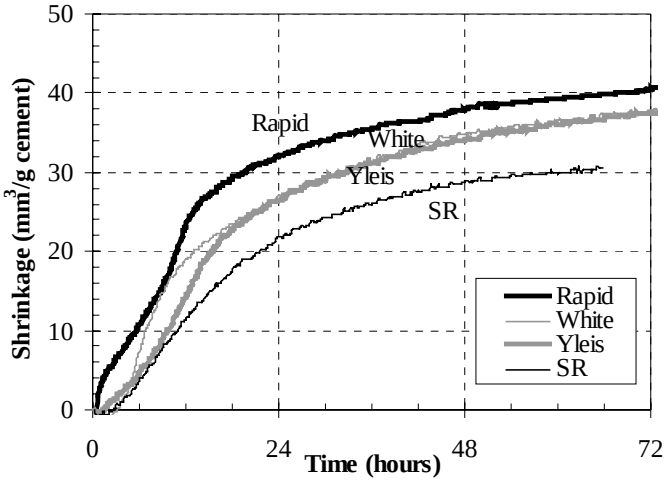

Figure 6.14. Volumetric shrinkage of four Finnish cement mortars in chemical shrinkage test, with w/c = 0.30, no superplasticizer and equivalent water amount of 195 kg/m^3.

A final set of tests was done with a Finnish gray mortar where the w/c ratio was again adjusted from 0.40 to 0.30. (Figure 6.15) In this set there were no chemical superplasticizers, the water amount remained at 275 kg/m^3 and the cement amount increased from 685 to 915 kg/m^3 (1155 to 1540 lb/yd^3). The mixture proportions can be found in Table 3.15. It was expected that the chemical shrinkage would be equivalent during the early ages since the shrinkage is measured in terms of mm^3 of shrinkage per gram of cement. As the cement amount changes the shrinkage would still be equivalent. This theory was not supported by the results shown in Figure 6.15.

During the first 12 hours the shrinkage amounts were nearly the same but as shrinkage progressed there was greater divergence. The mortars with a lower w/c ratio had the least amount of shrinkage because of the lack of water for further cement hydration. The cement paste within the mortar has a dense microstructure (high cement content) which prevents excess water from infiltrating the paste and aiding in hydration. This is the same principle that was shown for the cement pastes in Section 6.2, where at a w/c of 0.30 only 71% of the hydration can be achieved according to Power's models [1968].

In the mortars with the higher w/c ratio (i.e. 0.40) there is enough water for hydration, and thus chemical shrinkage, to continue. Also at the higher w/c the microstructure is not so dense and it is possible for excess water to penetrate the paste so the chemical reactions can proceed easier and with a higher shrinkage

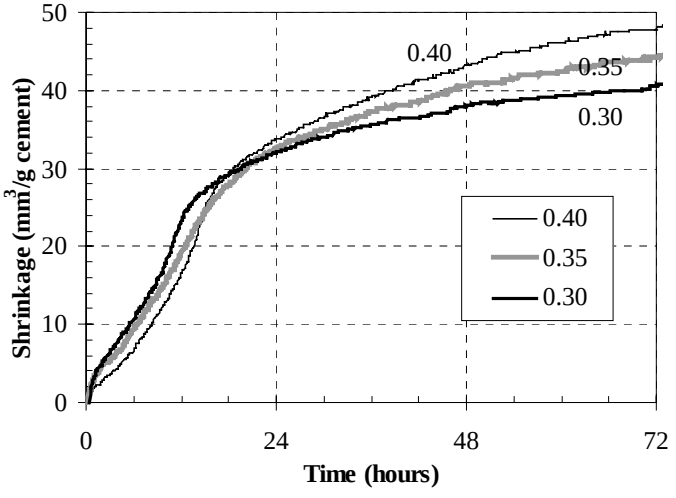

Figure 6.15. Volumetric shrinkage of Finnish mortars with changing w/c ratio in chemical shrinkage test, with no superplasticizer and equivalent water amount of 275 kg/m^3.

If the results are viewed for only the very early stage of the first 12 hours (Figure 6.16) the levels of chemical shrinkage with varying w/c ratio are reversed. The mortar with the lowest w/c ratio of 0.30 is reacting the fastest while the 0.40 mortar is slowest. The same trend held true in tests on pastes (Figures 6.10 and 6.11) but they are more pronounced in the case of mortars.

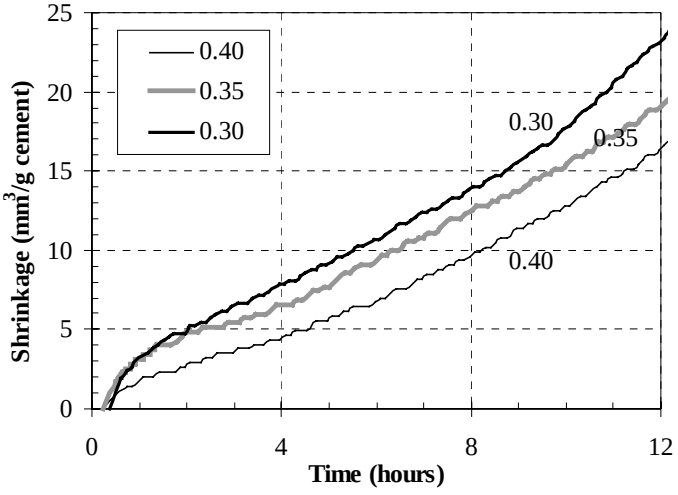

Figure 6.16. Volumetric shrinkage of same Finnish mortars with changing w/c ratio as in Figure 6.15, but shorter x-axis time scale.

There are a few possible explanations for this behavior of reversing the shrinkage magnitude with the changing w/c ratio. One likely cause is the presence of air pores in the cement paste. The air pores are flexible and are able to expand with the pressure change in the paste. In the chemical shrinkage test arrangement, air pores prevent infiltration of extra water and thus an expanding air pore will inhibit a measure of chemical shrinkage. At a higher w/c ratio (0.40) cement paste typically has a higher volume of air pores compared to a low w/c ratio mixture (0.30). Therefore the chemical shrinkage may be lower in the 0.40 mixture during the very early ages since the air pores can expand more and prevent the measurement of chemical shrinkage. As the concrete age approaches the initial setting time, the cohesion (stiffness) increases and the air pores are no longer able to expand. Then at the later ages the chemical shrinkage proceeds as expected where the magnitude is greater at higher w/c ratios.

Another possible cause of the reversal of shrinkage magnitudes with w/c ratio during the first hours is the effect of abrasion among the cement particles during mixing. At the lower w/c ratio (0.30) there is a greater amount of cement per volumetric unit of paste compared to the higher w/c ratio (0.40). During mixing of the low w/c mixture the cement particles come in contact with each other and the aggregate particles more often. There would be an abrasive action between

the particles, making them more reactive when in contact with water during the first hours. This notion of improved workability due to abrasion and grinding among the cement particles has been supported by Kronlöf's work [1997] on fine inert mineral fillers.

A third possibility for the reversal is merely the variation in hydration products of the reacting cement. At a higher w/c ratio there may be a greater consumption of water for the early ettringite formation. The growth of larger ettringite crystals may inhibit the hydration (and thus chemical shrinkage) rate of other compounds.

Pinpointing the exact cause of these changes in chemical shrinkage magnitudes in the first few hours was outside the scope of this work. In the future if a more precise explanation is sought it would be necessary to better assess the contribution of air voids, cement grinding and hydration products.

Additional tests were done on mortars with an altering w/c ratio but at slightly lower ratios and including a superplasticizer. These results are shown in Figure 6.17 for a w/c ratio from 0.40 to 0.25 and the cement increasing to 1095 kg/m^3. The mixture proportions can be found in Table 3.16. Again, the mortar with the highest w/c ratio had the greatest amount of chemical shrinkage due to the ability for the water infiltration with a less dense paste microstructure. This is the same trend that was shown with the mortars containing no superplasticizer (Figure 6.15) and the cement pastes containing superplasticizer (Figure 6.12).

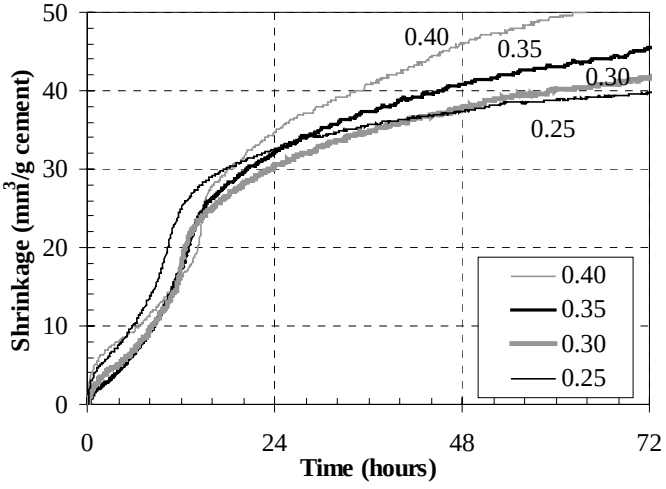

Figure 6.17. Volumetric shrinkage of Finnish mortars with changing w/c ratio in chemical shrinkage test, with superplasticizer and equivalent water amount of 275 kg/m^3.

6.2.3 Comparison of Predicted and Measured Values

The results from Sections 6.2.1 and 6.2.2 are compared in Table 6.7 for the variation in the predicted and measured values of chemical shrinkage. The values are reported at the age of 72 hours and the measured values are given for both paste and mortar. The predicted values are taken from Table 6.5 and the measured values are taken from the data presented in Figures 6.4 and 6.6 (Finnish and American pastes) and 6.13 (Finnish mortars). The values from Figure 6.4 are for a w/c ratio of 0.25 with superplasticizer, while the other mixtures are non-superplasticized at 0.30. If the results for the Finnish pastes were given at a w/c = 0.30, it is expected that the values would increase about 7%. This percentage increase was estimated from Figure 6.12 for changing w/c ratios.

Table 6.7. Comparison of predicted and measured chemical shrinkage at 72 hours.

Cement Type		Chemical Shrinkage (mm^3/g cement)		
		Predicted	Measured	
			Paste	Mortar
Finnish	Gray	35	39.6	40.6
	White	29	36.3	37.6
	SR	28	31.5	31.1
American	High	31	36.0	-
	Medium	30	32.0	-
	Low	27	32.8	-

The comparison shows that the measured chemical shrinkage of mortars is slightly greater than the pastes for gray and white Finnish cement. If an additional 7% increase in each of the Finnish pastes were also applied to get equivalent w/c ratios, all pastes would have slightly higher chemical shrinkage than the mortars.

Both the paste and mortar measured values are also slightly higher than the predicted values, with the measured mortar exceeding the predicted values by 7 to 30%. This indicates that the earlier prediction model proposed in Section 4.2 estimates the chemical shrinkage slightly lower then the true values.

The model in this work is still more accurate than the existing chemical shrinkage prediction models [Paulini 1992]. Paulini's model had greater estimates of ultimate chemical shrinkage compared to the model of this work, as earlier shown in the far right column of Table 6.3. Even though Paulini's predictions may have more accurately matched the measured values, his model is achieving these results somewhat by default. His is neglecting to consider the true hydration of the C_3A and is basing the shrinkage prediction on a hydration reaction (Equation 12) which may not be occurring throughout the reaction period in many cements. On the other hand, the model in this work is still predicting the chemical shrinkage fairly close to the actual measured value and in a more justified manner.

6.3 Measurements of Autogenous Shrinkage

6.3.1 Initial Data Output

Measuring autogenous shrinkage during the early ages was done at VTT using the slab test arrangement described in Section 5.2.1. In most of the following graphic results the autogenous shrinkage plotted on the y-axis is taken from the horizontal displacement. The shrinkage is given in units of mm/m, where 1 mm/m = 1000 με.

Figure 6.18 shows a typical early age autogenous shrinkage test result for a mortar with a w/c = 0.35 and 780 kg/m^3 of Finnish gray cement. On the slab there can be two measurements of each property (settlement, pressure, and horizontal shrinkage) but the average value is shown here for simplicity. Note that the magnitude of capillary pressure is given on the right y-axis.

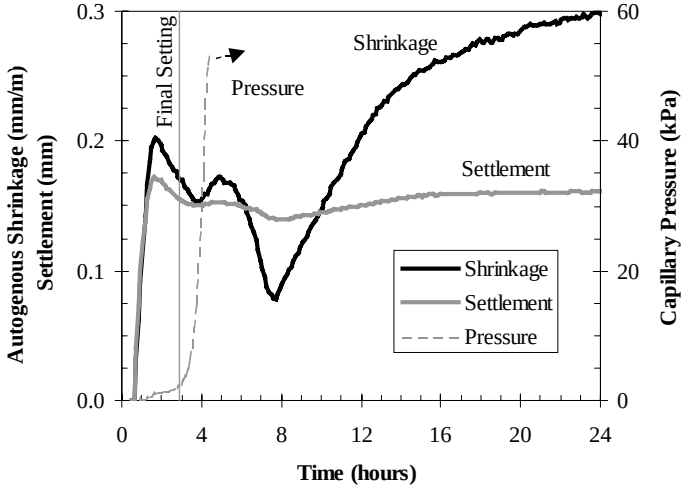

Figure 6.18. Typical early age autogenous shrinkage result.

In the test results presented in Figure 6.18 the values are not zeroed or referenced from a certain point, but are presented from the start of testing at 30 minutes. The vertical line shows the final set time at about 3 hours. Since there is so much activity during the first hours, the x-axis is magnified and another graphic is presented in Figure 6.19 for closer examination. In Figure 6.19, the vertical lines note both the initial and final setting times.

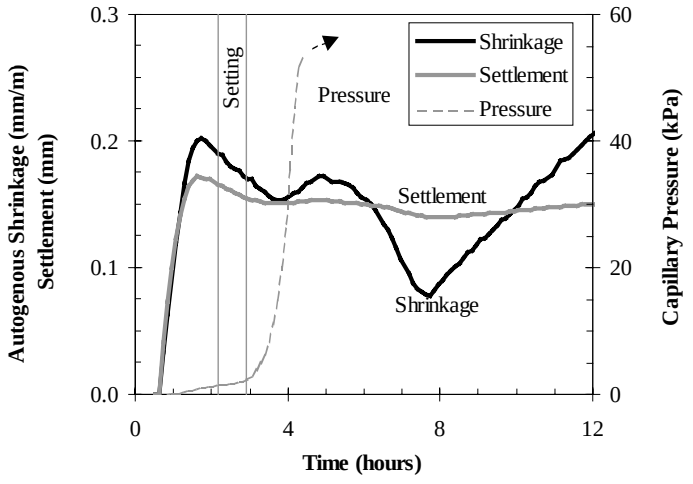

Figure 6.19. First 12 hours of the early age autogenous shrinkage result of Figure 6.18.

The first deformations of settlement and horizontal shrinkage occur immediately, from the age of about 30 to 90 minutes. After these deformations start, the capillary pressure also begins to develop and reaches a peak slightly over 50 kPa at about 4 ½ hours. The pressure will continue at a high level for many hours, though the physical measurement may have a "break through" and drop to a lower level (as explained in Section 5.2.3).

In the first hour the equipment arrangement correctly measures a large amount of settlement, or vertical shrinkage. This occurs due to the chemical shrinkage of the cement paste and the settlement of aggregate and cement particles. After about 90 minutes the rate of settlement slows due to the development of a loose internal skeleton that prevents further vertical movement.

The measurement of horizontal shrinkage has 5 distinct stages during the 12-hour test period. These stages can typically be found in the measurements of any cement paste, mortar or concrete. The stages are noted in Figure 6.20 and briefly described by the following points. The relevant time periods of each stage in Figure 6.20 are noted in parenthesis for this particular mixture. Some of these stages are also elaborated on in upcoming sub-sections.

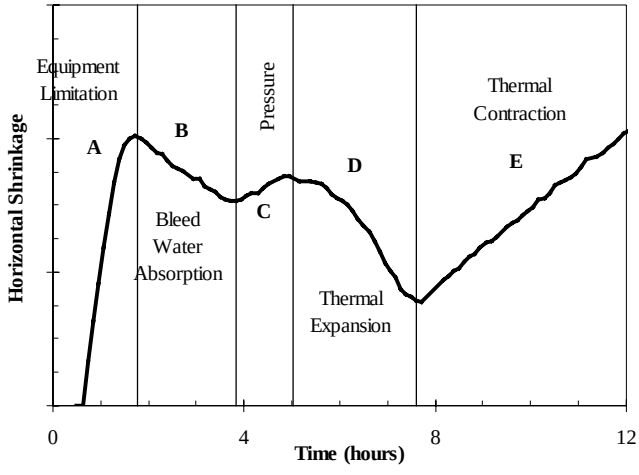

Figure 6.20. Various horizontal shrinkage stages in a typical early age slab test, including their governing factors.

- **A**: Very early stage:
  Equipment limitation due to settlement forces. (30 - 90 minutes)

  At the start of the test the equipment arrangement may measure excessively large horizontal shrinkage. Since the mortar is still liquid it is not possible for the mass to be displaced on the xy-plane. This measurement likely occurs as an artifact of the equipment arrangement, as the vertical settlement exerts a force on the measuring plates suspended vertically to detect horizontal movement. The measurement may be somewhat accurate but its reliability is questionable due to the limitations of the equipment. There is no consequence to this possibly erroneous measurement since the mortar can deform without stress prior to the initial setting time. This excessive shrinkage reading does not exist in the measurement of some mixtures, such as stiff mixtures with low workability and little settlement.

- **B**: Bleeding controlled stage:
  Bleed water absorption causes expansion. (90 minutes - 4 hours)

  As aggregate and cement particles settle, extra bleed water rises to the mortar's surface. Once the settlement in stage A is complete, the bleed water will be drawn back into the mortar by a small capillary suction. This re-absorption causes the mortar to expand.

- **C**: Pressure controlled stage:
  Development of pressure causes shrinkage. (4 + hours)

  After the bleed water has been fully re-absorbed the capillary pressure will develop. The capillary pressure is a result of the cement hydration, as described in Section 5.2.3. This pressure generates a stress, causing autogenous shrinkage. The shrinkage can be detected in both the vertical and horizontal directions. The capillary pressure will continue to instigate shrinkage into stages D and E but the shrinkage may be compensated by thermal changes.

- **D**: Thermally controlled stage:
  Cement heat of hydration causes thermal expansion. (5 - 8 hours)

  The hydration reaction of cement and water generates heat. The mortar will thermally expand as its temperature increases. This expansion exceeds the amount of shrinkage caused by the pressure in stage C. Therefore, the overall measurement shows a volume increase.

- **E**: Thermally controlled stage:
  End of cement heat generation causes thermal contraction. (8 + hours)

  This stage is the opposite of stage D since the mortar is now cooling due to the end of heat generation by the cement hydration. The cooling results in a contraction of the mortar, which will registers as a shrinkage. Some additional autogenous shrinkage may also be occurring due to continuing capillary pressure. At some point the cooling will end and the mortar temperature will reach equilibrium with the environment. The shrinkage can then continue at a slow, steady rate for many hours or even days as long-term autogenous shrinkage.

Before elaborating on the effects of bleed water and thermal expansion, it is important to examine the reference (zeroing) point used when interpreting horizontal shrinkage data and elaborate on how it is chosen.

6.3.2 Data Viewpoints and Their Uses

On first inspection, the horizontal shrinkage measured in the early age test arrangement seems to be literally “all over the place”. One may wonder how it is

ever possible to select a reference point from which to begin the comparisons of different concrete. That is why it is necessary to address the choice of such a zeroing point and reflect upon the uses for the different options.

There are three different reference points that can be selected for data interpretation: scientific, engineering, or structural. The selection of any of these points depends on the user and his or her purpose of conducting the test. It is important for this purpose to be identified prior to analyzing the results and drawing conclusions about the meanings. All of these reference points are valid in certain situations. The descriptions of the three options are as follows:

- Scientific

  From a scientific viewpoint, the data interpretation should begin from the very start of the test. This corresponds to the start of Stage A. There should be no manipulations or corrections applied to the test results. This viewpoint should be used if the fundamental principles controlling the shrinkage need to be identified.

  In this work, the scientific viewpoint cannot be accurately used for interpretation due to the extreme variation encountered in the first hour of measurements. In some cases there is a simple explanation for the shrinkage magnitude but not always. These early measurements are beyond the scope of the slab test arrangement. It has been seen that the non-homogeneous concrete provides too many “exceptions to the rules” to be able to identify the fundamental principles governing the shrinkage behavior.

  Using the scientific viewpoint of zeroing at the start of the test, any conclusions that are drawn in this work about the reactions in the first hours are only qualitative in nature.

- Engineering

  From an engineering viewpoint, the data interpretation should be done in a manner that provides conclusions for “all materials”. The shrinkage results should be analyzed to provide a guideline for the use of the concrete. They should not be dependent on the test arrangement, since the intent is to use the results for future material.

When analyzing the shrinkage data from an engineering viewpoint, the data must be corrected for any changes that are a function of the test arrangement. This means that the thermal movements caused by the cement hydration should be removed from the data prior to interpretation. The results would then be only a function of the material itself, independent of the size or shape of the element. The results can then be applied as generalizations about the particular concrete material being tested.

Using the engineering viewpoint in this work means that the reference point for the start of data interpretation is at the end of the bleeding stage. Bleeding and its implications are material properties and thus the reference point is after bleed water re-absorption. This corresponds to the start of Stage C. As earlier described, once the bleeding ends the capillary pressure, and thus true autogenous shrinkage, start. If there is no bleeding, the referencing point should be taken at the time of initial set. Prior to setting the material is still so fluid and no skeleton exists to restrain the stresses.

The engineering viewpoint requires correcting the data by removing the thermal dilation caused by hydration. Using the engineering reference point provides data that can be analyzed in a qualitative and quantitative manner.

- Structural

  From a structural viewpoint, the data interpretation is dependent on the test arrangement. The test arrangement is used to simulate an actual structure. This view considers the material properties as well as the constraints generated by the application for which they are used. This means that no corrections should be applied to the data and the reference (zeroing) point is selected for each particular test.

  When analyzing the shrinkage data from a structural viewpoint, the data is not corrected to remove the thermal dilation. The results are specific to the concrete mixture used in a 100-mm thick element (i.e. slab, floor, façade, etc.). This allows for interpretation of how the actual autogenous shrinkage magnitudes in a field situation will change as a result of altering material properties, such as cement type, w/c ratio, use of admixtures.

This method is useful when establishing trends resulting from adjustments to the mixture design. It may not give accurate quantitative results of the true autogenous shrinkage magnitude since the measurements include thermal dilation.

Using the structural viewpoint in this work means that the reference point for the start of data interpretation is when the expansion due to thermal changes is at its greatest. This corresponds to the start of Stage E. The thermal expansion generates compressive stress that is relieved by the relaxation upon cooling. Once there is relaxation then tensile stresses can be generated by the pressure-induced shrinkage. The time when these stresses start (after thermal expansion) is critical and this time is dependent on both the material and the size of the test specimen. The data can be analyzed qualitatively and quantitatively from the structural viewpoint.

Each of these three viewpoints can be used to establish the referencing point of the data. They all have merits for certain analysis intentions. When the scientific reference point is used, the accuracy is low and the results only qualitative. The engineering approach should be taken when the magnitude of the true autogenous shrinkage for a generalized material is of concern. A structural approach is the best option when the effects of mixture design are in consideration.

In the forthcoming analysis (Section 6.3.5) both the structural and engineering viewpoints are used for establishing the reference point of the autogenous shrinkage data. A summary table listing the values using the engineering viewpoint compared to the scientific viewpoint is included in Section 6.3.3.6. Prior to the analysis of this laboratory data, a few more points need to be clarified regarding the effects of bleed water and thermal dilation on the shrinkage stages (Sections 6.3.3 and Sections 6.3.4).

6.3.3 Effect of Bleed Water

When the mortar settles, excess mixing water rises in the concrete as *bleed water*. This water can appear on the surface of the slab or may be trapped under aggregate particles within the mortar. The maximum amount of bleed water is

present on the surface of the concrete at about the same time as the maximum settlement, which was about 90 minutes in Figure 6.19.

With no further settlement and a lack of a drying environment, the bleed water returns to the body. The bleed water is sucked back into the mortar to aid the cement hydration reactions. This suction force acting on the bleed water is confirmed by the presence of a small rise in capillary pressure at about 2 hours. The bleed water penetrates into the mortar and fills the voids that have been generated by the ongoing chemical shrinkage. This causes an expansion of the mortar, which can be seen in Figure 6.19 in both the vertical and horizontal directions from 2 to 4 hours. All of the bleed water must be re-absorbed prior to the development of significant capillary pressure. Without the significant capillary pressure there will be very little, if any, autogenous shrinkage.

After the bleed water is removed from the mortar surface, the continuing chemical shrinkage results in both vertical and horizontal shrinkage. In Figure 6.19 this period starts at the age of 4 hours, where the capillary pressure quickly begins to develop. This induces the gradual increase of shrinkage. From this point of 4 hours the true (engineering) autogenous shrinkage can be accurately measured.

It is very important to remember that the reference point for the autogenous shrinkage curves **should not** be taken until the bleed water has been re-absorbed into the concrete if the analysis is going to be quantitative. For this reason, interpretation of each test is concrete, or material, dependent.

In the example presented above, the point when the bleed water was fully-absorbed was only slightly beyond the final setting time of the mortar. This may not always be the case.

It would be erroneous to choose the zeroing point dependent on the setting time because in an extremely workable mixture the bleed water may still be present on the surface. The swelling of the mortar would continue and induce additional, non-consequential compressive strains. Only once these strains have relaxed into tension will there be a risk of cracking.

On the other hand, if a particular mortar mixture is stiff, there may be less settlement and no bleeding (i.e. upcoming in Figure 6.30 at w/c = 0.30). In such a case the autogenous shrinkage would start much earlier and may occur prior to the final setting time. It is possible that the autogenous shrinkage may begin from the start of testing time (prior to initial set) if the mixture is extremely stiff and rigid. In this case measurements are obtained during the "liquid" phase of free movement when no stresses occur and the selection of the reference point needs to be carefully evaluated. In this work, the earliest possible reference point was taken at the time of initial set when quantifying the autogenous shrinkage.

Any horizontal shrinkage prior to a defined "initial set" is an artifact of the test arrangement for measuring setting (as described for Stage A in Figure 6.20). The time when an initial skeleton is formed may be earlier than defined by the setting equipment. Examples of these types of mixtures with more or less bleed water will be given in the upcoming results in Section 6.3.5.

This limitation of autogenous shrinkage occurring after bleed water removal is true for any concrete, mortar or cement paste. As the slab thickness in this work was only 100 mm, it was assumed that the distance the rising bleed water moved to the surface was not significant enough to produce a moisture gradient over the cross-section during the first hours. This assumption was supported by the measurement of equivalent capillary pressure at various slab depths. In practice, if the slab was much thicker or the concrete was poured into a massively thick structure (such as a dam), there may be uneven moisture movement due to localized bleeding which would create a variation in the early age autogenous shrinkage over the element's cross-section.

The amount of bleed water in these tests is impossible to control by construction handling practices, since it is only a function of the mixture proportions. Even though a quantitative amount of external bleed water can be measured for different mixtures by another Finnish test standard (similar to ASTM C232), it was not done in this work. In the early age test arrangement it is not possible to directly measure the amount of water off of the slab test specimen without disrupting the mass. Therefore the estimate of bleed water for various mixtures was only done by visual observations.

When interpreting slab test data for cement paste and mortar is also important to note the effects of the temperature history in the material. Often coinciding with the time of bleed water re-absorption is the start of heat generation due to the cement hydration. The method of removing the thermal volume change due to this cement hydration for data interpretation from an engineering viewpoint is addressed in the following sub-section.

6.3.4 Effect of Hydration Heat

As cement reacts with water in the process of hydration, a large amount of heat can be generated. This thermal change resulting from the cement hydration was explained in Section 2.2.1 and discussions in Section 6.3.2 addressed how it can alter the reference point for data interpretation. If the data is to be analyzed from an engineering viewpoint, it is necessary to correct the measurements by removing the thermal dilation. Only after such a correction is it possible to make generalizations about the full magnitude of autogenous shrinkage that is expected for a material. The process of making such thermal corrections is detailed in the next paragraphs.

To account for the thermal dilation it is necessary to know how the temperature changes in the concrete with time. Sample temperature profiles for paste, mortar, and concrete are shown in Figure 6.21. The paste and mortar have w/c ratios of 0.35 and the concrete has a w/c ratio of 0.30 and includes superplasticizer. The mortar shown is the same one that was presented in the example of Figure 6.19 of Section 6.3.2. This concrete's temperature rose to a maximum of 36°C at 8 hours, while the mortar reached 42°C and the paste reached 71°C at 9 hours. It is important to note in this figure that the heat of hydration begins to develop at approximately 4 hours for this particular Finnish gray cement.

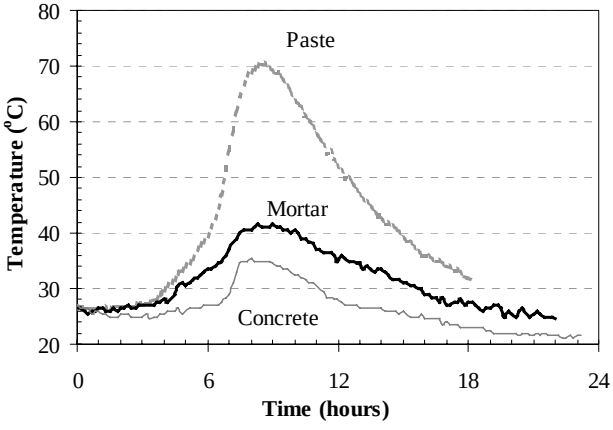

Figure 6.21. Sample temperature development with time since concrete mixing. Paste and mortar at w/c=0.35 and concrete with superplasticizer w/c=0.30.

As described in Section 2.2.1, the thermal dilation of concrete during the early ages is very difficult to measure. Hedlund [1996] had measured a value of approximately 25 με/°C for a concrete at the age of 10 hours. A best fit line approximated by Equation 27 was found based on Hedlund's and Weigler's data (Figure 2.10 Section 2.2.1) for concrete, as shown in Figure 6.22. This equation was used to estimate the thermal expansion during the early ages for the tests in this work.

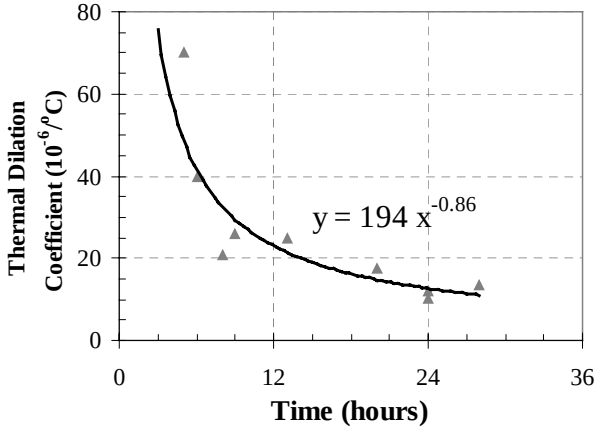

Figure 6.22. Early age thermal dilation coefficients for concrete, including best-fit line. [Hedlund 1996, Byfors 1980]

It must be noted that for mortars or paste the thermal dilation might be different than given by Hedlund's concrete estimates. On the other hand, the value of Hedlund's coefficient of thermal dilation is in-line with the values given in Finnish literature and presented in Table 2.3 of Section 2.2.1. [Jokela et al. 1980] In the mortar mixture of Figure 6.21 the aggregate-to-cement ratio was 1.5, which corresponds to a thermal dilation coefficient of 12.9 με/°C for mature concrete in Table 2.3.

$$TE = 193.9t^{-0.86} \quad , \quad \text{for } 3 < t < 24 \text{ hours} \tag{28}$$

where: TE = thermal expansion, με/°C, and
t = time, hours.

The thermal expansion coefficient was then adjusted to fit each mixture based on the maturity function given in Equation 28. This was done to correct for the variation in development of strength and temperature.

$$M = \sum \frac{T_C + 10}{T_O + 10} \times \Delta t \tag{29}$$

where: M = Maturity, hours,
T_C = concrete temperature, °C,
T_O = standard testing temperature, 20 °C, and
Δt = change in time, hours.

The maturity-adjusted thermal expansion coefficients were then multiplied by the mortar temperature history shown on the left axis of Figure 6.23 (same mortar data as in Figure 6.21) to give the thermal expansion values. These maturity adjusted thermal expansion results are given on the right y-axis of Figure 6.23 and are represented by the gray dashed line. This figure shows a volume change of -0.4 mm/m (expansion) can be expected due to the thermal changes in the mortar resulting from cement hydration. Note that the contraction due to cooling is less than the expansion generated with heating due to the lowering thermal dilation coefficient.

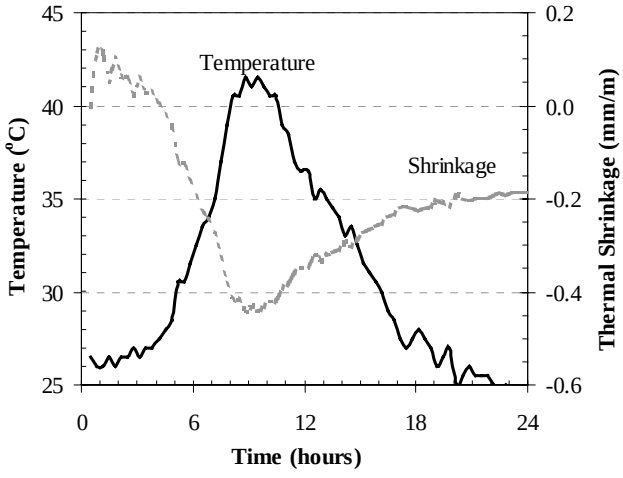

Figure 6.23. Temperature rise and resulting thermal expansion based on maturity for the mortar in Figure 6.26, due to a temperature rise to 42 ℃ at 9 hours.

These calculations of the mortar's thermal expansion adjusted for maturity provide a means for correcting the autogenous shrinkage slab data for the engineering viewpoint analysis. It is now possible to factor out the effects of thermal expansion from the measurements on the early age slab, which included the volume change due to both autogenous and thermal reactions.

If the early age test arrangement was thermally controlled to remove the effects of the cement hydration, then the resulting measurement would be a true autogenous shrinkage. Figure 6.24 shows the measured horizontal shrinkage of the mortar from Figure 6.18, zeroed at the start of stage C when the expansion due to re-absorption of bleeding ended. In the previous section this reference point was shown to be valid when interpreting data from an engineering viewpoint. The earlier horizontal shrinkage resulting from settlement and re-absorption of bleed water prior to 4 hours still exists but is omitted for this interpretation.

Above the measured line in Figure 6.24, the horizontal shrinkage has been re-calculated as a corrected shrinkage. This corrected shrinkage has removed the thermal dilation shown in Figure 6.23. The corrected isothermal shrinkage now shows a continuous autogenous shrinkage starting at 4 hours, resulting from the

increase in capillary pressure. This is the true "risky" autogenous shrinkage that should be considered when evaluation the final shrinkage magnitude and crack risk of the mortar from the engineering viewpoint.

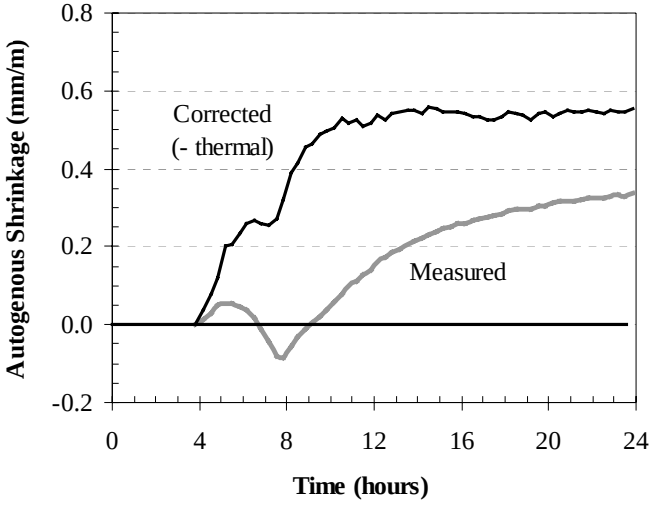

Figure 6.24. Basic measured mortar shrinkage and then corrected with maturity for actual value if thermally controlled, following Figures 6.18.

In Figure 6.24, the measured line correctly showed an autogenous shrinkage due to chemical shrinkage from 4 to 5 hours. But the small change or platform from 5 to 6 hours resulted from the increase in the mortar's temperature, generating an expansion that counteracted the shrinkage. From 6 to 8 hours the continued climb of the temperature resulted in expansion exceeding the amount of autogenous shrinkage. The expanding mortar fills the voids created by the chemical shrinkage reactions. The available expansion space can be slightly aided by the thermal expansion of the stainless steel mold, which is estimated to be 0.08 mm/m for a temperature rise of 5°C (17×10^{-6}/°C [Gere & Timoshenko 1990]). But there is still some restraint provided by the mold walls that inhibits the concrete from horizontally expanding as much as desired.

At 9 hours the mortar reached its peak temperature and thereafter started to cool, generating thermal contractions or shrinkage. Therefore the thermal shrinkage would be added to the autogenous shrinkage already underway (but undetected by the measured line). By subtracting out the length changes due to the thermal

dilation it is possible to get the corrected or true autogenous shrinkage, given by the gray line. As earlier described, for some analysis objectives it is accurate to also zero this corrected line at the point when the autogenous shrinkage started, after bleed water re-absorption.

Figure 6.24 shows that the true or corrected autogenous shrinkage would be greatest at about 10 hours (0.5 mm/m) and would remain at this platform level. The measured autogenous shrinkage shows a continuous shrinkage gain after 10 hours but this is actually due to the thermal contraction due to cooling which is removed in the corrected line. In the corrected line there is small dip from 6 - 7 hours where the mortar is no longer shrinking. This is a limitation of the applied correction method, representing the mortar trying to thermally expand more than was allowed by the space generated by the chemical shrinkage. Such a phenomenon exists in tests where the material was not shrinking in the first hours, such as when bleed water was present, and thus there was a lack of space generated for the later expansion.

With the rigid mold restrain, the mortar is not allowed to expand as much as desired and a “hold” resulted on the amount of further movement (shown by the flat part of the “measured” curve right before 8 hours). Therefore, if a dip or shelf is present in the engineering data results the early age autogenous shrinkage will be slightly underestimated or conservative.

A best-fit line could be drawn to approximate the unrestrained autogenous shrinkage, correcting for the dip and simulating free movement. The line should extend with an equal shrinkage rate or slope of the line from 4 to 6 hours and move parallel to the shrinkage resuming after 9 hours. This approximate curve is a estimate of the corrected curve of Figure 6.24 and is shown in Figure 6.25.

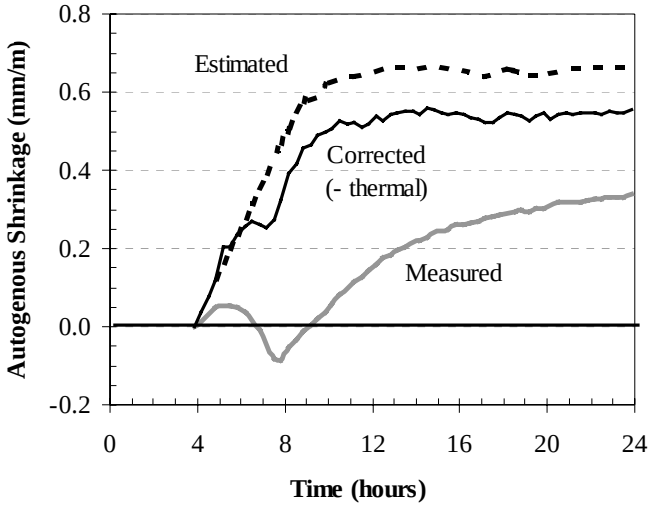

Figure 6.25. Estimated autogenous shrinkage of Figure 6.24, removing the shrinkage shelf at 6 hours in the corrected curve caused by mold restraint of the thermal expansion.

This example has shown that the slab-measured values underestimate the true autogenous shrinkage because of the influences of thermal dilation. If the data analysis is to be performed from the engineering viewpoint (to make generalizations about the tested materials), it is necessary to make such thermal corrections to all data prior to interpretation.

6.3.5 Effect of Capillary Pressure

During the early age a capillary pressure will develop due to the reactions within concrete. As described in Section 2.2.3, as the pressure builds up it induces stresses pulling the capillary pore walls closer together. The moving paste registers as the early age shrinkage and therefore the development of pressure is an indicator of the instigation of volume change.

Capillary pressure was measured in each early age autogenous shrinkage test. A typical result with the autogenous shrinkage increasing at the same time as the pressure development was given in Figure 6.19 of Section 6.3.1. The pressure was responsible for stage C of the shrinkage (Figure 6.20) and continues to contribute in the next stages. Further examples of the relationship of developing

pressure to shrinkage will be given in the upcoming results of the effect of mixture designs (Section 6.3.7).

6.3.6 Repeatability

The repeatability of the early age test method was evaluated to check the validity of the horizontal shrinkage equipment. Since the test arrangement had been developed and recently modified at VTT, the repeatability tests insured the pertinence of the equipment measurements in this work. The validity could be checked from two different approaches: from the start or end of testing.

Typically a repeatability analysis is taken from the reference point at the beginning of the test. For the data interpreted by the structural viewpoint in this work, this was at the time of maximum thermal expansion. The shrinkage curves were equivalent from this start point and then diverged as they approached 24 hours at the end of the test. On the other hand, the repeatability could be referenced at the end of the test and viewed in reverse. This provides a means of evaluating at what point, or how early, the test method is measuring data with too much divergence from the mean. It is known that at 24 hours the concrete has hardened and gained enough strength to resist shrinking stresses, so the change in all data measurements should be nearly zero during the last hours. Therefore, the repeatability data curves could be zeroed at either the start or end of the data curves.

The early age slab test repeatability for one mortar is shown in Figure 6.26. This data reference point was taken at the point of maximum thermal expansion (approximately 8 hours), in accordance with the structural viewpoint for analyses of concrete that is material- and test arrangement dependent. The data is not thermally corrected prior to the zeroing. Tests A1 and A2 are two simultaneous measurements on the same slab, while tests B and C are tests done on repeated mixtures the following days.

From the data presented in Figure 6.26, the reliability that the results are within the 90% probability range is about 15%. This is given in Table 6.8, with the values of 10 and 17% error at the ages of 12 and 24 hours, respectively. The coefficient of variation was also found to be approximately 10%, which was an acceptable level considering the non-homogenous nature of concrete materials.

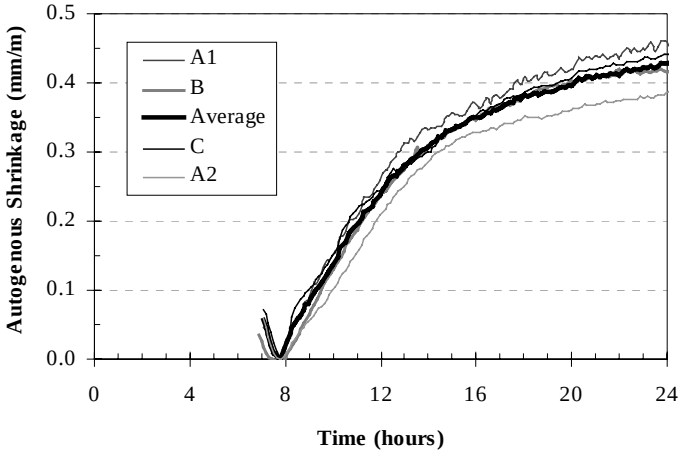

Figure 6.26. Repeatability of autogenous shrinkage test, on mortars with w/c = 0.35 and 780 kg/m^3 Finnish gray cement, no superplasticizer. Reference (zeroing) point of results at maximum thermal expansion for structural viewpoint analysis.

Table 6.8. Average values of shrinkage at 12 and 24 hours for 3 mortar tests from Figure 6.26. Average, standard deviation, variation and error within 90% probability given in bottom rows.

Test	Shrinkage (mm/m)	
	12 hours	24 hours
A1	0.27	0.45
B	0.23	0.42
C	0.24	0.44
A2	0.21	0.39
Average	0.24	0.43
SD	0.03	0.03
Variation (%)	12.5	7.0
Error (±%)	17.3	10.3

The repeatability can also be presented for data where the thermal corrections are applied. This would be beneficial when doing analysis from the engineering viewpoint with the intention of interpreting general material properties. Figure

6.27 shows the repeatability of two mixtures with a w/c = 0.40 and 685 kg/m^3 of Finnish gray cement. The data was taken from two measurements on one slab and a third measurement on a second slab. The temperature history was only taken once for the mixtures, which had a peak temperature of 38ºC at 11.5 hours.

For this set of tests the reference point should be at the end of bleed water re-absorption, about 2 hours. When checking the repeatability, it is another option to zero all measurements at the final measuring point and work in reverse to see when the data diverges. Therefore, it is important to note in Figure 6.27 that the results have been shifted so that all horizontal shrinkage is equivalent to 0.40 mm/m at 24 hours. Thus the curves should be viewed in reverse, progressing to the left towards t = 0 hours. Using this frame of reference, it is possible to see where the error arose when comparing the 3 measurements.

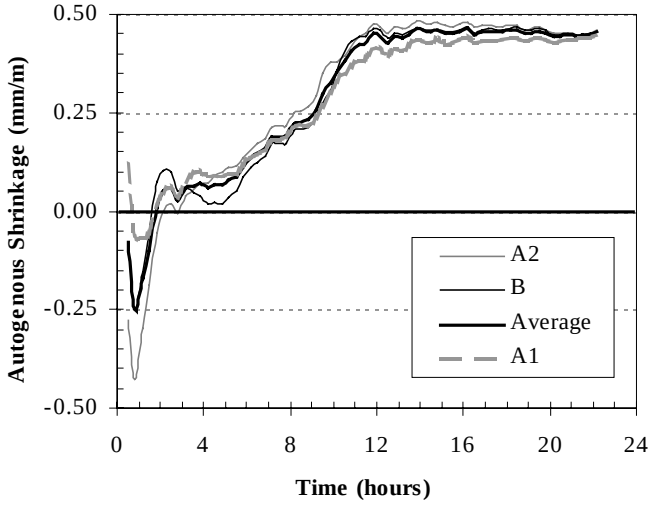

Figure 6.27. Repeatability of autogenous shrinkage test from engineering viewpoint, on mortar with w/c = 0.40 and 685 kg/m^3 Finnish gray cement, no superplasticizer.

The repeatability of this second set of measurements is also quite good. There is not much variation in the data from the age of 8 to 22 hours. Visually assessing Figure 6.27 shows that the results begin to diverge prior to 4 hours, which would be the actual reference (zeroing) point for the engineering viewpoint. This validates the test method for early age shrinkage with acceptable repeatability.

Table 6.9 includes the statistical analysis for the data from Figure 6.27. The reliability that the results are within the 90% probability range is about 15% if the average is taken from the 8 and 12-hour error values. In this case the results were referenced together from 24 hours and viewed in reverse, so it is important that there is not much variation or error from 8 to 12 hours. The coefficient of variation was also found to be approximately 10%, which was an acceptable level considering the non-homogenous nature of concrete materials.

Table 6.9. Average values and statistical analysis of shrinkage at 4, 8 and 12 hours for mortar tests of Figure 6.27.

	Shrinkage (mm/m)			
Test	4 hours	8 hours	12 hours	20 hours
A1	0.09	0.21	0.41	0.43
B	0.02	0.21	0.46	0.45
A2	0.07	0.25	0.47	0.45
Average	0.06	0.22	0.45	0.44
SD	0.04	0.02	0.03	0.01
Variation (%)	60.1	10.3	7.2	2.6
Error (±%)	99.2	17.1	11.9	4.3

Possible sources of error in the early age shrinkage test arrangement include:

- friction of the mold walls and concrete inhibiting horizontal and vertical shrinkage (though attempts were made to eliminate the friction by the plastic and talc liner),
- restraint provided by the mold walls inhibiting expansion due to thermal heat of hydration,
- contact between the LVDT pin and holder (though they should be non-contact and free to move) that would reduce the amount of movement detected, and
- air bubbles penetrating the capillary pressure transducer preventing a measure of internal pressure and only registering air pressure readings.

6.3.7 Effect of Mixture Design

This section presents the early age autogenous shrinkage results of the slab test when the mixture design were altered. The main tests were done on mortars, since they allow comparison to the chemical shrinkage tests. Testing mortars had the secondary effect of complicating the data interpretation due to their greater thermal change during the early ages compared to concrete. The mixture parameters that were altered included water-to-cement ratio (w/c), the use of a superplasticizer admixture, and Finnish cement type. The tests are summarized in Table 6.10 along with their measured setting times and temperature histories. All mixtures had materials at 20°C at the start of mixing. The time when the bleed water was re-absorbed is also listed, but these times are based on estimates from the horizontal shrinkage data (as described in Section 6.3.1 at the end of stage B). Finally, the time when the capillary pressure started to develop is noted in Table 6.10 based on the test data. This development point was taken when the pressure reached a level of 3kPa.

Table 6.10. Summary of early age autogenous slab test mixtures.

Type	w/c	SP	Cement	Initial Set (hr:min)	Bleeding Done (hr:min)	Pressure Start (hr:min)	Temperature Peak (°C)	Temperature Time (hr:min)
Paste	0.35	-	Rapid	3:15	4:10	4:10	70.3	9:00
Mortar	0.30	-	Rapid	1:30	-	2:15	44.0	7:50
Mortar	0.35	-	Rapid	2:10	3:50	3:10	41.5	8:50
Mortar	0.40	-	Rapid	2:25	4:30	4:10	37.8	11:50
Mortar	0.45	-	Rapid	3:35	7:50	6:30	34.5	12:10
Mortar	0.30	1%	Rapid	1:30	-	2:30	47.5	8:00
Mortar	0.30	-	Yleis	2:20	2:30	3:20	42.5	9:30
Mortar	0.30	-	White	1:55	3:10	3:20	39.5	7:20
Mortar	0.30	-	SR	2:35	4:10	-	36.5	10:00
Concrete	0.30	5%	Rapid	0:35	-	3:00	35.5	8:00
Concrete	0.35	2%	Rapid	2:35	-	2:25	34.0	9:00

All of the results in the following sub-sections are presented using both the structural and engineering viewpoints, as graphs ‘a’ and ‘c’. This means that the

referencing (zeroing) point is taken from a different point for the two different graphic depictions of each test scenario. The temperature histories of the mixtures in each scenario are also presented prior to the engineering data (graph 'b'), since the engineering data requires removal of the thermal dilation to show the pure autogenous shrinkage. The engineering viewpoint data is useful if numeric modeling were to be done, since it gives a quantitative amount of the early age autogenous shrinkage.

Interpretation the data from a structural viewpoint is sufficient when the goal is to identify trends when altering the mixture designs. This data represent what would be expected in field practice on a 100 mm deep slab. This is a representative depth of floor slabs and façade elements in Finland. There is a higher confidence in the reliability of the structural viewpoint raw data actually measured in the slab test arrangement prior to manipulation with the assumed thermal corrections.

Both depictions by engineering or structural referencing show the same trends when the material parameters are changed yet the final magnitude is slightly different. The ultimate early age autogenous shrinkage (at 24 hours) is higher when the structural viewpoint is used since it also includes the thermal contraction resulting in the cooling material. A table summarizing the variation in the 12 and 24 hour magnitude of each of these mixtures from both the structural and engineering is presented in Section 6.3.7.6.

After the shrinkage representations in each of the following sub-sections there is also a figure showing the corresponding development of capillary pressure, as mentioned in Section 6.3.5. Note that the pressures usually reach a sudden break-through maximum but this is merely a limitation of the equipment (see Section 5.2.3). The main observation from the pressure figures should be the time when pressure starts. The onset of pressure corresponds to the time when shrinkage starts, as long as the bleed water has been removed.

6.3.7.1 Cement Paste

Early age measurements of autogenous shrinkage for cement pastes are not very representative of the true behavior of concrete because of their large thermal changes. The high heat of hydration of the cement paste will result in a large

thermal expansion and thus the slab shrinkage measurements will include this change. As described in Section 6.1.2, it would be very difficult to have a practical “slab” measuring arrangement that could keep the cement paste in isothermal conditions through the test. Figure 6.28 shows one of the few tests done on cement paste in the autogenous shrinkage test arrangement. The paste can be compared to a similar mortar at the same w/c ratio of 0.35 with no superplasticizer. Figure 6.28a presents the data from the structural viewpoint where the referencing is done at the time of maximum thermal expansion. Figure 6.28b presents the thermal change due to cement hydration, which are used to correct the data for the presentation of the engineering viewpoint data in Figure 6.28c. Note that the mortar mixture given in Figure 6.28 is the same mortar that was detailed in Figures 6.23 to 6.26.

For the structural viewpoint, the data was referenced at the time of maximum thermal expansion. This reference point was different for each mixture, depending on the time when the peak temperature occurred (Figure 6.28b). For the engineering viewpoint, the data was referenced at the time when all of the bleed water was reabsorbed to the mixture and thus there was an end of expansion prior to capillary pressure development. For the mortar and neat paste mixtures of Figure 6.28c this was at about 4 hours. If there had been no bleeding the reference point would have been taken at the time of initial set. As will be seen in all the forthcoming tests, these referencing points changes for each mixture depending on the bleeding and temperature.

As expected, the neat paste had much greater shrinkage than the mortar due to the lack of aggregate providing restraint. The difference in the two mixtures was nearly the same when presented from either the structural or engineering viewpoint, with both analysis methods showing the neat paste having about 1.7 times greater shrinkage compared to the mortar. The engineering viewpoint data would have increased if the later expansion due to cooling could be corrected for the paste with better thermal dilation assumptions.

In the engineering presentation, the autogenous shrinkage had ended by about 12 hours, at which time the material had hardened enough to resist the forces causing shrinkage. This is different than the data presented by the structural viewpoint, where the magnitude of shrinkage continued to increase throughout

the 24-hour test. The same trend will be shown in additional mortar graphs of this section.

In the engineering data presentation, both mixtures exhibited a shelf at approximately 6 to 8 hours where there was greater thermal expansion than autogenous shrinkage and the mold was restraining the movement. Therefore it is expected that on a larger slab with free movement the mixtures could have a slightly greater final magnitude of autogenous shrinkage at 24 hours. This correction was applied and is represented by the dashed line for each mixture. The paste magnitude did not change when removing the shelf, while the mortar mixture had a greater ultimate shrinkage. This was earlier described in Section 6.3.4 and Figure 6.25.

(a) Structural Viewpoint

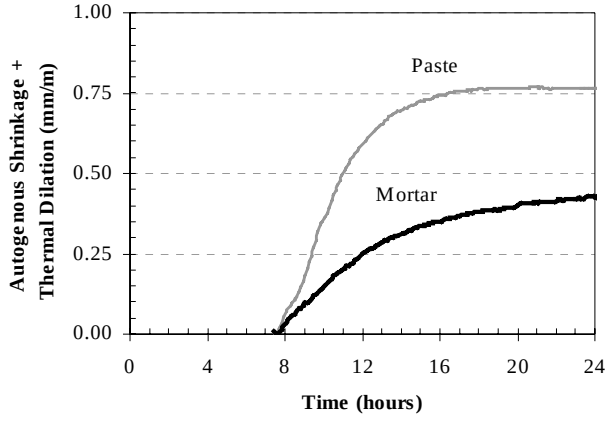

(b) Thermal Change

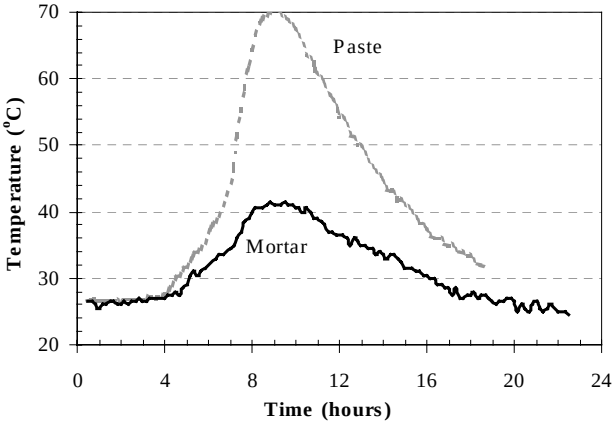

(c) Engineering Viewpoint

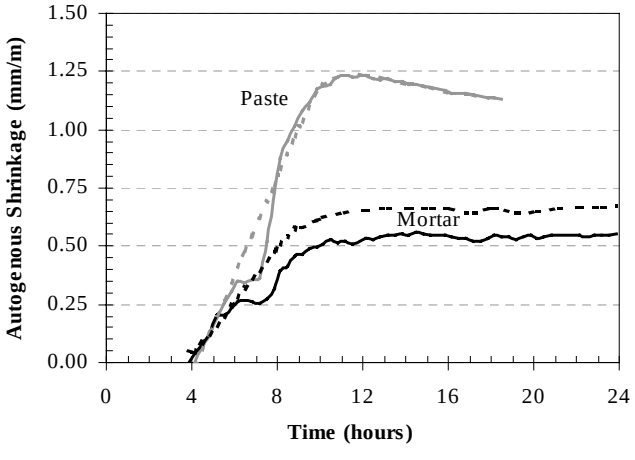

Figure 6.28. Comparison of mortar and paste in autogenous shrinkage test, with w/c = 0.35 and no superplasticizer.

The paste mixture in Figure 6.28c also showed a slight expansion beyond 12 hours. This is probably not an accurate depiction resulting from too great of a calculated thermal contraction as the mixture cooled. A more accurate measure of the thermal dilation coefficient would be required to improve the paste's true autogenous shrinkage estimate in the first day.

Figure 6.29 shows the pressure build-up corresponding to the shrinkages of Figure 6.28. In the case of the mortar mixture, the bleed water was not fully absorbed until 3 hours and 50 minutes (Table 6.10) so the onset of pressure before that time did not contribute to the shrinkage (Figure 6.28c). The paste bleed water was absorbed at 4 hours and 10 minutes, at which time both the pressure and shrinkage started.

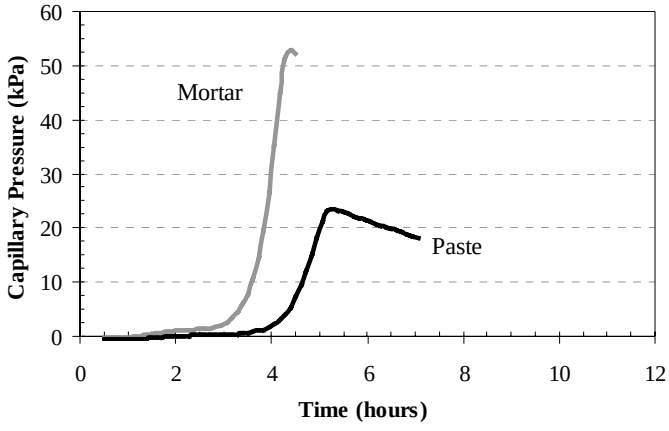

Figure 6.29. Comparison of capillary pressure for mortar and paste in autogenous shrinkage test from Figure 6.28, with w/c = 0.35 and no superplasticizer.

6.3.7.2 Water-to-Cement Ratio

The next set of tests investigated the changes in autogenous shrinkage magnitude due to the variation in w/c ratio of mortars. The w/c ratio was changed from 0.30 to 0.45 while the water amount was held constant at 275 kg/m^3. This corresponds to an increasing cement content and paste content while the aggregate amount remained constant. No superplasticizers were added to the mortars so the workability varied with the four mixtures. Again, the structural viewpoint is presented is Figure 6.30a, with the temperature profile in Figure

6.30b and the engineering viewpoint data in Figure 6.30c. The mortar with a w/c of 0.35 is the same mixture that was presented in Figure 6.28.

In Figure 6.30a for the structural viewpoint, the data was referenced at the time of maximum thermal expansion. The mixture with a w/c ratio of 0.30 was quite stiff and had very low workability, probably corresponding to a slump of 0 mm. It also had the earliest temperature peak but it never showed an accumulative expansion so the data was referenced at the time of initial set (90 minutes). The other three mixtures all showed a thermal expansion exceeding the amount of shrinkage after the bleed water absorption period and were then zeroed at the low point. This referencing point coincided with the time of maximum thermal expansion, as can be seen in Figure 6.30b.

In Figure 6.30c for the engineering viewpoint, the data was referenced at the time when the bleed water absorption was completed. For the mixture with a w/c of 0.30 there was no bleeding so the referencing was done at 90 minutes, the time of initial set. All the mortar mixtures of this test set had increasing workability and also increasing bleeding amounts as the w/c increased, and thus the referencing point was later with succeeding w/c ratios.

Again there was a shelf in the data of the 0.35 w/c mixture, due to the restraint provided by the mold as thermal expansion exceeded pure autogenous shrinkage at about 6 hours. The dashed line for the 0.35 w/c mixture estimates the corrected curve.

The trend of increasing shrinkage at a lower w/c ratio held true in both the structural and engineering viewpoints. Again, the structural data (Figure 6.30a) showed a continued increase in shrinkage over the 24-hour test period, while the engineering data (Figure 6.30c) showed the shrinkage ending at about the time of peak temperature. The temperature peaks were lower and slightly later as the w/c ratio increased, as seen from Figure 6.30b.

As expected, the mortar with the lowest w/c ratio had the greatest amount of autogenous shrinkage. This is because the mixtures have increasing cement at the lower w/c ratios. As seen from the chemical shrinkage tests, with equivalent cement content the chemical shrinkage was constant (Figure 6.11 in Section 6.2.1) but as the cement content increased the shrinkage also increased. Since the

chemical shrinkage drives the autogenous shrinkage, the same trend was seen here in the slab test results.

Most of the mixtures presented from the engineering viewpoint had slightly greater ultimate (24 hour) shrinkage than the data presented by the structural viewpoint. Only the mixture with a w/c of 0.45 had less shrinkage when thermally corrected in the engineering viewpoint compared to the original raw data. The pure autogenous shrinkage values taken from the engineering viewpoint were increased approximately 38 to 55% at the low w/c compared to the structural viewpoint, while it was decreased 12% at the 0.45 w/c. Using the pure autogenous shrinkage (Figure 6.30c), the mortar with a w/c of 0.30 had six times the amount of shrinkage as the 0.45 mortar.

(a) Structural Viewpoint

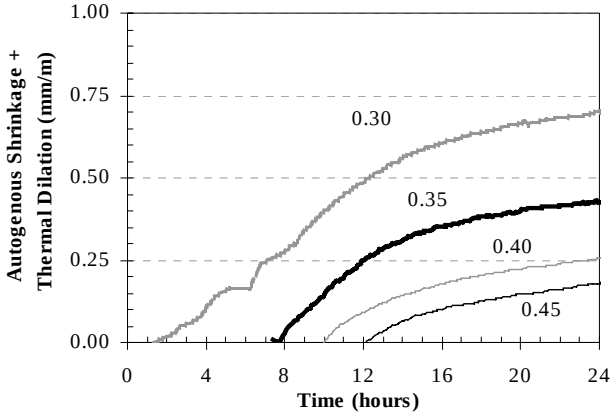

(b) Thermal Change

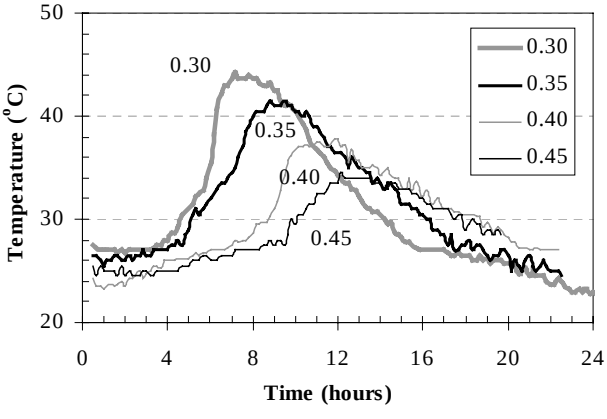

(c) Engineering Viewpoint

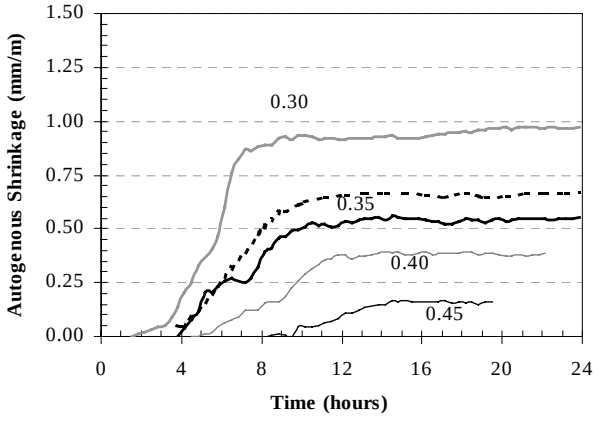

Figure 6.30. Comparison of changing w/c ratio in autogenous shrinkage test, with water amount = 275 kg/m^3 and no superplasticizer.

Figure 6.31 shows the pressure build-up corresponding to the shrinkages of Figure 6.30. As expected, as the w/c ratio of the mortar mixtures was lowered the capillary pressure started earlier. This is due to the finer pores in the microstructure and lower amount of water in the mixtures at low w/c ratios. The 0.30 w/c mixture had an initial setting time of 1 hour and 30 minutes (Table 6.10), no bleeding, and the pressure began rising at about 2 hours. Near the same time the shrinkage began. The other mixtures had later setting times and a delayed onset of pressure, as well as a delayed start of horizontal shrinking. Since the mortars with w/c ratios of 0.40 and 0.45 had much later bleed water absorption times (4:30 and 7:50, in Table 6.10) the early development of capillary pressure did not induce shrinkage.

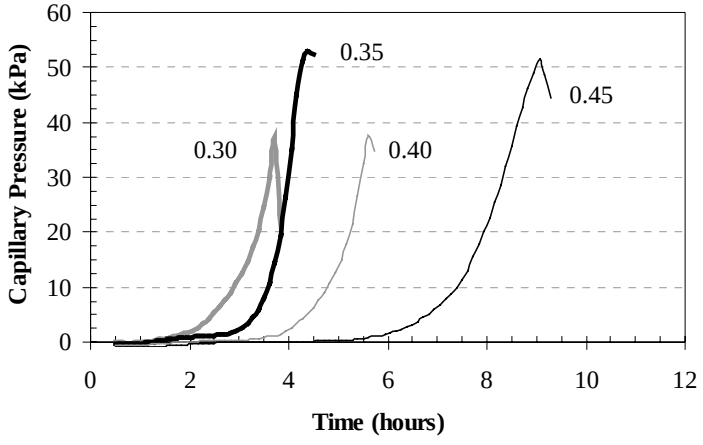

Figure 6.31. Comparison of capillary pressure changing w/c ratio in autogenous shrinkage test from Figure 6.30, with water amount = 275 kg/m^3 and no superplasticizer.

6.3.7.3 Superplasticizers

To test mortars at a lower w/c ratio it would be necessary to add a superplasticizer to the mixture to improve the workability and allow for adequate placement of the mixture. The effect on autogenous shrinkage when a superplasticizer (SP) was added to a mortar with a w/c of 0.30 is shown in Figure 6.32. Both mixtures had identical proportioning except for the addition of the chemical. Therefore, their workabilities were different but both mixtures still

had little, if any bleed water. The non-superplasticized mixture is the same as the mortar with a w/c of 0.30 in Figure 6.30.

Since there was little bleeding and no signs of expansion due to bleed water re-absorption, the data curves were referenced at the time of initial set (90 minutes). In this case the setting time was not delayed with the addition of the superplasticizer, as is often expected. Both the structural viewpoint (Figure 6.32a) and engineering viewpoint (Figure 6.32c) data are referenced at the same point.

Since the structural data includes thermal dilation, it had a lower ultimate shrinkage than the reference mixture. The thermal dilation coefficient is great in the first hours of expansion than during cooling and contraction in the later hours. When the structural viewpoint data is referenced after the thermal expansion, the contraction provided by cooling is less than was created by the expansion. Thus the ultimate structural data is less than the values obtained by the engineering viewpoint. The ultimate autogenous shrinkage magnitude (24 hours) for the data presented by the engineering viewpoint of Figure 6.32c was 20 to 40% greater (no SP and SP, respectively) than the data by the structural viewpoint of Figure 6.32a.

The temperature peak of the two mixtures was at about the same time of 8 hours, though the superplasticized mortar had a slightly greater temperature rise. The engineering data of Figure 6.32c platformed near this time of peak temperatures while the structural data of Figure 6.32a continued to show increased autogenous shrinkage due to the thermal contraction. Even with this difference of shrinkage rate, the variation between the two mixtures was nearly the same by either representation due to their similar temperature histories. From the structural viewpoint the superplasticized mixture had shrinkage 78% greater than the reference mixture, while from the engineering viewpoint the increase was only 50%. The greater autogenous shrinkage with superplasticizer was a result of the improved cement dispersion and faster rate of hydration reactions generating shrinkage. An identical trend was shown in the chemical shrinkage tests for the same Finnish gray cement paste (Figure 6.7 in Section 6.2.1).

(a) Structural Viewpoint

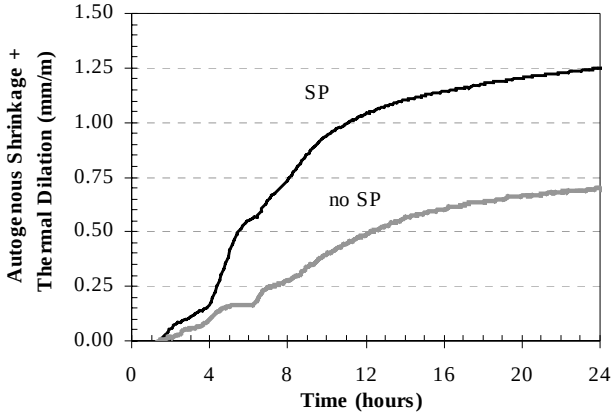

(b) Thermal Change

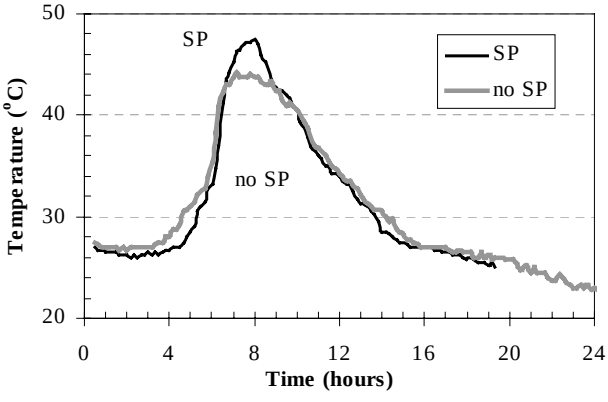

(c) Engineering Viewpoint

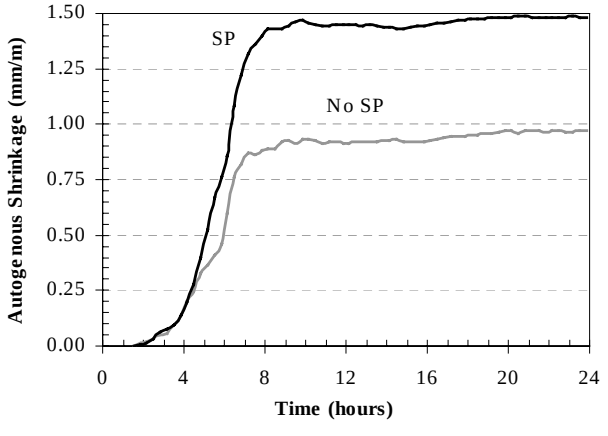

Figure 6.32. Comparison of adding superplasticizer in autogenous shrinkage test, with w/c = 0.30 and water amount = 275 kg/m^3.

Figure 6.33 shows the pressure build-up corresponding to the shrinkages of Figure 6.32. In both mixtures the capillary pressure began to develop at 2 hours. Neither of these mixtures had any bleeding so the shrinkage curves were referenced for both viewpoints at the time of initial setting (90 minutes), which is also when the capillary pressure began to rise.

One important pressure aspect to note from Figure 6.29 is that the rate of pressure development was greater for the non-superplasticized mixture (no SP), yet this mixture had a lower amount of shrinkage in both Figure 6.30a and 6.30c. The rates of pressure development for many mixtures in this work were evaluated by taking the first derivatives of the pressure curves and trying to establish a relation to the amount of shrinkage. No direct correlation existed that held true for all mixtures. For instance, in the tests comparing mortar and pastes, (Figures 6.28 and 6.29) the pressure developed earlier in the mortar mixture and at a greater rate. Yet there was still bleeding in the mortar mixture until about 4 hours so this pressure did not contribute to any shrinkage during that time. Therefore, it was concluded that it is not possible to correlate the rate or acceleration of capillary pressure with the magnitude of early age autogenous shrinkage.

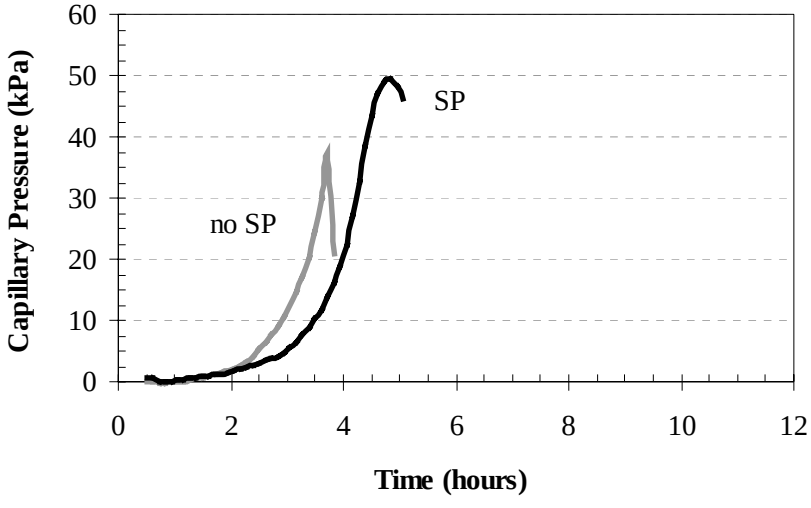

Figure 6.33. Comparison of capillary pressure for adding superplasticizer in autogenous shrinkage test from Figure 6.31, with w/c = 0.30 and water amount = 275 kg/m^3.

6.3.7.4 Cement Type

Another set of autogenous shrinkage tests was done on mortars with varying Finnish cement types. Figure 6.34 shows the changes in shrinkage for the 4 different types of Finnish cement. The mixture designs of all 4 mixtures were identical, with a w/c ratio of 0.30. The aggregate gradations were not adjusted to account for the fine material, so the workability of the mixtures varied a lot. The fineness of the cements contributed to the workability and amount of bleeding. The Rapid cement is ground the finest and thus had the lowest workability. The 'Rapid' mixture is the same non-plasticized mixture that was presented in Figures 6.29 and 6.30.

In Figure 6.34a for the structural viewpoint, the data was referenced at the time of maximum thermal expansion. The mixture made from Rapid cement had low workability and no bleeding. It showed no expansion so the data was referenced at the time of initial set, 90 minutes. The mixtures made with the three other Finnish cements all showed a thermal expansion exceeding the amount of shrinkage after the bleed water absorption period and were then zeroed at the low point. This referencing point coincided with the time of maximum thermal expansion, as can be seen in Figure 6.34b.

Recall from the Materials section that Yleis cement is derived from the same clinker as Rapid cement, with the addition of limestone and slag. This combination causes Yleis to have a slower cement hydration reaction and delayed time of maximum heat generation. The SR cement has a low and late heat generation because of the lower C_3S content (which is the greatest heat generator) and lower C_3A content (causing a later set time).

In Figure 6.34c for the engineering viewpoint, the data was referenced at the time when the bleed water absorption was completed. For the mixture made from Rapid cement there was no bleeding so the referencing was done at the time of setting, as in the structural viewpoint data. With the various other cements, the workability increased along with the amount of bleeding. Yleis and White cement mixtures had a peak amount of bleed water absorption (expansion) at 2.5 and 3.2 hours, respectively. The SR cement mixture was even later at 4.2 hours.

The mortar made from Yleis cement exhibited a shelf in the engineering data due to the mold restraint while thermally expanding. This was again corrected and estimated by the dashed line in Figure 6.34c for the Yleis curve. The ultimate magnitude of the Yleis mortar is then slightly greater than the original calculated value.

The trend in both from both the structural and engineering viewpoints shows the gray cement (Rapid and Yleis) mortars have greater autogenous shrinkage than the White or SR cement mixtures.

Again, the structural data (Figure 6.34a) showed a continued increase in shrinkage over the 24-hour test period, while the engineering data (Figure 6.34c) showed the shrinkage ending at about the time of peak temperature. The Yleis cement mixture was slightly different, since it continued to shrinkage for a longer period of time. This was earlier justified because of the presence of inert filler in the cement and its slow reaction rate. The Yleis cement mortar is the only mixture where the shrinkage magnitude changed the order of results between the structural and engineering viewpoint, since it exceeded the Rapid cement mixture for pure autogenous shrinkage (Figure 6.34c).

Most of these results are in agreement with the chemical shrinkage results presented earlier (Figure 6.4 in Section 6.2.1 for paste, Figure 6.14 in Section 6.2.2 for mortar), where the Rapid or gray cements showed the greatest shrinkage and the SR had the least shrinkage. From the engineering viewpoint, the Rapid cement had 40% greater shrinkage than the White cement and 137% greater than the SR cement. For the structural viewpoint, these differences increased to 130% and 159% for the White and SR cement compared to the Rapid, respectively.

(a) Structural Viewpoint

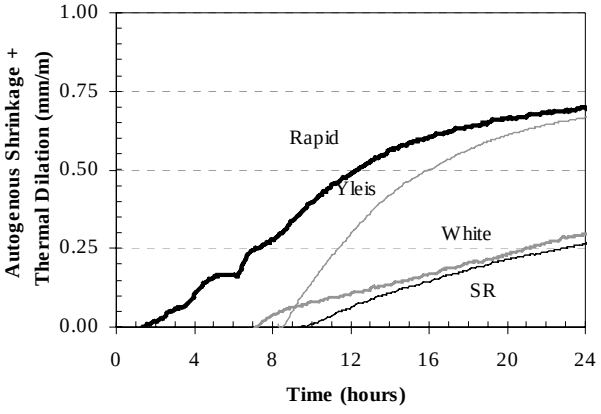

(b) Thermal Change

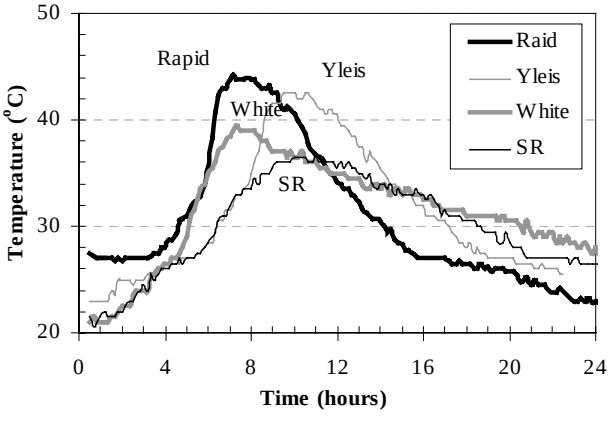

(c) Engineering Viewpoint

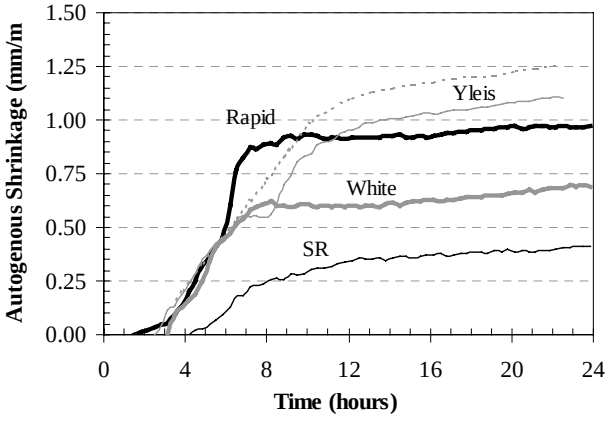

Figure 6.34. Comparison of various Finnish cements in autogenous shrinkage test, with w/c = 0.30 and water amount = 275 kg/m^3.

Figure 6.35 shows the pressure build-up corresponding to the shrinkages of Figure 6.34. Similar to the shrinkage trends, the mortar made with Rapid cement had the pressure developing earliest at about 2 hours. The mortars made with both White and Yleis cements had the pressure start at 3 hours and again the shrinkage started at nearly the same time (Figure 6.34c). The pressure in the Yleis cement mixture did not reach a very high level compared to the Rapid and White cement mixtures but it was maintained for a long time period. There was an error in all pressure transducer readings of the SR cement mixture, with no development measured so no conclusions can be drawn about this mixture.

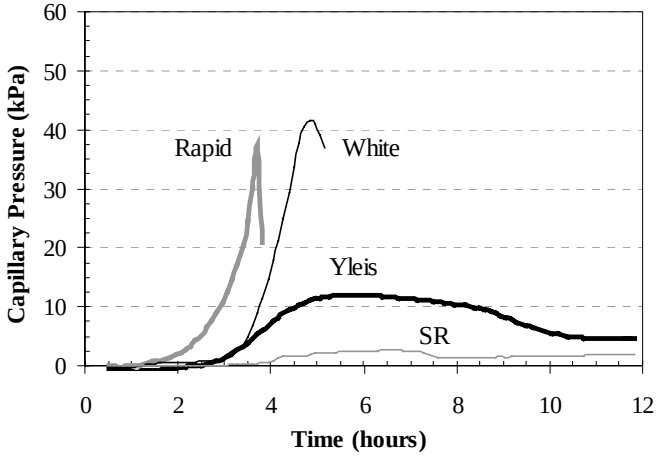

Figure 6.35. Comparison of capillary pressure for various Finnish cements in autogenous shrinkage from Figure 6.34, with w/c = 0.30 and water amount = 275 kg/m^3.

6.3.7.5 Concrete Autogenous Shrinkage

A final set of tests was done to evaluate the early age autogenous shrinkage of concrete. All of the previous results have been for mortars with a maximum aggregate size of 2 mm but in this test series the aggregate size was increased to 10 mm and there was 70 - 73% aggregate in the mixtures. The water amount was constant for the two mixtures at 165 kg/m^3 while the w/c ratio was lowered from 0.35 to 0.30 and more superplasticizer was added (2 to 5%). Both mixtures had good workability, with a visual estimation of an expected slump of 50 to 100 mm.

Figure 6.36 shows the structural viewpoint results of the tests on concrete with the two difference w/c ratios. Similar to the mortar tests, the temperature rise due to cement hydration was measured and is shown in Figure 6.36b. The shrinkage from the engineering viewpoint is corrected for thermal dilation and is given in Figure 6.36c. Neither mixture had any bleeding and therefore the results are zeroed at the time of initial setting for both mixtures in the structural and engineering viewpoint presentations. The initial setting time was shortened from 2 ½ hours to ½ hour at the lower w/c ratio. This was attributed to the lower w/c ratio having quicker hydration. The final setting time was also later at the higher w/c ratio (4 hours compared to 3 hours) where there was less superplasticizer. These tests showed no drastic delay of setting time with the addition of the naphthalene-based superplasticizer.

Figure 6.36 supports the mortar test results, with greater autogenous shrinkage occurring in the mixture with a lower w/c ratio. This is due to the denser microstructure and probably an earlier development of capillary pressure. The 0.35 w/c ratio mixture was also expected to have slightly less shrinkage due to its lower amount of cement than the 0.30 mixture.

Both mixtures had high initial temperatures at 30 minutes (Figure 6.36b) even though the mixing ingredients started at 20 °C. This is due to their high cement contents and some heat generation during mixing. During the first few hours after placement both mixture are cooling, thus the engineering viewpoint data (Figure 6.36c) showed an expansion in the first hours. The concrete with a 0.35 w/c ratio could still be referenced at the time of initial setting (2 hours and 35 minutes) and the pure autogenous shrinkage started soon after this point. On the other hand, the concrete with the lower 0.30 w/c ratio did not show autogenous shrinkage until about 2 hours. Therefore the final magnitude of autogenous shrinkage was lower when comparing the structural and engineering data for the 0.30 w/c mixture. The 0.35 mixture had nearly the same amount of shrinkage in both presentations. From the structural viewpoint the 0.30 w/c ratio mixture had shrinkage 25% greater than the 0.35 w/c ratio mixture, while from the engineering viewpoint the increase was only 3%.

(a) Structural Viewpoint

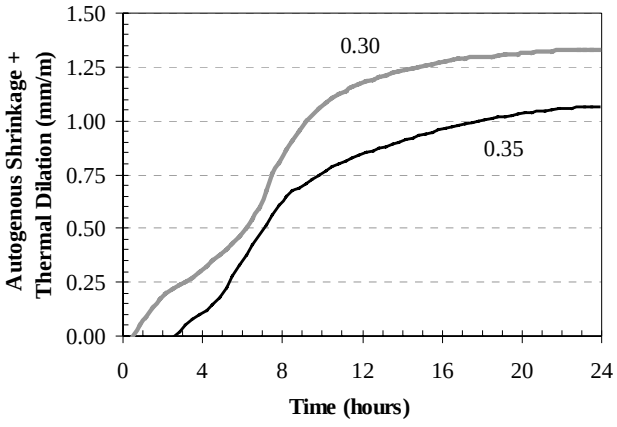

(b) Thermal Change

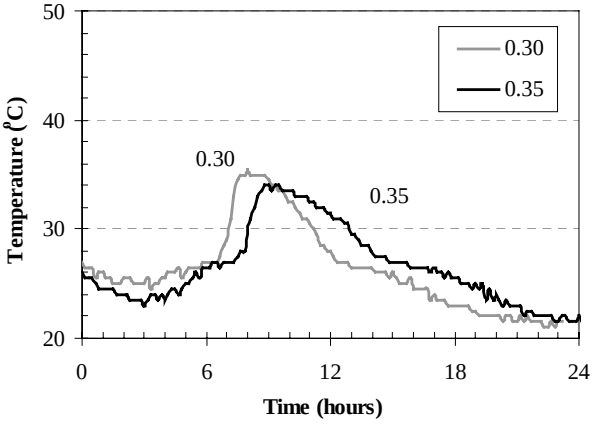

(c) Engineering Viewpoint

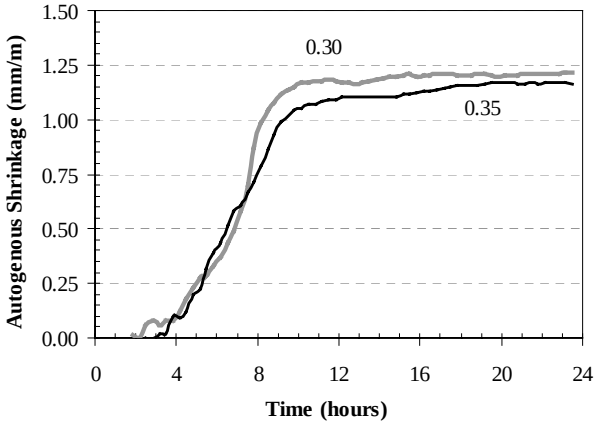

Figure 6.36. Comparison of concretes with different w/c ratios in autogenous shrinkage test; water amount = 275 kg/m^3, superplasticizer of 2% (0.35 w/c) and 5% (0.30 w/c).

The temperature peaks of the two mixtures were slightly different, with the 0.35 w/c concrete having a peak at 9 hours compared to the 0.30 w/c concrete's peak at 8 hours. The 0.35 w/c concrete also had a slightly lower temperature peak of 34°C (compared to 35.5°C for the 0.30 w/c concrete) due to its lower amount of cement. The engineering data of Figure 6.36c platformed near these times of peak temperatures while the structural data of Figure 6.36a continued to show increased autogenous shrinkage due to the thermal contractions.

Figure 6.37 shows the capillary pressure build-up corresponding to the shrinkages of Figure 6.36. There is an error in the readings for the concrete with a w/c ratio of 0.30, since it did not start to develop until much later and there is not a clear, early peak. It is expected that a proper reading would show the 0.30 concrete had capillary pressure development start earlier than the 0.35 concrete mixture. The concrete with a 0.35 w/c ratio had the pressure start to increase at about 4 hours, which corresponds to its time of the higher autogenous shrinkage rate in Figure 6.36.

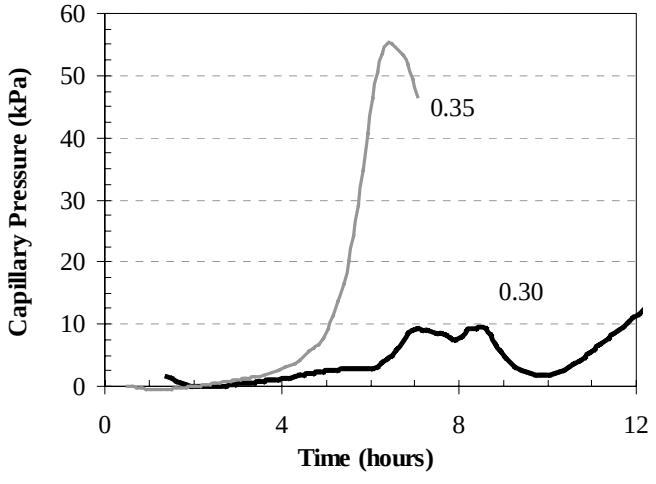

Figure 6.37. Comparison of capillary pressure for different concretes in autogenous shrinkage test from Figure 6.36, with w/c = 0.30 and 0.35.

Another important point to realize from Figure 6.36 is that the autogenous shrinkage magnitude for the concrete with a w/c ratio of 0.30 is nearly equivalent to the shrinkage of the mortar mixture with a 0.30 w/c ratio (Figure 6.30). The comparison of these two mixtures is presented in Figure 6.38. The

concrete mixture had less cement (545 kg/m^3, as given in Table 3.17 Section 3.5.2) compared to the mortar mixture (915 kg/m^3) so the amount of chemical shrinkage would be less in the concrete. It was also expected, based on the mortar and paste comparisons in Figure 6.28, that the concrete mixture would have less shrinkage than the mortar since the concrete has more aggregate restraining the shrinkable paste. Both of these theories held true, with the concrete shrinking less than the mortar, though there was still sufficient stresses to induce a high amount of shrinkage in the concrete. The same comparison cannot be made between the mortar and concrete at the 0.35 w/c ratios since the mortar did not contain superplasticizer.

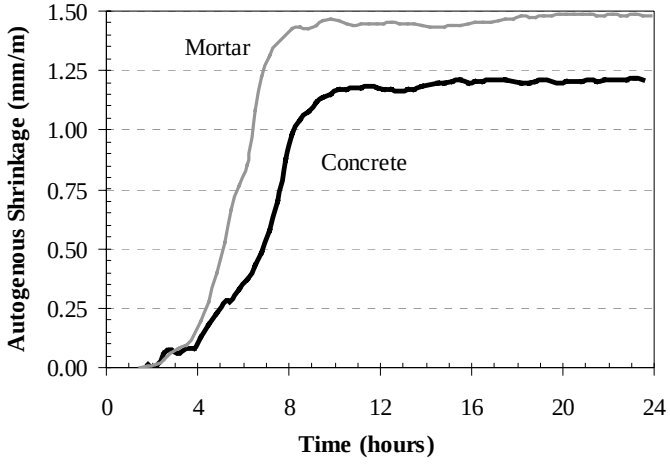

Figure 6.38. Comparison of autogenous shrinkage from the engineering viewpoint for mortar and concrete at 0.30 w/c ratio and containing superplasticizer.

6.3.7.6 Comparison of Viewpoints

The autogenous shrinkage data for the mortars and concretes presented in Figures 6.28 to 6.36 was presented from both the structural and engineering viewpoints. The engineering data provided a more accurate measure of the "true" autogenous shrinkage, assuming the values of thermal dilation coefficient are nearly correct. The structural viewpoint data provided a measure of what would be seen in a similar field slab.

Table 6.11 summarizes the differences in the data when interpreting from these two different perspectives, at both 12 and 24 hours. As noted during the analysis of the data, the engineering data results were greater than the structural data due to the smaller thermal coefficient of contraction compared to expansion. The engineering data also reached a platform level near the time of peak temperature in most cases.

The values used for the paste, 0.35 w/c mortar, and Yleis mortar mixtures all used the estimated corrected values from the engineering viewpoint. Recall these corrections were done to adjust for the shelf due to mold restraint during thermal expansion. Also note in Table 6.11 (*) that for the paste mixture, the 24 hour engineering data would probably be closer to the 12 hour value, since the thermal dilation coefficient is too great during the cooling period, leading to expansion when correcting the data.

Table 6.11. Comparison of mortars of Figures 6.28 to 6.31 from the structural and engineering viewpoints.

Mixture			Autogenous Shrinkage (mm/m)			
			Structural		Engineering	
Cement	w/c	Other	12 hr	24 hr	12 hr	24 hr
Rapid	0.35	Paste	0.59	0.76	1.23	1.13 *
Rapid	0.30	Mortar	0.49	0.70	0.92	0.97
Rapid	0.35	Mortar	0.25	0.43	0.65	0.67
Rapid	0.40	Mortar	0.09	0.26	0.38	0.39
Rapid	0.45	Mortar	0.00	0.18	0.11	0.16
Rapid	0.30	Mortar + SP	1.04	1.25	1.45	1.48
Yleis	0.30	Mortar	0.40	0.77	1.10	1.26
White	0.30	Mortar	0.05	0.24	0.60	0.70
SR	0.30	Mortar	0.01	0.21	0.35	0.42
Rapid	0.30	Concrete + 5% SP	1.17	1.33	1.17	1.21
Rapid	0.35	Concrete + 2% SP	0.84	1.07	1.10	1.17

* Note: expected to be higher if thermal dilation of paste was more accurate

In most cases the engineering viewpoint (thermally corrected) yielded early age autogenous shrinkage magnitudes 10 to 190% greater than the structural viewpoint data at the age of 24 hours. The exceptions to this trend were in the

mortar with a w/c of 0.45 (12% less) and the concrete with a w/c of 0.30 (10% less). The mortar mixture did not follow the trend due to the thermal dilation affect on the small shrinkage scale. The concrete mixture did not follow the trend due to the later time of initial readings or referencing.

6.4 Comparison of Chemical and Autogenous Shrinkage

As described in previous sections, autogenous shrinkage is driven by the chemical shrinkage of the cement paste within the mortar. Therefore, it can be informative to view the horizontal and vertical shrinkage (settlement) along with the chemical shrinkage. To do this, it is first necessary to convert the autogenous shrinkage measured in the slab tests to volumetric units. This example uses a mortar presented in Figure 6.32, made from Rapid cement, with a w/c ratio of 0.30 and superplasticizer. The settlement was first divided by the height of the slab, 0.1 m, to get the units of mm/m. The horizontal and vertical displacement of the slab then had comparable units and could be graphically shown together, as in Figure 6.39. Both horizontal and vertical shrinkage have been corrected according to the engineering viewpoint to remove the dilation due to cement hydration. The gray dashed vertical lines at approximately 1 ½ and 2 ½ hours represent the times of the mortar's initial and final set. The dark dashed curve shows the capillary pressure in 10s of kPa, which starts to develop after the initial set in this case.

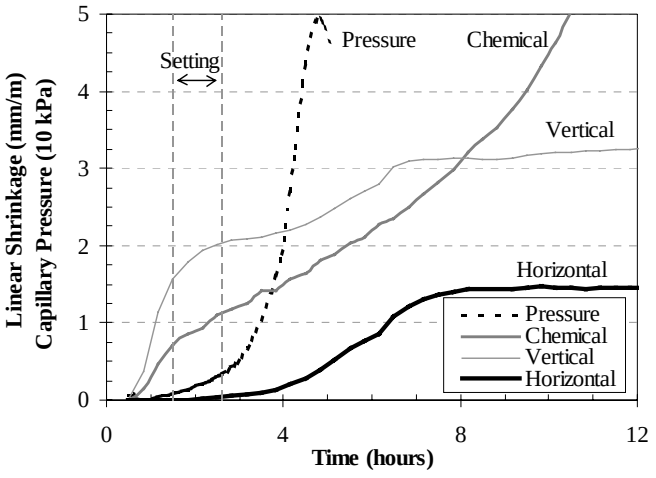

Figure 6.39. Horizontal and vertical shrinkage of mortar (Rapid mortar with w/c = 0.30 and superplasticizer), with curves corrected to remove changes due to thermal dilation.

During the first hours it is seen that all of the autogenous shrinkage is attributed to vertical movement, or settlement. Later there is an increase in both the horizontal and vertical shrinkage once the pressure started to rise and reached about 10 kPa. Further analysis of this graph will be given as a volumetric comparison of autogenous shrinkage and chemical shrinkage in the upcoming paragraphs.

To convert the autogenous shrinkages of Figure 6.39 to a volume, Equation 29 could be used with the results expressed in units of mm^3/ mm^3. It is also possible to approximate a unitless volume change since the autogenous shrinkage presented in this work have been in terms of strain, mm/m. The approximation of the volume change of the autogenous shrinkage strain can be found from Equation 30. This approximation is valid when the magnitude of change is relatively small compared to the original distance. In Equation 30, the horizontal components, x and y, are taken as twice the horizontal shrinkage measured in the slab test, while the vertical component, z, is taken as the settlement. For a slab of 10 m in length with a shrinkage of 5 mm, the error from approximating the volume change by either Equation 29 or 30 is only 0.025%.

$$\frac{\Delta V}{V} = \frac{\left[(x+\Delta x)\times(y+\Delta y)\times(z+\Delta z)\right] - xyz}{xyz} \tag{30}$$

$$\frac{\Delta V}{V} = \varepsilon_x + \varepsilon_y + \varepsilon_Z \tag{31}$$

In order to compare the autogenous shrinkage to the chemical shrinkage, it was necessary to also convert the chemical shrinkage to similar units. The chemical shrinkage measurement of mm^3/g of cement was first changed to a volumetric measure of mm^3/mm^3 using the amount of cement in the mixture. The equation for this conversion is given in Equation 31, where a chemical shrinkage of 10 cm^3/g of cement (for a mortar mixture with 915 kg/m^3 of cement) produced a volumetric shrinkage of 0.00915 mm^3/mm^3. If needed, this volumetric chemical shrinkage could be converted to a linear shrinkage (mm/m) using Equation 7 presented in Section 2.2.3. From this equation it can be calculated that 0.00915 mm^3/mm^3 of volumetric shrinkage is equivalent to 3.05 mm/m of linear shrinkage.

$$V_{CS} = CS \times V_{cem} \times 10^{-6} \tag{32}$$

where: V_{CS} = Volume of chemical shrinkage (mm^3/mm^3),
CS = Amount of chemical shrinkage from bottle test results (cm^3/g of cement), and
V_{cem} = Volume of cement in mixture (kg/m^3).

After making the necessary conversions, it is possible to volumetrically compare the chemical and autogenous shrinkage, as shown in Figure 6.40. This presentation is for the same mortar that was shown in Figure 6.39. Figure 6.40 shows that during the first hours the autogenous shrinkage is controlled by chemical shrinkage. Parallel lines have been drawn on the figure to identify the similar shapes of the chemical and autogenous shrinkage curves.

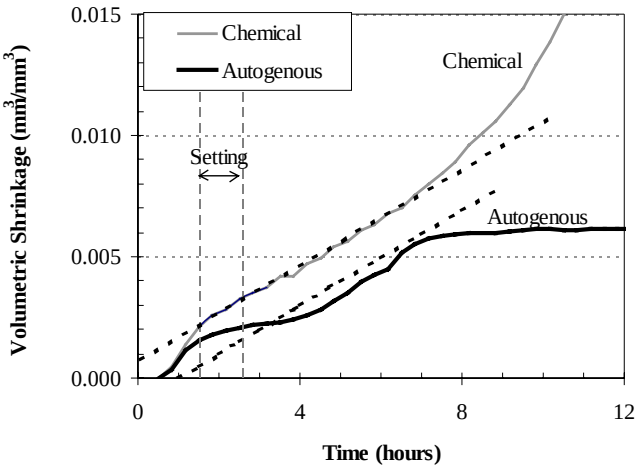

Figure 6.40. Volumetric chemical and autogenous shrinkage for mortar from Figures 6.18 and 6.33 (Rapid mortar with w/c = 0.30 and superplasticizer).

In Figure 6.40, prior to setting all autogenous movement is attributed to settlement. Once a skeleton has formed at about the time of setting the chemical and autogenous shrinkages diverge since there is some strength. The mortar has stiffened enough to resist some of the chemical shrinkage. At about 4 hours the autogenous shrinkage again increases as a result of the capillary pressure. By about 7 hours, or 4 hours after the final setting time, the mortar is again stiff enough due to hardening to resist most of the shrinkage due to both chemical changes and pressure.

This example supports the theories proposed in this work (and in Section 2.2.4.3) that autogenous shrinkage is driven by both chemical shrinkage and capillary pressure during the early ages. Not all of the mixtures tested in this program followed such clear paths but the same general trend was evident.

As a summary, Table 6.12 shows the comparison of autogenous and chemical shrinkage during this period when they are both increasing in a parallel manner. Tests included in the table cover many of the mortar mixtures and one paste mixture presented in Sections 6.2 and 6.3. Comparisons are not made for the concrete autogenous tests since no companion chemical tests could be done with the larger aggregate size. The data is given for the horizontal autogenous shrinkage and the linearized chemical shrinkage, as presented in Figure 6.39.

The duration of comparison is from the start of testing by the engineering viewpoint (initial set or end of bleeding time) until 4 hours after the final set. This selection of "4 hours after final setting" was chosen because it had the greatest correlation compared to other referencing points, such as time of peak temperature, 2 hours after setting, etc.

Table 6.12. Comparison of chemical and autogenous shrinkage from the start of engineering data measurements (initial set or end of bleeding) until 4 hours beyond final set time. Only the first mixture is paste while the remaining mixtures are mortar.

Mixture			Shrinkage (mm/m)		Autogenous %
Cement	w/c	Other	Autogenous	Chemical	of Chemical
Rapid	0.35	Paste	0.96	2.08	46
Rapid	0.30	+ SP	1.08	1.65	65
Rapid	0.30	-	0.76	2.26	34
Rapid	0.35	-	0.26	1.16	22
Rapid	0.40	-	0.12	0.87	14
Rapid	0.45	-	0.00	0.39	0
Yleis	0.30	-	0.42	1.60	26
White	0.30	-	0.54	2.84	19
SR	0.30	-	0.23	1.26	18

In Table 6.12 it is seen that all of the autogenous shrinkage values in this work are less than the chemical shrinkage for the same time period. The final column in the table shows the magnitude of autogenous shrinkage compared to chemical shrinkage as a percentage. The autogenous shrinkage ranged from 0 to 65% of the chemical shrinkage, with an average contribution of 27%. These values are not constant, as expected, since the chemical shrinkage is only dependent on the amount of cement in the mixture. The other mixture parameters, such as w/c ratio or use of superplasticizers, control the paste microstructure and likelihood of shrinkage. In each mixture there is a different amount of capillary pressure and different rate of shrinkage due to the paste properties.

For comparison purposes long term drying shrinkage is usually about 0.5 to 1 mm/m, which is similar in magnitude to the early age autogenous shrinkage measured in this work.

Figure 6.41 graphically represents the values given in Table 6.12 for the 4 different mortar test series of Figures 6.28 to 6.31: a) material type, b) w/c ratio, c) use of superplasticizer, and d) cement type.

Overall, the autogenous shrinkage and chemical shrinkage are not equivalent during the first 24 hours due to the many factors in all three early ages. Even during the middle "skeleton formation" stage, the values given in Table 6.12 and Figure 6.41 have shown that there is not a direct correlation between the two types of shrinkage. Also in the other stages there are differences due factors such as bleed water, thermal dilation, strength development (setting) and restraint provided by aggregate particles. These will be elaborated on in the next section on modeling of autogenous shrinkage.

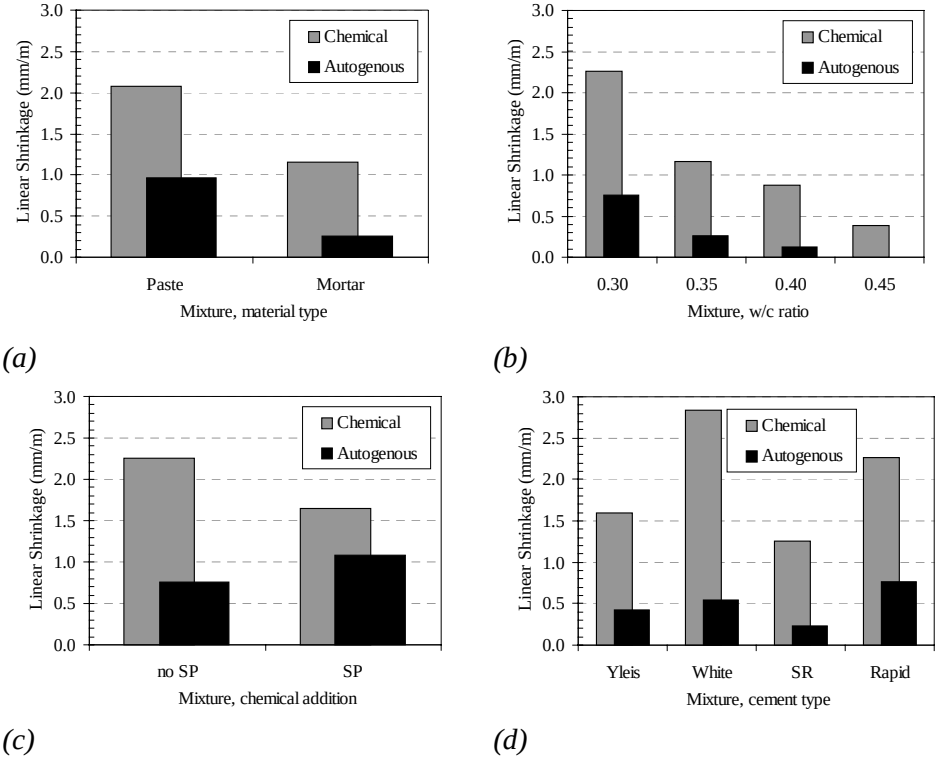

Figure 6.41. Comparison of chemical to autogenous shrinkage from start of engineering data (initial set or end of bleeding) until 4 hours beyond final set time, as given in Table 6.12.

6.5 Modeling Early Age Autogenous Shrinkage

As described in previous sections, autogenous shrinkage occurs over 3 distinct stages: liquid, skeleton formation and hardening. In all of these phases the driving force is chemical shrinkage. Chemical shrinkage occurs since the reaction product of the cement and water consumes less volume than the initial material inputs. The chemical shrinkage is unavoidable and will always exist due to this cement hydration. For this reason, autogenous shrinkage can not be avoided but it may be minimal due to other mixture parameters.

To quantify the amount of early age autogenous shrinkage expected from any particular concrete, ideally one would hope to correlate the amount of autogenous shrinkage to the amount or rate of chemical shrinkage. This is not possible due to the other mixture parameters altering the behavior of the concrete during the first day. But for comparison purposes, it is helpful to address a few points that show why the two measurements diverge.

Figure 6.42 depicts the correlation between autogenous and chemical shrinkage during the early ages, in accordance with the different hydration stages described in Section 2.1. This autogenous shrinkage would be the pure value, as seen from the engineering viewpoint.

In this first phase the concrete is very fluid. While a *liquid*, the autogenous shrinkage may be fully attributed to chemical shrinkage in terms of settlement (vertical displacement). But during this phase the early age test arrangement used in this work cannot accurately quantify the autogenous shrinkage magnitude. This is not a concern for modeling field concrete practice, since during the liquid stage the concrete with high plasticity is not effected by stresses. Most volume change by settlement is compensated by rising bleed water. The chemical shrinkage is progressing but there is no resulting harmful autogenous shrinkage in the slab test. The earliest the autogenous shrinkage can begin is at the time of initial setting, as earlier defined in this work (Section 6.3.1).

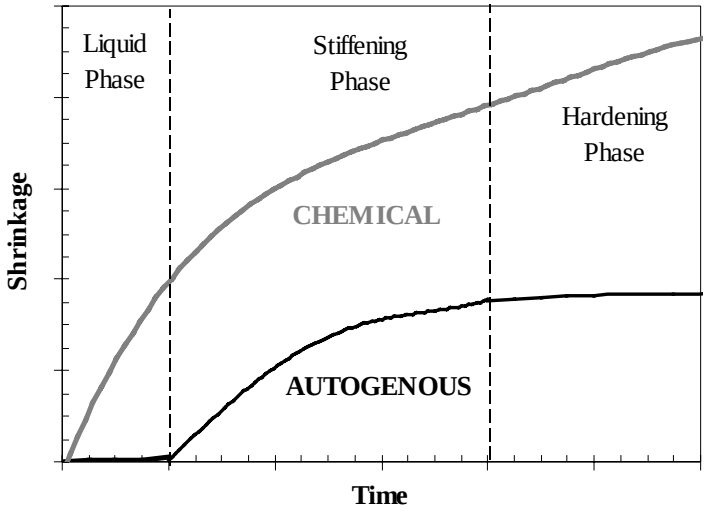

Figure 6.42. Stages of autogenous and chemical shrinkage during early hydration.

In the next phase where the concrete begins to stiffen and *form a skeleton* the chemical shrinkage stresses induce a strain in the concrete so there will be autogenous shrinkage. Ideally, the autogenous shrinkage curve would be parallel to the chemical shrinkage as long as there is insufficient strength in the concrete to resist the forces. This means *the autogenous shrinkage is nearly equal to chemical shrinkage* for a short period during setting and the few hours afterwards. The best correlation was found during the time period of final set plus 4 hours, with improved correlation in the lower w/c ratio mixtures. Test results detailed in Sections 6.4 showed that the formation of the skeleton provides enough restraint to resist the chemical shrinkage and therefore the curves are not parallel for a very long duration. During this phase the water and cement reaction product takes less volume and the capillary pressure is pulling the pore walls closer to induce a volume change. During this stage the setting will also proceed, but not necessarily at the start of the skeleton formation.

As shown in Figure 6.40, the chemical and autogenous shrinkage amounts can be equivalent even if for only a short period of the early age reaction. Another case in which the chemical and autogenous shrinkage are equivalent during the early ages is when conducting theoretical autogenous tests with a thin rubber membrane test, as shown in Figures 2.25 and described in Section 2.3.1 [Justnes

et al. 1996, Hammer 1999] Extensive work in Norway has proven that the rubber membrane test models the autogenous shrinkage of a mass which begins to lose water from the internal pores after the initial reactions. This typically takes place at 6 to 12 hours, at which point there is a divergence from the chemical shrinkage, as shown in Figure 2.18 of Section 2.2.4. Until this divergence, the two measurements are equivalent, showing that all internal volume changes are merely attributed to the cement's chemical reactions. As earlier explained, the rubber membrane test is not a realistic measure of an actual concrete slab's shrinkage due to the confinement of the mass.

It is understood that the chemical shrinkage due to cement hydration with water causes a decrease in the resultant paste volume. During the skeletal phase, the movement of water due to hydration causes the largest pores to lose their water. This loss in water volume causes a pressure in the capillary water spaces, which excerpts a pulling or suction force on the capillary pores (as earlier described in Section 2.2.3 and Figure 2.13). The capillary water pressure is a stress, leading to a strain in the concrete as a meniscus is forced into the capillary water spaces. The strain in the concrete is the autogenous shrinkage.

The likelihood of autogenous shrinkage development due to the chemical shrinkage is dependent on the microstructure of the cement paste. Following the sample graphic used earlier (Figure 2.4), another two sample cement pastes are demonstrated in Figure 6.43. These show the variation in microstructure of a dense (top) and coarse (bottom) cement paste. [Kronlöf 1999] After hydration the dense microstructure has very few open spaces or voids (top right) while the coarse microstructure (bottom right) is still very open.

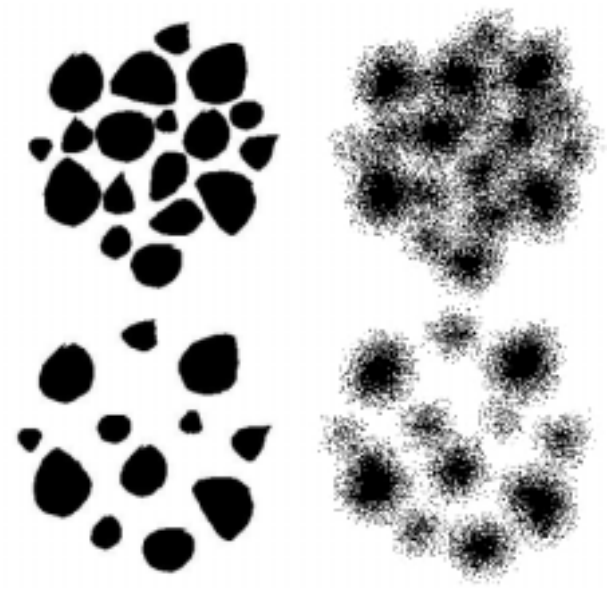

Figure 6.43. Samples of a dense (top) and coarse (bottom) microstructure, before (left) and after (right) hydration. [Kronlöf 1999]

If there is a coarse pore structure of the cement paste it will be easy for the meniscus to penetrate the capillary pore space between hydration particles once the pressure development begins (Figure 6.44a). Therefore there is not much of a pressure increase and thus no resulting early age autogenous shrinkage. Recall that the most likely occurrence of a coarse pore structure is in concrete with higher w/c ratios (greater than approximately 0.42 [Powers 1968]).

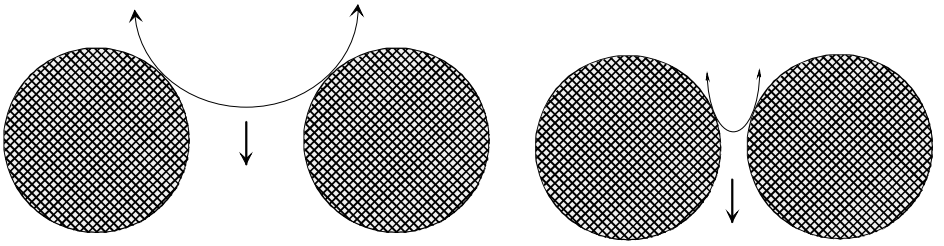

(a) *(b)*

Figure 6.44 Penetration of meniscus to a) coarse and b) fine paste pores structure.

The magnitude of early age autogenous shrinkage will then be much greater in concrete with a dense microstructure, which would be a result of a lower w/c or

additives such as silica fume. With this dense microstructure the meniscus has a smaller radius of curvature and penetrates farther between the capillary pores, as shown in Figure 6.44b. This requires a much higher pressure that will draw in the capillary pore walls and result in shrinkage. It is for this reason that early age autogenous shrinkage is increasing with lowering of the w/c ratio, as earlier described in Section 2.2.4.

After the final setting time the concrete has started to harden. Although there is usually still sufficient water within the mass to allow cement hydration, the development of a more rigid structure restricts autogenous shrinkage. The elastic modulus is getting larger and it restrains the resulting chemical shrinkage so that there is less and less autogenous shrinkage measured in the slab test. Later in this stage the relative humidity within the pores will lower due to the need for water for cement hydration. The pores will lose their water and the resulting shrinkage is a result of self-desiccation, which has been well documented by other researchers [Baroghel-Bouny 1996, Tazawa & Miyazawa 1995b, Igarashi et al. 1999].

Moving into this hardening or *stiffening stage* leads to the measurement of long-term autogenous shrinkage. In this late-age stage the concrete's stiff microstructure prevents water access and movement for the cement hydration. As the cement hydration requires extra water, it must be extracted from the internal moisture of the air pores in order to proceed. The lowering of the internal relative humidity is also dependent on the capillary pore structure and is accounted for in these long-term models. This phenomenon of humidity dependence on pore radius was described earlier in Section 2.2.3 using the Kelvin equation and work by Washburn [1921]. During the initial hours the relative humidity had been high enough (~100 %) that no water removal (or self-desiccation) from the internal pores was instigated.

In summary, ideally the autogenous shrinkage should be equivalent to the chemical shrinkage if there were no exterior restraints or influencing factors. In reality the concrete has other contributing factors, such as bleeding, thermal dilation, and modulus development, which prevent this clear correlation. The discussion on modeling of autogenous shrinkage to this point has assumed that there is no bleed water, or free water, on the concrete surface. The presence of bleed water will delay the onset of autogenous shrinkage until it has been

removed or completely drawn back into the concrete, as addressed in Section 6.3.3. The implications of other such factors will be addressed in the next section on concrete design for minimizing autogenous shrinkage.

6.6 Implications to Concrete Design

Autogenous shrinkage has been defined as the shrinkage due to internal changes and without moisture transfer to the surrounding environment. This also means that autogenous shrinkage cannot be controlled by adjusting construction practice, such as placing, finishing, curing, etc. The magnitude of autogenous shrinkage is strictly based on the chosen materials and the mixture design of the concrete. Like any other type of concrete shrinkage, autogenous volume reductions put the concrete at risk of cracking and reduces its durability.

The main factor governing autogenous shrinkage is the water-to-cement ratio. As shown by Powers [1968], when the w/c ratio is less than approximately 0.42 there is not enough water for the cement hydration. This level for the w/c of 0.42 is only an estimate, since the actual ratio at which autogenous shrinkage can develop can range from 0.38 to 0.45, depending on the cement chemistry. The limits on the w/c ratio have previously only been a concern for later age (> 24 hour) autogenous shrinkage because of the self-desiccation behavior.

Recall from Section 2.2.4.4 that the amount of long term autogenous shrinkage could be 1 mm/m, or about 1000 με, at the lower w/c ratios near 0.20 [Baroghel-Bouny 1996, Tazawa & Miyazawa 1995b]. Long-term autogenous shrinkage taken at 90 days for a w/c ratio of 0.38 would be approximately 0.65 mm/m according to Figure 2.20. Compared to the value of 0.15 mm/m measured for the concrete in this work (Figure 6.36), these values are of the same order of magnitude. Therefore, it must be re-emphasized that the *early age* autogenous shrinkage can be nearly the same amount as later measured by standard length change tests over a *long period*. This work has shown that it is important to include the assessment of early age deformations and not be limited to the long-term investigations.

At early ages there are a few factors in addition to the w/c ratio that are also contributing to the autogenous shrinkage. Figure 6.45 shows the three main

parameters effecting the magnitude of early age autogenous shrinkage. The mixture parameters that alter the bleeding, chemical shrinkage, and time of hardening (stiffening) are all held responsible for the shifting of the autogenous shrinkage.

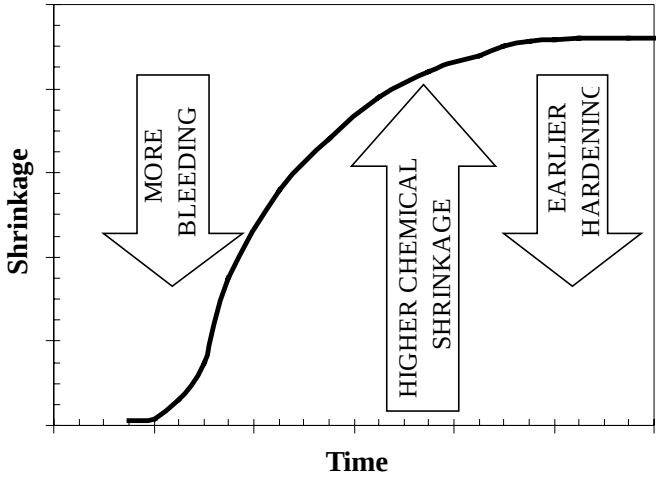

Figure 6.45. Direction of shift in early age autogenous shrinkage when influenced by other material factors.

Chemical shrinkage provides the potential for greater autogenous shrinkage. The bleeding and hardening are material parameters that affect the autogenous shrinkage in reality. All three of these factors are mixture dependent and inter-related. Yet the sum autogenous shrinkage accounting for all three factors simultaneously cannot be predicted by a numeric model. The factors governing each of the three parameters in Figure 6.45 are addressed in the next sub-sections.

6.6.1 Chemical Shrinkage

As demonstrated in Figure 6.45, one of the main parameters controlling the amount of early age autogenous shrinkage is the chemical shrinkage. This chemical volume reduction due to the reaction of water and cement cannot be avoided since the product consumes less space than the constitutes. If the rate or

total amount of chemical shrinkage increases then there is greater potential for higher autogenous shrinkage.

The amount of chemical shrinkage is dependent on the type of cement chosen, with the cements having a high C_3A content also having the greatest shrinkage. As shown in the predicted amounts of chemical shrinkage (Table 6.4), there was a 30% difference in the amount of expected shrinkage at 12 hours. This was validated in Figures 6.4 for pastes and Figure 6.14 for mortars, where Finnish gray and USA "high" cements had the highest C_3A content and also the greatest chemical shrinkage.

The rate of chemical shrinkage can be altered by many factors. The most common cause of a faster rate is the use of finer cement, since there is a greater surface area in contact with the water for hydration. Other properties of the mixture design that improve the cement dispersion will also increase the chemical shrinkage rate, such as using superplasticizers or more aggregate.

If the w/c ratio is very low (i.e. 0.20) the chemical shrinkage may stop in the early ages due to the lack of water for hydration. In this case, even though the chemical reaction has ceased the autogenous shrinkage can continue since the water will then be taken from the capillary pores. The relative humidity of the pores will be lowered and the self-desiccation will promote the autogenous shrinkage at an earlier age rather than the chemical shrinkage.

An increase in the concrete temperature will also accelerate the rate of chemical shrinkage. Such a temperature increase may be due to the actual materials used or the surrounding environmental conditions.

6.6.2 Bleeding

The presence of free water on the concrete surface or within the concrete will decrease the magnitude of early age autogenous shrinkage since the extra water must be re-absorption by the cement paste prior to the start of shrinking. In this work the free water has always been attributed to rising bleed water. In actuality, the free water could also be a result of internal moisture sources or moist curing.

An example of an internal moisture source is the use of lightweight aggregates. The lightweight aggregates can replace all or even a small percentage of the normal mixture proportioned aggregate. The lightweight aggregates hold water within the concrete and provide an extra source to aid cement hydration. It is expected that they would promote decreased autogenous shrinkage.

To reduce early age autogenous shrinkage by providing more surface water by curing, there must be an excessive amount of water. This could be achieved by the old-fashion method of ponding or by heavy misting. To get the delay of autogenous shrinkage onset, it is not sufficient to only have a surrounding relative humidity of 100% (i.e. achieved by fog spraying). There must actually be a thin layer of water on top of the concrete to prevent the meniscus from curving lower between the pores. External curing is also limited to influencing only the top surface of the concrete, whereas excess bleed water can also be trapped internally under aggregate.

As shown in some of the tests in this work, bleed water will inhibit the start of autogenous shrinkage. Typically in practice it is not desirable to have excess bleed water on the concrete surface since it can indicate segregation and delays the finishing of the concrete. An increase in the amount of bleed water can be a result of such things as:

- using too much mixing water,
- using coarser ground cement,
- decreased the amount of cement, and
- using a lower volume of fine aggregate.

The early age autogenous shrinkage would increase if the bleed water was decreased or omitted. This could be achieved by doing the opposite of the adjustments listed above, as well as by using chemical and mineral admixtures (such as superplasticizer and silica fume). In high strength and high performance concrete where the w/c ratio is less than about 0.42 there is the greatest risk of autogenous shrinkage. It is in this case where it is also very likely to be using such admixtures that promote greater autogenous shrinkage by reducing bleeding. Thus the concrete has an even greater risk of cracking.

Bleeding can be a risk is all types of concrete, not excluding large constructions with thick slabs or elements. In such large constructions the water may not rise to the surface but it is still possible that there is localized bleeding which can be trapped under aggregates or formwork. Any such types of bleeding, external or internal, will reduce the early age autogenous shrinkage.

6.6.3 Hardening

The final key contributor to the early age autogenous shrinkage magnitude is the time of hardening. This corresponds to the time when the concrete has enough stiffness to resist the shrinkage stresses. The time can be measured and correlated to some period after the initial set. Any material or construction parameters causing a delay of setting will prolong the period when early age autogenous shrinkage occurs. These delays can be caused by factors such as the use of: retarders, superplasticizers, fly ash, some shrinkage reducing admixtures, etc.. Placing concrete in cold weather may delay the setting time and thus prolong the autogenous shrinkage but such alterations to curing conditions were not evaluated in this work.

If the temperature, of either the materials or the surrounding environment, was increased the time of hardening would be earlier. This plays the opposite role of the chemical shrinkage, which would be faster and promoting more autogenous shrinkage with the temperature increase. Therefore, it is demonstrated how the factors of Figure 6.45 are inter-related and there is not one simple model to predict ultimate autogenous shrinkage in the early ages. An external factor can simultaneously help and hinder the forces driving autogenous shrinkage. Each concrete case has to be independently evaluated based on its chemistry, bleeding potential, and likely time of stiffening.

6.7 Future Work

This work aimed at developing a test method to measure early age autogenous shrinkage and identifying factors contributing to its magnitude from 0 to 24 hours. A relationship was established between the chemical and autogenous shrinkage, but this was only valid for the very first hours of the testing, prior to development of a rigid skeleton resisting shrinkage forces. It was not possible to

establish a quantitative model to predict the early age shrinkage due to the material parameters that vary for every concrete, such as bleeding and hardening.

A few topics could be elaborated on in future work to improve the understanding of early age autogenous shrinkage. These topics are listed in the points below.

- Chemical shrinkage tests could be elaborated on, such as determining the role of air voids and repeating the test with varying cement fineness to assess the influence on reaction rates.

- The slab test arrangement could be modified to include different dimensions. A deeper mold would allow study of the effect of rising bleed water and trapped internal bleed water.

- The slab test arrangement could be more thermally controlled to eliminate the need to make thermal dilation coefficient assumptions for the engineering viewpoint corrections.

- More tests could be done at various temperatures, in attempt to establish a clearer trend between the time of stiffening and rate of chemical shrinkage. For instance, at a warmer temperature it would be beneficial to know if the autogenous shrinkage is greater due to higher chemical shrinkage or if it is lower since the concrete hardens sooner.

- Alternative materials could be tested to determine their influence on the magnitude of autogenous shrinkage. For example, it would be informative to replace part of the cement with silica fume or fly ash to determine the change in chemical shrinkage, capillary pressure development (pore size distribution), bleeding, and time of hardening. Another example would be to use some lightweight aggregate to see if they provide an excess water source similar to bleeding to reduce autogenous shrinkage.

7. Conclusions

The concept of autogenous shrinkage has been around for over 100 years. Historically, it was not a concern since concrete was typically made at much higher w/c ratios and lower strength. In recent years autogenous shrinkage has returned to the forefront of concrete technology discussions, especially with the documentation of field cracking and durability problems in modern high performance concretes. Cracking during the first day under ideal curing conditions has heightened the discussions and need for research. This worked aimed at developing a test method to measure early age autogenous shrinkage and identifying the factors contributing to early age autogenous shrinkage.

Any type of concrete shrinkage is a durability problem. As the concrete shrinks it must relieve the stresses and form a crack if no other joint is provided for the movement. In the early ages there have been more citations of pavement and floor cracking, even with ideal curing practice. These cracks may likely be a result of autogenous shrinkage.

Autogenous shrinkage results from chemical changes in the cement paste of concrete. It becomes a risk when the water-to-cement ratio is below the range of 0.40 to 0.45 since the cement does not have enough water for hydration. Early age autogenous shrinkage is defined in this work as the volume changes occurring during the first 24 hours after concrete mixing. At the age of about 12 hours the concrete is usually stiff enough to resist many of the shrinkage stresses. Prior to this point the tensile capacity is very low and the concrete is at a great risk of cracking due to any shrinkage stresses.

Figure 7.1 recalls the discussions in Section 2 on shrinkage types and stages. This work was focused on the autogenous shrinkage during the first day, which is a small part of the pie consisting of total shrinkage. If concrete is subjected to drying shrinkage in the early ages, the contribution of early age autogenous shrinkage to total shrinkage will likely be negligible. On the other hand, if there is ideal curing of high strength concrete the contribution of early age autogenous shrinkage to total shrinkage can be significant. Such ideal curing is also applicable to some confined structural concrete elements, such as a steel encased pier column where the concrete cannot be drying once placed and consolidated.

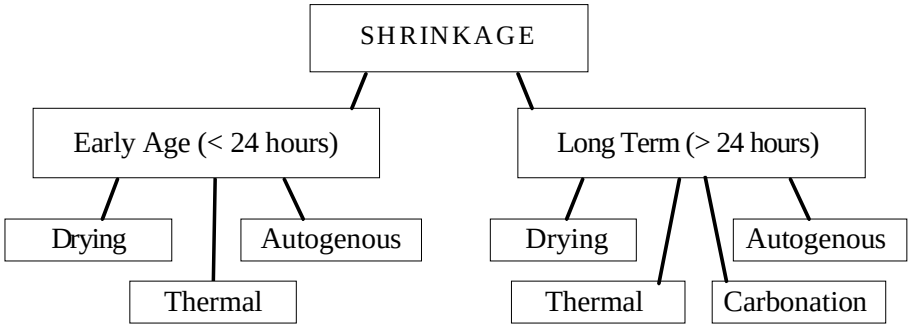

Figure 7.1. Diagram of shrinkage types and stages.

Autogenous shrinkage is occurring over three distinct phases, while the concrete is liquid, forming a skeleton, and hardened. During the first stage there will be no harmful shrinkage since the material is still fluid and plastic. The autogenous shrinkage is equivalent to chemical shrinkage and is seen in the slab tests as settlement. In the slab test the horizontal measure of autogenous shrinkage can start only at the time of initial set and it continues to be driven by chemical shrinkage if the concrete does not have enough stiffness. If there is bleed water on the surface, it must be re-absorbed prior to the onset of autogenous shrinkage. During the skeleton formation stage the concrete is setting and developing capillary pressure that causes the meniscus to move into the pore spaces (pulling on the paste with shrinkage forces). The autogenous shrinkage is equivalent to the chemical shrinkage for a short time period. Once the concrete has hardened enough it can resist the shrinkage forces and any further autogenous shrinkage is mostly due to self-desiccation.

The shrinkage in the three stages (liquid, skeleton formation, and hardening) can be measured respectively by a chemical bottle test, slab test, and standard beam length-change test. The tests in this work on both chemical shrinkage and autogenous shrinkage found the following general trends when comparing mixture designs of paste, mortar or concrete:

- Shrinkage was lower when paste content was lowered (increasing aggregate content, concrete < mortar < paste),
- Shrinkage was lower at high w/c ratios compared to low w/c ratios (i.e. 0.40 < 0.35 < 0.30),
- Shrinkage was lower if bleed water was present on the material surface,

- Shrinkage was higher when superplasticizer was added, due to better cement dispersion,
- Shrinkage potential is higher for cements with a high C_3A content,
- Shrinkage may be higher if the setting time is delayed (by chemicals, temperature, etc.).

Since autogenous shrinkage cannot be controlled by construction practice, it is important to properly design the concrete mixture to minimize the factors contributing to autogenous shrinkage. There are three main factors to consider:

- Early age autogenous shrinkage is closely related to chemical shrinkage during the very early ages (i.e. 2 to 8 hours) and thus it is highly affected by the cement chemistry and fineness.
- Any mixture parameters that delay the stiffening and strength development of concrete will prolong the period of early age autogenous shrinkage.
- Bleed water will reduce autogenous shrinkage but care should be taken before recommending excess bleeding if the concrete's surface properties, such as wear resistance, are a concern.

Long term autogenous shrinkage has been well documented and is attributed to self-desiccation as the internal pores lose water for continued cement hydration. At early ages autogenous shrinkage can be of the same order of magnitude as long-term shrinkage and it should be accounted for when documenting the total amount of volume deformation.

Acknowledgements

I would like to acknowledge a few organizations for supporting this work, both in the USA and Finland: the Valle Scandinavian Exchange program for providing funding to originally venture to Helsinki and then remain an extra year to begin my doctoral research, the Fulbright Association for funding my second official year on a research exchange, and the National Science Foundation International Programs dissertation enhancement awards for funding to complete laboratory testing. I am also very grateful to VTT, The Technical Research Centre of Finland, for welcoming me to their outstanding research family of building material experts for the duration of this research.

I have appreciated the flexibility of my review committee and our UW Department of Civil and Environmental Engineering, who have allowed me to conduct most of my work from the other side of the world without too many flights home to Seattle.

A great thanks to my advisor, Don Janssen, for his continuous support over the many years. Thank you for your endless guidance and putting up with my frustrations.

Finally, I want to gratefully acknowledge the support of my family and friends throughout this great endeavor. Kiitoksia paljon.

References

ACI 209-92, "Prediction of Creep, Shrinkage, and Temperature Effects in Concrete Structures," Committee 209, American Concrete Institute, Michigan, 1997.

Acker, P., Comportement mécanique du béton: apports de l'approche physico-chimique. *Rapport de Recherche LPC*, N° 152, 1988.

Baroghel-Bouny, V., "Texture and Moisture Properties of Ordinary and High-Performance Cementitious Materials," Proceedings of Seminaire RILEM 'Benton: du Materiau a la Structure', September 1996, Arles, France.

Betonistandardit, 1992, Suomen Standardisoimisliitto, SFS r.y. Helsinki, 365 pp.

Bjøntegaard, Øyvind, Thermal Dilation and Autogenous Deformation as Driving Foreces to Self-Induced Stresses in High Performance Concrete, Doctoral Dissertation, the Norwegian University of Science and Technology, 1999, 256 pp.

Boivin, S., Acker, P., Rigaud, S., and Clavaud, B., "Experimental Assessment of Chemical Shrinkage of Hydrating Cement Paste," Autogenous Shrinkage of Concrete, edited by Ei-ichi Tazawa, E & FN Spon, London, 1999, pp. 81 - 92.

Brinker, C. J. and Scherer, G.W., Sol-Gel Science: The Physics and Chemistry of Sol-Gel Processing, Academic Press, Inc., San Diego, 1990, 908 pp.

Brooks, J.J., Megat Johari, M.A., and Mazloom, M., "Effect of Admixtures on the Setting Times of High-Strength Concrete," *Cement & Concrete Composites*, Vol. 22, 2000, pp. 293 - 301.

Byfors, J., Plain Concrete at Early Ages, Swedish Cement and Concrete Research Institute, Report 3:80, 1980, 464 pp.

CEB-FIP, *Model Code for Concrete Structures*, Comité Éuro-International du Béton – Fédération Internationale de la Précontrainte, 1990.

Czernin, W., *Cement Chemistry and Physics for Civil Engineers*, 2nd Edition, Foreign Publication Inc., New York, 1980.

Emborg, M., Thermal Stresses in Concrete Structures at Early Ages, Doctoral Thesis, Luleå University of Technology, Luleå, Sweden, 1989, 285 pp.

Engstrand, J., "Shrinkage Reducing Admixture for Cementitious Compositions," *ConChem-Journal*, Vol. 4, 1997, pp. 149 - 151.

Eurocode 2: Design of Concrete Structures – Part 1: General Rules and Rules for Buildings, European Draft Standard prEN 1992-1 (2nd Draft), Brussels, 2001, 222 pp.

Gangé, R., Aouad, I., Shen, J. and Poulin, C., "Development of a New Experimental Technique for the Study of the Autogenous Shrinkage of Cement Paste," *Materials and Structures*, Vol. 32, 1999, pp. 635 - 642.

Gere, J.M. and Timoshenko, S.P., Mechanics of Materials, 3rd Edition, PWS-KENT Publishing Company, Boston, 1990, 807 pp.

Geiker, M. and Knudsen, T., "Chemical Shrinkage of Portland Cement Pastes," *Cement and Concrete Research*, Vol. 12, pp. 603 - 610, 1982.

Grzybowski, M. and Shah, S.P., "Shrinkage Cracking of Fiber Reinforced Concrete," *ACI Materials Journal*, Vol. 87, No. 2, 1990, pp. 138 - 148.

Hammer, T.A., "Test Methods for Linear Measurement of Autogenous Shrinkage Before Setting," Autogenous Shrinkage of Concrete, edited by Ei-ichi Tazawa, E & FN Spon, London, 1999, pp. 143 - 154.

Hedlund, H., Stresses in High Performance Concrete Due to Temperature and Moisture Variations at Early Ages, Licentiate Thesis, Luleå University of Technology, Luleå, Sweden, 1996, 240 pp.

Heikkilä, E., Product Manager, Finnsementti Oy, personal conversations and e-mails, Fall 2000.

Holt, E., “Where Did These Cracks Come From?” *Concrete International*, Vol. 22, No. 9, 2000, pp. 57 - 60.

Holt, E., "Early Age Autogenous Shrinkage of Concrete", doctoral dissertation, University of Washington, Seattle, 2001, 209 pp.

Holt, E. and Leivo, M., “Shrinkage Tendencies of Facade Concrete,” Internal Research Report, VTT Building Technology, Technical Research Centre of Finland, 1996, 26 pp.

Holt, E. and Leivo, M., “Methods of Reducing Early Age Shrinkage,” Shrinkage 2000: Proceedings of the International RILEM Workshop, Baroghel-Bouny, V. & Aitcin, P. editors, RILEM Publications Vol. 1, Paris, 2000, pp. 435 - 447.

Igarashi, S., Bentur, A., and Kovler, K., “Stresses and Creep Relaxation Induced in Restrained Autogenous Shrinkage of High-Strength Pastes and Concrete,” *Advances in Cement Research*, Vol. 11, No. 4, 1999, pp. 169 - 177.

Janz, M., Moisture Transport and Fixation in Porous Materials at High Moisture Levels, Doctoral Dissertation, Report TVBM-1018, Lund Institute of Technology, Lund 2000, 33 p. + 6 papers.

Japan Concrete Institute, Technical Committee on Autogenous Shrinkage of Concrete “Committee Report,” Autogenous Shrinkage of Concrete, edited by Ei-ichi Tazawa, E & FN Spon, London, 1999, pp. 1 - 62.

Jensen, O.M. and Hansen, P.F., “A Dilatometer for Measuring Autogenous Deformation in Hardening Portland Cement,” *Materials and Structures*, Vol. 28, 1995, pp. 406 - 409.

Jokela, J., Kukko, H., Metso, J., Pihlajavaara, S., Sarja, A., Vesikari, E., and Virtanen, J., Kovettuneen Betonin Perusominaisuudet, Tiedonanto 74 (Basic Properties of Hardened Concrete, Research Notes 74 – in Finnish), VTT, Espoo, Finland, 1980, 102 p.

Justnes, H., Clemmens, F., Depuydt, P., Van Gemert, D., and Sellevold, E.J., “Correlating the Deviation Point Between External and Total Chemical

Shrinkage with Setting Time and Other Characteristics of Hydrating Cement Paste," Shrinkage 2000: Proceedings of the International RILEM Workshop, Baroghel-Bouny, V. & Aitcin, P. editors, RILEM Publications Vol. 1, Paris, 2000, 17 pp. 57 - 73.

Justnes, H., Sellevold, E.J., Reyniers. B., Van Loo, D., Van Gemert, A., Verboven, F., and Van Gemert, D., "The Influence of Cement Characteristics on Chemical Shrinkage," Autogenous Shrinkage of Concrete, edited by Ei-ichi Tazawa, E & FN Spon, London, 1999, pp. 71 - 80.

Justnes, H., Van Gemert, A., Verboven, F., and Sellevold, E.J., "Total and External Chemical Shrinkage of Low W/C Ratio Cement Pastes," *Advances in Cement Research*, Vol. 8, No. 31, July 1996, pp. 121 - 126.

Kasai, Y., Yokoyama, K., and Matsui, I., "Tensile Properties of Early Age Concrete," Mechanical Behavior of Materials, Society of Materials Science, Vol. 4, Japan, 1972, pp. 288 - 299.

Kell, G.S., "Volume Properties of Ordinary Water," *Journal of Chemical Engineering Data*, Vol. 12, pp. 67 - 68, 1967.

Kinuthia, J.M., Wild, S., Sabir, B.B. and Bai, J., "Self-Compensating Autogenous Shrinkage in Portland Cement-Metakaolin-Fly Ash Pastes," *Advances in Cement Research*, Vol. 12, No. 1, 2000, pp. 35 - 43.

Koenders, E.A.B. Simulation of Volume Changes in Hardened Cement-Based Materials, Ph.D. dissertation, Delft University Press, 1997, 171 pp.

Kosmatka, S. and Panarese, W., Design and Control of Concrete Mixtures, 13th Edition, Portland Cement Association, Skokie, 1988, 205 pp.

Kronlöf, A., Personal Slides, Betoniyhdistys (Finnish Concrete Association), 1999.

Kronlöf, A., Filler Effect of Inert Mineral Powder in Concrete, VTT Publication No. 322, VTT Building Technology, Espoo, Finland, 1997, 155 p. + app. 32 p.

Kronlöf, A., Leivo, M. and Sipari, P., "Experimental Study on the Basic Phenomena of Shrinkage and Cracking of Fresh Mortar," *Cement and Concrete Research*, Vol. 25, No. 8, 1995, pp. 1747-1754.

Lea, F.M., The Chemistry of Cement and Concrete, 3rd Edition, Chemical Publishing Company, Inc., New York, 1971, 727 pp.

Lea's Chemistry of Cement and Concrete, 4th Edition, edited by Peter C. Hewlett, Arnold, Great Britain, 1998, 1053 pp.

Le Chatelier, H., Sur les changements de volume qui accompagnent le durcissement des ciments. *Bulletin de la Société d'Encouragement pour l'industrie Nationale*, 5eme série, tome 5, 1900.

Leivo, M. and Holt, E., "Autogenous Volume Changes at Early Ages" Self-Desiccation and Its Importance in Concrete, B. Persson and G. Fagerlund editors, Lund University, Lund Institute of Technology, Report TVBM-3075, Lund 1997, pp. 88 - 98.

Leivo, M. and Holt, E., "Betonin kutistuma", VTT Tiedotteita 2076 ("Concrete Shrinkage", VTT Research Notes No. 2076, *in Finnish*), Espoo, 2001, 57 p.

Lynam, C.G., *Growth and Movement in Portland Cement Concrete*, Oxford University Press, London, 1934, pp. 25 - 45.

Mak, S.L., Ritchie, D., Taylor, A., and Diggins, R., "Temperature Effects on Early Age Autogenous Shrinkage in High Performance Concretes," Autogenous Shrinkage of Concrete, edited by Ei-ichi Tazawa, E & FN Spon, London, 1999, pp. 155 - 166.

Mannonen, R., The Effects of Addition Time of Sulphonated Naphthalene-based Superplasticizer on the Properties of Concrete, Doctoral dissertation, Helsinki University of Technology, Espoo, Finland, 1996, 140 pp.

Mehta, P.K. and Monteiro, J.M., Concrete: Structure, Properties and Materials, 2nd Edition, Prentice Hall, Inc., 1993, 548 pp.

Mindess, S. and Young, J.F., Concrete, Prentice-Hall, Inc., 1981, 671 pp.

Neville, A.M., Properties of Concrete, 2nd Edition, Pitman Publishing, London, 1978, 687 pp.

Paulini, P., "A Weighing Method for Cement Hydration," 9th International Congress on the Chemistry of Cement, New Delhi, India, 1992, pp. 248 - 254.

Paulini, P., "Outlines of Hydraulic Hardening - an Energetic Approach," Workshop NTNU/SINTEF - Trondheim, Norway, Early Volume Changes and Reactions in Paste - Mortar - Concrete. November 28-29, 1996.

Paulini, P., "Reaction Mechanisms of Concrete Admixtures," *Cement and Concrete Research*, Vol. 20, 1990, pp. 910 - 918.

Powers, T.C., "Absorption of Water by Portland Cement Paste during the Hardening Process," *Industrial and Engineering Chemistry*, Vol. 27, No. 7, 1935.

Powers, T.C. and Brownyard, T.L., "Studies of the Physical Properties of Hardened Portland Cement Paste," Bulletin 22, Portland Cement Association, Chicago, 1948, 992 pp.

Powers, T.C., Properties of Fresh Concrete, John Wiley and Sons, Inc., 1968, 664 pp.

Radocea, A., A Study on the Mechanisms of Plastic Shrinkage of Cement-Based Materials, doctoral dissertation, CTH Göteborg, Sweden, 1992, 125 pp.

Radocea, A., "Autogenous Volume Change of Concrete at Early Ages Model and Experimental Data," Self-Desiccation and Its Importance in Concrete, B. Persson and G. Fagerlund editors, Lund University, Lund Institute of Technology, Report TVBM-3075, Lund, Sweden, 1997, pp. 56 - 71.

Scherer, G.W., "Structure and Properties of Gels," *Cement and Concrete Research*, Vol. 29, 1999, pp. 1149 - 1157.

Spiegel, M., Schaum's Outline of Theory and Problems of Statistics, McGraw-Hill, New York, 1961.

Taylor, H.F.W., Cement Chemistry, 2nd Edition, Thomas Telford, New York, 1997, 459 pp.

Tazawa, E. and Miyazawa, S., "Chemical Shrinkage and Autogenous Shrinkage of Hydrating Cement Paste," *Cement and Concrete Research*, Vol. 25, No. 2, 1995a, pp. 288 - 292.

Tazawa, E. and Miyazawa, S., "Experimental Study on Mechanisms of Autogenous Shrinkage of Concrete," *Cement and Concrete Research*, Vol. 25, No. 8, 1995b, pp. 1633 - 1638.

Tazawa, E. and Miyazawa, S., "Influences of Cement and Admixtures on Autogenous Shrinkage of Cement Paste," *Cement and Concrete Research*, Vol. 25, No. 2, 1995c, pp. 281 - 287.

Uno, P.J., "Plastic Shrinkage Cracking and Evaporation Formulas," *ACI Materials Journal*, Vol. 95, No. 4, July 1998, pp. 365 - 375.

Viirola, H. and Raivio, P., "Portlandsementin hydrataatio," VTT Tiedotteita 2041 ("Portland Cement Hydration", VTT Research Notes No. 2041, *in Finnish*), Espoo, 2000, 61 pp.

Washburn, E.W., "Note on a Method of Determining the Distribution for Pore Sizes in a Porous Material," *National Academy of Science Proceedings*, Vol. 7, 1921, pp. 115 - 116.

Whiting, D. A., Detwiler, R.J. and Lagergren, E.S., "Cracking Tendency and Drying Shrinkage of Silica Fume Concrete for Bridge Deck Applications," *ACI Materials Journal*, Vol. 9, No. 1, 2000, pp. 71 - 77.

Whitman, F.H., "On the Action of Capillary Pressure in Fresh Concrete," *Cement and Concrete Research*, Pergamon Press, Inc., Vol. 6, 1976, pp. 49 - 56.

Winslow, D.N., “The Rate of Absorption of Aggregates,” *Cement, Concrete, and Aggregates*, CCAGDP, Vol. 9, No. 2, Winter 1987, pp. 154 - 158.

Young, J.F., *Powder Technology*, Vol. 9, 1974, pp. 173 - 179.

Appendix A: Chemistry

The following Table (A.1) presents the common elements used in cement chemistry, along with their molecular weights. The table also gives some of the common abbreviations for compounds and their weights.

Table A.1. Molecular weights of elements and compounds.

Elements / Compounds		g/mol
Ca		40.08
O		16.00
Si		28.09
S		32.07
H		1.01
Al		26.98
Fe		55.85
C	CaO	56.08
S	SiO_2	60.08
$\overline{S}$	SO_3	80.06
H	H_2O	18.01
CH	$Ca(OH)_2$	74.09
A	Al_2O_3	101.96
F	Fe_2O_3	159.69

The following table (A.2) presents the densities assumed for the chemical shrinkage reactions presented in Section 4, along with their references. Bold values are the ones used, with alternative values also presented with citation.

Table A.2. Cement compound densities used for chemical shrinkage calculations. Bold values are actual ones used.

Compound	Density (g/cm^3)	Reference	Assumptions
H	**0.9982**	Paulini 1992	
C_3S	**3.13**	Lea 1971	
	3.15	Justnes et al. 1999	
$C_3S_2H_3$	**2.63**	Lea 1971, Paulini 1992	Afwillite
	2.44	Lea 1971	Tobermorite
CH	**2.23**	Lea 1971	
	2.24	Justnes et al. 1999	
C_2S	**3.28**	Lea 1971, Paulini 1992	Beta
C_4AF	**3.97**	Lea 1971	
CH	**2.23**	Lea 1971	
C_3AH_6	**2.52**	Lea 1971	
C_3FH_6	**2.64**	Paulini 1992	
C_3A	**3.001**	Paulini 1992	
	3.03	Justnes et al. 1999	
	3.04	Lea 1971	
$C\bar{S}H_2$	**2.32**	Lea 1970, Justnes et al. 1999	
$C_6A\bar{S}_3H_{32}$	**1.78**	Justnes et al. 1999	
	1.73	Lea 1971	
$C_4A\bar{S}H_{12}$	**1.99**	Lea 1971	

Appendix B: Calibrations

Calibrations of the linear variable differential transformers (LVDTs) and the pressure transducers were done each year to ensure no variation in the measurements. The LVDTs were calibrated using a "Digimatic" micrometer tool, number 164-161 manufactured by the Mitutoyo company. It measured a range of 0-50 mm with a precision of 0.001 mm and an error of ±2 μm.

Figures B.1 and B.2 give the calibration graphs of the 6 LVDT gauges used on the early age test equipment. The corresponding R^2 values on the linear trendlines are given in Table B.1. Gauges 0 - 1 and 5 - 6 were used as the 2 pairs for measuring horizontal displacement and they are noted as "H" in Table B.1. Gauges 2 and 7 were used for vertical displacement (settlement).

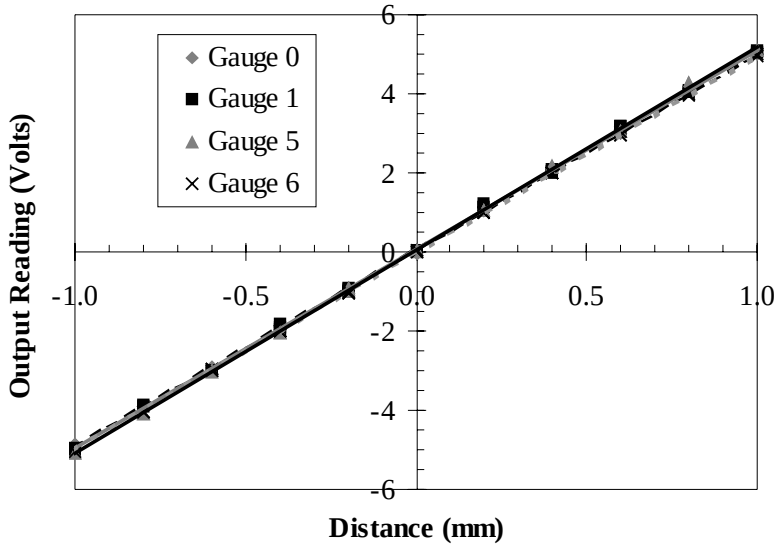

Figure B.1. Calibration of LVDTs measuring horizontal displacement.

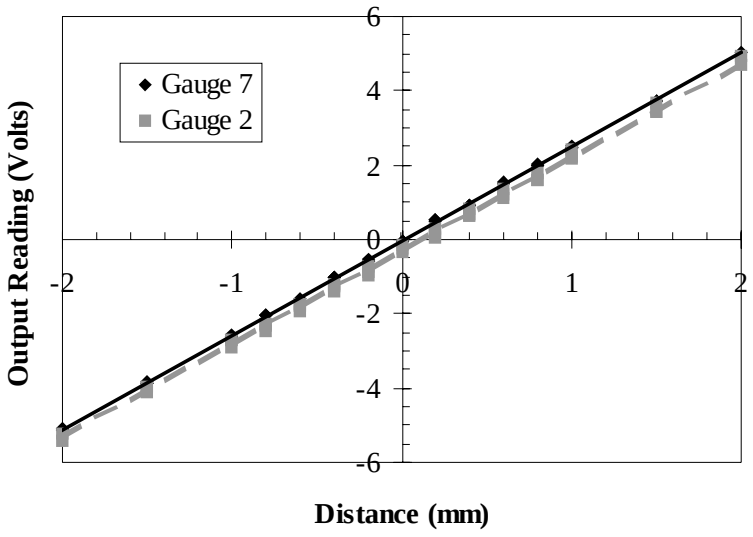

Figure B.2. Calibration of LVDTs measuring vertical displacement.

Table B.1. Square of the correlation coefficient (R^2) for linear trendline of LVDT and pressure transducer gauges. Coefficient a = 1/slope of line.

Gauge	Measure	Line Equation	Coefficient, a	R^2	SD
0	LVDT – H	y = 4.9623 x + 0.0503	0.2015	0.9999	0.033
1	LVDT – H	y = 5.0194 x + 0.0812	0.1992	0.9996	0.059
2	LVDT	y = 2.5222 x - 0.2876	-0.3983	0.9984	0.082
5	LVDT – H	y = 5.1399 x + 0.0375	0.1946	0.9997	0.056
6	LVDT – H	y = 4.9982 x - 0.0067	-0.2001	0.9999	0.027
7	LVDT	y = 2.5344 x - 0.0407	-0.3946	0.9998	0.031
3	Pressure	y = 1.1371 x + 3.2750	0.8794	0.9928	0.066
4	Pressure	y = 1.1297 x + 1.5325	0.8852	0.9999	0.030

Figure B.3 gives the calibration graph of the 2 pressure transducers used to measuring internal capillary water pressure development. The corresponding R^2 values and standard deviation, SD, are also given above in Table B.1.

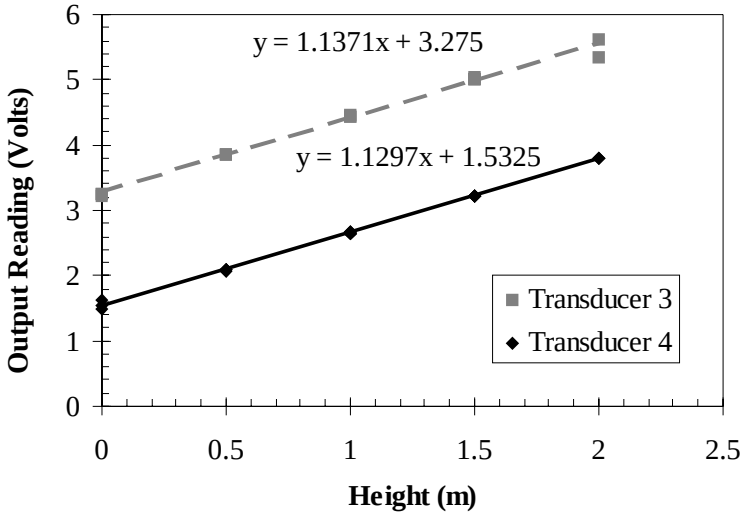

Figure B.3. Calibration of pressure transducers.

The equation used to convert the voltage readings taken by the computer to actual pressure and distance measurements are given by Equations B.1 to B.3. The equations are all based on the calibrations presented above.

$$P = -9.81 \times V \times a \tag{1}$$

$$D = 9/7 \times V \times a \tag{2}$$

$$S = \frac{D_0 + D_1}{X} \tag{3}$$

Where: P = Capillary Pressure (Pa),
V = Output Reading (Volts),
a = Coefficient, = 1/slope of calibration line,
D = Distance a gauge moves (mm),
S = Shrinkage (mm/m), and
X = Distance between gauges (m).

The precision of each measuring device was calculated based on the actual calibrations rather than the values specified on the equipment. For instance, the

data converter manufacturer listed a linearity error < 0.1% while the LVDTs had an error listed of 0.2%. These values were replaced with actual errors calculated from the above calibrations.

Using basic statistical equations, the error was calculated as the square root of the sum of the individual squared error components. The error calculations are shown by Equations B.4 to B.8 and are elaborated on in the next steps for the horizontal shrinkage measuring LVDT.

$$\text{Error}_{\text{total}} = \sqrt{(\text{distance})^2 + (\text{LVDT})^2} \tag{4}$$

The distance error was taken as the precision of measuring over the range used when calibrating the VDT. For instance, the horizontal calibration was done over 2 mm and measured at a precision of 0.001 mm. Therefore the distance error is 0.05%, as calculated in Equation B.5.

$$\text{Error}_{\text{distance}} = \frac{0.001}{2} \times 100 = 0.05\% \tag{5}$$

The error for the actual LVDT voltage output was based on the standard deviation of the values predicted by the linear equations presented in Table B.1. Assuming a 90% likelihood of the data falling within this bell-distribution, the standard deviation was multiplied by 1.65 to get the error range. [Spiegel 1961] For instance, the average standard deviation of the 4 horizontal LVDTs (numbers 0, 1, 5 and 6) was 0.044 volts. This corresponded to a standard deviation in the length (according to equation B.2) of 0.0112 mm.

$$Error_{LVDT} = 0.044 \times 1.65 = 0.0726\% \tag{6}$$

The total error was then calculated using Equation B.4 and shown in Equation B.7.

$$Error_{total} = \sqrt{(0.05)^2 + (0.0726)^2} = 0.088\% \tag{7}$$

Finally, the measuring precision of the horizontal LVDTs was then determined over the range used in practice. In the test arrangement, the distance between the pair of horizontal LVDT gauges was 0.2 m. The LVDT gauge itself was measuring over a range of 1 mm. The final precision of the total horizontal LVDT measurement was then calculated to be 5 με, as shown in Equation B.8.

$$Accuracy_{LVDT} = \frac{1 \times 0.00088}{0.2} \times 1000 = 4.4\ \mu\varepsilon \tag{8}$$

The same type of calculations were done for the other measuring devices: the settlement LVDT and the pressure transducers. The summary of each calibration and the input parameters is given in Table B.2.

Table B.2. Parameters for calibration of horizontal and vertical LVDTs, as well as capillary pressure transducers.

	Horizontal LVDT	Vertical LVDT	Capillary Pressure
Calibration distance (mm)	2	4	2000
Calibrating tool precision (mm)	0.001	0.001	1
Error in calibration tool (%)	0.050	0.025	0.050
Average SD (Volts, Table B.1)	0.044	0.056	0.048
SD range (Volts)	10	10	4.2
90% range of within SD (%)	0.07	0.09	1.89
Total Error (%)	0.09	0.10	1.89
Test measure range (mm/mm/kPa)	1	2	60
Final Accuracy (μm/μm/kPa)	0.88	1.9	1.1

The calibration of the Italian Penetration Test apparatus was done by noting the time of the machine penetration timer compared to a standard clock. There was a nearly perfect correlation, as shown in Figure B.4.

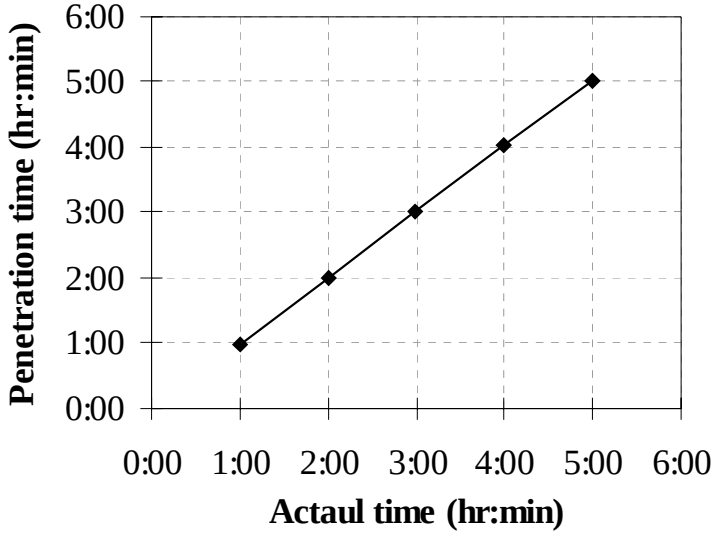

Figure B4. Calibration of penetration test timer compared to real time. $R^2 = 1$.

Appendix C: Finnish Standards

Some of the concrete work followed test procedures detailed in Finnish national standards, Betonistandardit [1992]. A brief summary of each of these standards is presented here for reference. The corresponding American ASTM standard that is closest to the Finnish standard is listed in parenthesis after the titles.

- SFS 5283: Fresh Concrete: Sampling (ASTM C 172)
  This test method follows the ISO 2736/1 standard. It requires that 1.5 times the amount of concrete needed is sampled before use.

- SFS 5284: Fresh Concrete: Consistency, Slump Test (ASTM C 143)
  This test method follows the ISO 4109 standard. The slump cone should be removed from the concrete in 5 to 10 seconds. The slump is measured from the highest point of the slumped concrete.

- SFS 5285: Fresh Concrete: Consistency, Vebe Test (ASTM C 1170)
  This test method follows the ISO 4110 standard. The test uses equipment to measure the consistency while vibrating the concrete. The “vebe” is measure of time (in seconds) for the slump cone concrete to fully collapse.

- SFS 5313: Fresh Concrete: Air Content (ASTM C 231)
  This test method is for a 1-liter mortar sample. The method is similar to SFS 5287 for concrete (7-liter sample) which follows the ISO 4848 method.

- SFS 5341: Concrete: Test Specimens, Making and Curing (ASTM C 192)
  This test method follows the ISO 2736/2 standard, describing how to make test samples and use the vibrating table for consolidation.

Published by

Vuorimiehentie 5, P.O.Box 2000, FIN-02044 VTT, Finland
Phone internat. +358 9 4561
Fax +358 9 456 4374

Series title, number and report code of publication

VTT Publications 446
VTT-PUBS-446

Author(s)
Holt, Erika E.

Title

Early age autogenous shrinkage of concrete

Abstract

Volume change of concrete resulting from structural and environmental factors is an acceptable phenomenon. In the majority of cases this volume change, or shrinkage, is assumed to begin at the time of loading or drying. In reality, a volume change commences immediately after the cement and water come in contact during concrete mixing. These early age volume changes are typically ignored in design of concrete structures since their magnitude can be much less than shrinkage resulting from drying. But even when the concrete curing conditions are ideal, the first day shrinkage can significantly contribute to the ultimate shrinkage and thus the cracking risk.

The goal of this work was to establish a clearer understanding of the mechanisms causing autogenous shrinkage of concrete during the early ages. Autogenous shrinkage is a volume change resulting when there is no moisture transfer to the surrounding environment. It is most prominent in high strength, or high performance concrete where the water-to-cement ratio is under approximately 0.42. Autogenous shrinkage at later ages has been well documented and explained by self-desiccation behavior but the presence of autogenous shrinkage during the first day of concrete hardening has not been theoretically explained.

This work aimed at developing a test method to assess the shrinkage occurring immediately after mixing the concrete and continuing for the first 24 hours. Once a test method was established it was possible to investigate the chemical and physical phenomena causing the autogenous shrinkage in the first hours for neat paste, mortar and concrete. The shrinkage was well correlated to the cements' chemistry and the development of internal capillary pressure within the cement paste. Material parameters influencing the magnitude of the early age autogenous shrinkage were studied, such as the use of superplasticizer and different cement types. The three factors most significantly contributing to the autogenous shrinkage were identified as the concrete's chemical shrinkage, amount of bleeding, and time of hardening. Finally, a generalized model was proposed for reducing early age autogenous shrinkage in future practice.

Keywords

concrete, shrinkage, fresh concrete, volume change, measuring methods, tests, modeling

Activity unit

VTT Building and Transport, Materials and Products, Kemistintie 3, P.O.Box 1805,
FIN–02044 VTT, Finland

ISBN	Project number
951–38–5870–7 (soft back ed.) 951–38–6250–X (URL: http://www.vtt.fi/inf/pdf/)	

Date	Language	Pages	Price
October 2001	English	184 p. + app. 9 p.	D

Name of project	Commissioned by

Series title and ISSN	Sold by
VTT Publications 1235–0621 (soft back ed.) 1455–0849(URL: http://www.vtt.fi/inf/pdf/)	VTT Information Service P.O.Box 2000, FIN-02044 VTT, Finland Phone internat. +358 9 456 4404 Fax +358 9 456 4374

This publication is based on dissertation work done in cooperation with the University of Washington. The research aimed at assessing concrete volume changes occurring in the very early ages due to autogenous reactions. By improving the understanding of autogenous shrinkage, it is possible to take precautions to minimize shrinkage and thus cracking so that more durable structures are constructed. No such measurements of very early age autogenous shrinkage have been done in the past due to the difficulties in measuring fresh concrete. A test arrangement was developed to simultaneously measure vertical (settlement) and horizontal shrinkage, capillary pressure, setting time, temperature and chemical shrinkage from the age of 30 minutes until 24 hours. Early age autogenous shrinkage was correlated to the cements' chemistry and the development of capillary pressure within the paste. Material parameters, such as w/c ratio, superplasticizer dosage, cement type and aggregate restraint, influenced the magnitude of autogenous shrinkage due to their effects on bleeding amount

Tätä julkaisua myy
VTT TIETOPALVELU
PL 2000
02044 VTT
Puh. (09) 456 4404
Faksi (09) 456 4374

Denna publikation säljs av
VTT INFORMATIONSTJÄNST
PB 2000
02044 VTT
Tel. (09) 456 4404
Fax (09) 456 4374

This publication is available from
VTT INFORMATION SERVICE
P.O.Box 2000
FIN–02044 VTT, Finland
Phone internat. + 358 9 456 4404
Fax + 358 9 456 4374

ISBN 951–38–5870–7 (soft back ed.)
ISSN 1235–0621 (soft back ed.)

ISBN 951–38–6250–X (URL: http://www.vtt.fi/inf/pdf/)
ISSN 1455–0849 (URL: http://www.vtt.fi/inf/pdf/)